

Group 9
4/27/2021

EEL 4914

Final Project Document

High Capacity Battery Solar Powered System (HCBSPS)



UNIVERSITY OF CENTRAL FLORIDA
Department of Electrical Engineering and Computer Science

Dr. Lei Wei
Senior Design 1

GROUP 9

Josiah Best - Electrical Engineering
Mike Howell - Electrical Engineering
Eduard Meighan - Electrical Engineering
Jason Rodriguez - Computer Engineering

TABLE OF CONTENTS

| | |
|--|-----------|
| 1.0 Executive Summary | 1 |
| 2.0 Project Description | 3 |
| 2.1 Motivation | 3 |
| 2.2 Goals & Objectives | 3 |
| 2.3 Solar Assembly Basics | 4 |
| 2.4 Engineering Specifications | 6 |
| 2.5 Software Specifications | 7 |
| 3.0 Project Research | 10 |
| 3.1 Microcontroller | 10 |
| 3.1.1 Inter-Integrated Circuit | 11 |
| 3.1.2 Serial Peripheral Interface | 12 |
| 3.1.3 Universal Asynchronous Receiver-Transmitter | 13 |
| 3.1.4 Peripheral Options | 15 |
| 3.1.4.1 1.8" TFT Display Breakout Board and Shield | 15 |
| 3.1.4.2 2.4" TFT LCD with Touchscreen and Breakout Board w/MicroSD Socket | 15 |
| 3.1.4.3 2.8" TFT LCD with Capacitive Touchscreen and Breakout Board w/MicroSD Socket | 16 |
| 3.1.4.4 Adafruit BME280 I2C or SPI Temperature Humidity Pressure Sensor - STEMMA QT | 18 |
| 3.1.4.5 MCP9808 High Accuracy I2C Temperature Sensor Breakout Board | 18 |
| 3.1.5 Pulse Width Modulation | 18 |
| 3.1.6 Microcontroller Options | 20 |
| 3.1.6.1 Atmega2560 | 20 |
| 3.1.6.2 ATSAM21G18 ARM Cortex M0+ | 22 |
| 3.1.6.3 MSP430 LaunchPads | 26 |
| 3.1.7 Chosen Parts | 27 |
| 3.2 Solar Panel | 28 |
| 3.2.1 Crystalline, Polycrystalline and Amorphous Solids | 31 |
| 3.2.2 Technical Specifications of Solar Panels to Understand | 32 |
| 3.2.3 Solar Panel Types | 33 |
| 3.2.3.1 Monocrystalline Solar Panels | 33 |
| 3.2.3.2 Polycrystalline Solar Panels | 34 |
| 3.2.3.3 Amorphous Solar Panels | 34 |

| | |
|---|-----------|
| 3.2.4 Solar Panel Options | 34 |
| 3.2.4.1 Renogy 100W 12V Monocrystalline Foldable Suitcase Solar Panel | 34 |
| 3.2.4.2 Renogy 100W 12V Monocrystalline Ridgid Solar Panel | 35 |
| 3.2.4.3 HQST 100W 12V Monocrystalline Ridgid Solar Panel | 35 |
| 3.2.4.4 WindyNation 100W 12V Polycrystalline Solar Panel | 35 |
| 3.2.4.5 RICH SOLAR 100W 12V Polycrystalline Solar Panel | 36 |
| 3.2.4.6 Our Solar Panel Choice | 36 |
| 3.3 Charge Controllers | 37 |
| 3.3.1 PWM vs MPPT | 38 |
| 3.3.2 Which type of charge controller to use? | 40 |
| 3.3.3 PWM Functionalities and Examples | 40 |
| 3.3.4 MPPT Functionalities and Examples | 45 |
| 3.3.5 Which type of controller we will use and why? | 49 |
| 3.4 Relays | 50 |
| 3.4.1 Types of Relays | 51 |
| 3.4.2 Out Relay | 51 |
| 3.5 LCD Display & GUI | 51 |
| 3.5.1 Researching the 2.8" TFT LCD with Capacitive Touchscreen | 51 |
| 3.5.2 The Graphical User Interface | 53 |
| 3.6 Temperature Sensor | 56 |
| 3.7 Voltage Regulators | 56 |
| 3.7.1 Types of Regulators | 56 |
| 3.7.2 Voltage Regulators in our Project | 57 |
| 3.8 Battery Management System (BMS) | 58 |
| 3.8.1 What Makes Up the BMS | 59 |
| 3.8.2 Comparison of Different BMS's | 62 |
| 3.8.2.1 HEYO Smart BMS F4S12V60A BT | 62 |
| 3.8.2.2 DALY Waterproof LiFePO4 BMS | 63 |
| 3.8.2.3 MGod Smart LiFePO4 BMS | 63 |
| 3.8.2.4 GFS-SP04S020 LiFePO4 Smart BMS | 63 |
| 3.8.3 Our Battery Management System | 64 |
| 3.9 Rechargeable Battery | 67 |
| 3.9.1 Voltage Characteristic (Redox Reactions) | 67 |
| 3.9.2 Galvanic and Electrolytic Cells | 68 |
| 3.9.3 Rechargeable versus Non-Rechargeable | 69 |
| 3.9.4 Discharge Rate (C-Rate) | 70 |
| 3.9.5 Depth of Discharge/State of Charge | 71 |

| | |
|---|-----------|
| 3.9.6 The Effects of Ambient Temperature On Batteries | 72 |
| 3.9.7 Deep Cycle Versus Non-Deep Cycle Batteries | 72 |
| 3.9.8 Battery Energy Density | 73 |
| 3.9.9 Thermal Runaway | 74 |
| 3.9.10 Rechargeable Deep-Cycle Battery Types | 74 |
| 3.9.10.1 Nickel Cadmium Batteries | 74 |
| 3.9.10.2 Nickel-Metal-Hydride Batteries | 75 |
| 3.9.10.3 Lithium-Ion Batteries | 75 |
| 3.9.10.4 Sealed Lead Acid Batteries (SLA) | 75 |
| 3.9.10.5 Lithium Iron Phosphate Batteries | 76 |
| 3.9.11 Battery Options | 77 |
| 3.9.11.1 (4) VariCore 3.2V 200Ah Lithium Iron Phosphate Battery Cells | 77 |
| 3.9.11.2 Expert Power 12V 200Ah Lithium Iron Phosphate Battery | 77 |
| 3.9.11.3 LBP 12V 200Ah Lithium-Ion Battery | 78 |
| 3.9.11.4 Renogy 12V 200Ah AGM Battery | 78 |
| 3.9.12 Our Battery Choice | 78 |
| 3.10 Inverters | 79 |
| 3.10.1 Power Factor and Total Harmonic Distortion | 80 |
| 3.10.2 Different Types of Inverters | 83 |
| 3.10.3 Square Wave Inverters | 83 |
| 3.10.4 Modified Square Wave Inverters | 84 |
| 3.10.5 Pure Sine Wave Inverters | 84 |
| 3.10.6 Which Inverter We Will Use and Why? | 85 |
| 3.11 Soldering | 87 |
| 3.11.1 Soldering Standards In the Industry | 88 |
| 3.11.2 Soldering In Our Project | 88 |
| 3.12 Selecting Proper Gauge Wires | 89 |
| 3.12.1 Wire Gauges That We Plan to Use | 90 |
| 3.13 Transistors | 91 |
| 3.14 MOSFETS | 92 |
| 3.15 Current Sensors | 93 |
| 4.0 Design Constraints and Standards | 97 |
| 4.1 Constraints | 97 |
| 4.2 Design Standards | 97 |
| 4.2.1 Battery Standards | 98 |
| 4.2.2 IEEE Standards | 99 |
| 4.2.3 IPC PCB Standards | 99 |

| | |
|--|------------|
| 4.2.4 C/C++ Language Standards | 100 |
| 5.0 Project Design | 101 |
| 5.1 Software Design | 101 |
| 5.1.1 Charging Algorithm for Lithium Iron Phosphate Batteries | 101 |
| 5.1.1.1 The Bulk Stage | 101 |
| 5.1.1.2 The Absorption Stage | 103 |
| 5.1.1.3 The Float Stage | 104 |
| 5.1.1.4 The Algorithm | 105 |
| 5.1.1.5 Voltage and Current Measurements | 106 |
| 5.1.2 GUI Design | 107 |
| 5.2 Hardware Design | 110 |
| 5.2.1 Solar Charge Controller PCB | 110 |
| 5.2.2 Lithium Iron Phosphate Battery Assembly | 117 |
| 5.2.2.1 BMS Attachment to Battery Assembly | 118 |
| 5.2.2.2 Battery Assembly Custom Enclosure Design | 120 |
| 5.2.3 Custom Solar Charge Controller Enclosure Design | 122 |
| 5.2.4 Solar Panel Connection to Solar Charge Controller | 123 |
| 5.2.5 Battery to Inverter Connection | 124 |
| 8.0 Budget and Funding | 125 |
| 8.1 Milestones | 126 |
| 8.1.1 Project Milestones SD1 | 126 |
| 8.1.2 Project Milestones SD2 | 126 |

FIGURE INDEX

| | |
|---|----|
| Figure 1 - Basic Solar Assembly | 5 |
| Figure 2 - Block Diagram & Division of Labor | 7 |
| Figure 3 - House of Quality | 9 |
| Figure 4 - Typical I2C Connection | 11 |
| Figure 5 - SCL & SDA Signals | 12 |
| Figure 6 - Typical SPI Connection | 12 |
| Figure 7 - Example of SPI Signals | 13 |
| Figure 8 - Typical UART Connection | 13 |
| Figure 9 - Contents of a UART Packet | 14 |
| Figure 10 - Resistive Touch Screen | 16 |
| Figure 11 - Capacitive Touch Screen | 17 |
| Figure 12 - PWM Waveform by Duty Cycles | 18 |
| Figure 13 - Analog to Digital Conversion | 19 |
| Figure 14 - Sleep Modes for the Atmega2560 | 21 |
| Figure 15 - Current Consumption in ACTIVE mode | 23 |
| Figure 16 - Sleep Modes for ATSAMD21G18 ARM Cortex M0 | 24 |
| Figure 17 - AHB & APB Architecture | 24 |
| Figure 18 - Number of Pages According To Datasheet | 25 |
| Figure 19 - Sleep modes for MSP430G2553 | 27 |
| Figure 20 - Silicon Wafer After Slurry Sawing | 29 |
| Figure 21 - Textured Silicon Surface | 30 |
| Figure 22 - Atomic Structures of Crystalline, Polycrystalline, and Amorphous Solids | 32 |
| Figure 23 - Open and Short Circuit Diagram | 33 |
| Figure 24 - MPPT vs. PWM Analog Circuit | 38 |
| Figure 25 - Losses with PWM Controller | 39 |
| Figure 26 - Losses with MPPT Controller | 40 |
| Figure 27 - OLYS Solar Charge Controller | 41 |
| Figure 28 - MORPROSTAR-15M Solar Charge Controller | 43 |
| Figure 29 - PS-MPPT-25M Solar Charge Controller | 45 |
| Figure 30 - GV-10-LI-14.2V Solar Charge Controller | 47 |
| Figure 31 - Basic Relay Diagram | 50 |
| Figure 32 - Viewing Angles of a Screen | 52 |
| Figure 33 - Observer Below Screen | 52 |
| Figure 34 - Synchronous Baud Rate Equation | 53 |
| Figure 35 - Screen Coordinate | 54 |
| Figure 36 - Color Representation In 16-Bits | 54 |

| | |
|--|-----|
| Figure 37 - Setter Functions | 55 |
| Figure 38 - Drawing Text | 55 |
| Figure 39 - drawBitmap() Function and its Parameters | 55 |
| Figure 40 - BMS System Diagram | 59 |
| Figure 41 - FET Connection Between the Load and Charger | 60 |
| Figure 42 - FET Setup of Simultaneous Charging and Discharging | 60 |
| Figure 43 - Bypass FET Slowing the Charge Rate | 61 |
| Figure 44 - Active Balancing During Discharge Cycle | 62 |
| Figure 45 - BMS Wiring Diagram | 65 |
| Figure 46 - Potential Difference Between Two Electrodes | 67 |
| Figure 47 - Galvanic and Electrolytic Cells | 69 |
| Figure 48 - Discharge Curve of Battery Compared to Other Power Storage Devices | 70 |
| Figure 49 - Depth of Discharge and State of Charge | 71 |
| Figure 50 - Purely Resistive Circuit Current and Voltage Phase | 80 |
| Figure 51 - Inductive Circuit Current and Voltage Phase | 80 |
| Figure 52 - Capacitive Circuit Current and Voltage Phase | 81 |
| Figure 53 - Harmonics of a Square Wave Inverter Output | 83 |
| Figure 54 - Waveform of a Modified Square Wave Inverter Output | 84 |
| Figure 55 - Waveform of a Pure Sine Wave Inverter Output | 85 |
| Figure 56 - Sine Wave Inverter Diagram | 85 |
| Figure 57 - EDECOA DPM30 3000W Power Inverter | 86 |
| Figure 58 - NPN Transistor Diagram | 91 |
| Figure 59 - NPN Transistor Electron Flow | 91 |
| Figure 60 - NPN BJT | 92 |
| Figure 61 - N Channel MOSFET | 93 |
| Figure 62 - P Channel MOSFET | 93 |
| Figure 63 - Relationship Between Output Voltage and Sensed Current | 94 |
| Figure 64 - Voltage Division and Scale Factor for ACS712 | 95 |
| Figure 65 - MLX9122 Properties | 96 |
| Figure 66 - Charging Profile for LiFePO4 | 101 |
| Figure 67 - Bulk Stage Charging Algorithm | 102 |
| Figure 68 - Absorption Stage Charging Algorithm | 103 |
| Figure 69 - PID Equation | 103 |
| Figure 70 - PID Function Syntax | 104 |
| Figure 71 - Float Stage Charging Algorithm | 104 |
| Figure 72 - The Charging Algorithm | 106 |
| Figure 73 - Main Menu Screen | 107 |
| Figure 74 - Text File Output Example | 108 |
| Figure 75 - Settings Screen | 108 |
| Figure 76 - Time & Date Settings | 109 |

| | |
|---|-----|
| Figure 77 - Graphs Screen | 109 |
| Figure 78 - Overall Schematic for PCB Charge Controller | 111 |
| Figure 79 - Schematic of Current Sensor and TVS Diode | 112 |
| Figure 80 - Schematic of Voltage Dividers, Diodes, PMOS, and NPN BJT | 114 |
| Figure 81 - Schematic Focus on Fuse, Current Sensor, Battery and Load Terminals | 117 |
| Figure 82 - Battery Cell Connection With Included Bus Bars | 118 |
| Figure 83 - BMS Components and Dimensions | 119 |
| Figure 84 - BMS to Battery Cells Connection | 120 |
| Figure 85 - Custom Plexiglass Battery Assembly Enclosure | 121 |
| Figure 86 - Custom Solar Charge Controller Enclosure Front and Bottom | 122 |
| Figure 87 - Custom Solar Charge Controller Enclosure Side View | 123 |
| Figure 88 - Connecting the Solar Panel to Our Charge Controller | 123 |
| Figure 89 - Connecting the Inverter to the Battery | 124 |

TABLE LIST

| | |
|---|-----|
| Table 1 - Engineering Specifications | 6 |
| Table 2 - Software Specifications | 7 |
| Table 3 - Selected Parts and Reasons | 28 |
| Table 4 - Solar Panel Comparison | 37 |
| Table 5 - Technical Parameters of OLYS (Model SEC10 and SEC20) Charge Controller | 42 |
| Table 6 - Technical Parameters of MORNINGSTAR Charge Controller (All Models) | 44 |
| Table 7 - Technical Parameters Morningstar PS-MPPT Charge Controller (All Models) | 46 |
| Table 8 - Technical Parameters GV-10-LI-14.2V Solar Charge Controller | 48 |
| Table 9 - Comparing PWM vs MPPT Controllers | 49 |
| Table 10 - MP2307 and D24V22F9 Comparison | 58 |
| Table 11 - Comparison of BMS's | 64 |
| Table 12 - BMS Specifications Table | 66 |
| Table 13 - Battery Comparison | 79 |
| Table 14 - Specifications For DPM30 3000W Power Inverter | 87 |
| Table 15 - Nominal Wire Sizing Chart | 90 |
| Table 16 - ACS712 & MLX9122 Comparison | 96 |
| Table 17 - BJT Comparison | 114 |
| Table 18 - MOSFET Comparison | 115 |
| Table 19 - Budget and Funding | 125 |
| Table 20 - SD1 Milestones | 126 |
| Table 21 - SD2 Milestones | 126 |

EQUATIONS LIST

| | |
|--|----|
| Equation 1 - Power Factor in RMS | 50 |
| Equation 2 - Harmonic Current | 50 |
| Equation 3 - Apparent Power | 50 |
| Equation 4 - Revised Power Factor | 51 |
| Equation 5 - Simplified Power Factor | 51 |
| Equation 6 - Total Harmonic Distortion | 51 |
| Equation 7 - Relating Distortion Factor to THD | 51 |
| Equation 8 - Revised Conceptual Power Factor | 52 |
| Equation 9 - Revised Mathematical Power Factor | 52 |

1.0 Executive Summary

As civilization progresses, and pollution becomes more rampant, the world struggles with the same problem day to day with little in terms of an affordable long term solution. While there are several different energies that are considered “renewable”, the problem continues to center around affordability and efficiency. The one source of energy that is quite possibly the easiest to use is solar. While solar is still far from being fully efficient, it can be utilized more practically by the everyday person. As it stands, hydro and wind energies can require sources out of your control, while solar energy is typically abundant for many hours of the day. What is even more difficult is a solution that is not only clean, but portable. What we aim to accomplish is an affordable and easy to use solution to portable solar energy.

Our project aims to create an affordable high capacity solar assembly with a touchscreen interface that can be used in situations where standard power is not readily available. Whether this be when you’re camping or if you’re unlucky enough to have your power knocked out by a catastrophic event, our device offers a convenient and affordable solution. We estimate achieving a 12V 200 Ah battery by either sourcing an affordable pre-built battery, or buying and connecting individual battery cells in series/parallel to achieve our desired capacity.

The battery will be monitored by a charge controller that is based on a microcontroller and PCB. There will actually be two different systems monitoring the lithium iron phosphate battery bank. These two systems will be our charge controller that will control the amount of charge going into the battery and a battery management system which will make sure that the battery is charged equally. The charge controller will control and display the battery’s state and charging information from the solar panel on a touchscreen LCD screen. This will help preserve the life span of the battery and improve efficiency. The LCD will display information regarding the battery using graphics that is easy to understand. This will not only increase longevity of the device but also inform the user of many statuses. Many smartphones display charge levels by representing that information using a filled battery icon as well as including the numerical level. We will be using that design philosophy when creating the graphical user interface.

Though there are other high capacity batteries that can be charged with solar, their price points are not affordable for many households. For most people this is not an option. We want to demonstrate that affordability in this design IS possible, while also adding a feature that no other battery assembly has at our price point...an LCD touchscreen display as explained above.

In the solar industry, there are two types of charge controllers. Pulse Width Modulation (PWM) driven charge controllers and Maximum Power Point Tracking (MPPT) charge controllers. MPPT charge controllers are more efficient and can offer up to 80 amps or more in some cases. PWMs can only provide up to 60 amps. However, for this project, we will be creating a PWM charge controller. Our goal for this project is to provide an affordable and robust solution. PWM charge controllers have been around much longer compared to MPPT controllers and are generally cheaper. They are well established and simpler to implement. For our design we realize that MPPT The charge controller will

primarily serve a better purpose in terms of efficiency and scalability but we will stick with the PWM design as to reduce cost and complexity due to time and budget constraints. The temperature sensor will also monitor the temperature of the battery. Safety is very important for us, and due to this we will be choosing a battery type that is safe under extreme conditions and doesn't run a high risk of melting or exploding. Lithium iron phosphate batteries are known to be a good substitute for lithium ion as in the lithium ion thermal runaway may occur. We mitigate this problem by switching battery types. Additionally because of the importance of safety in our project, we will be monitoring ambient temperature using temperature sensors and using that to adjust specific aspects of our battery charging and discharging via the charge controller and a battery management system.

In terms of the solar panel, we will be using a foldable monocrystalline panel. This was chosen beforehand due to it being donated. This panel provides convenience due to its portability and has good ratings as per the manufacturer. Because one of the utilities for our project is producing power if power had been cut off by a storm event, this would be important. Not all days after a hurricane will be sunny, so it's imperative that the solar panel still charges the battery in these circumstances.

For functionality, our solar powered battery assembly will have the capacity to charge phones, computers, small refrigerators, small campers, and fans in times of need. (More specific info on what can be connected to the solar assembly will be discussed in our design section, section 5.0). No one wants to sleep when it's 90 degrees without AC or fans or have to deal with loud generators that release gaseous fumes, guzzle gas, and malfunction consistently. Our affordable green solution will remedy each of these problems, while keeping money in the customer's wallet.

One thing to note early on is that to power such AC devices, there has to be a clean signal via the inverter that we will use. Although we will explore all inverter types in our research section of our paper, we will mainly focus on a modified square wave inverter. Since our inverter was donated to us we will make use of it in our design. A pure sine wave inverter is the best type to use when producing "clean" power void of any distortion or interference, but for our application a modified square realization should be adequate. As a result of the imperfect power conversion we do expect to have residual heat and possible "buzzing" as a result of the losses that we have calculated in our design to occur.

The "brain" of our entire system will be our microcontroller. This will have various uses as outlined in one of the previous paragraphs. It will keep statuses on charging conditions of the batteries. It will communicate with the solar charge controller that we plan to build as a custom PCB. It will relay information to the touch screen whereby the user can see these said statuses. It will communicate and power a temperature sensor which will monitor the heat coming off of our system. It will be coded to keep the charging process fluid, safe and as efficient as possible so as to prolong the life of not only our batteries, but of our system as an entire entity. Finally this project is a microscale of what can be achieved. With a MPPT controller and a larger solar panel as well as a larger battery bank with a pure sine wave inverter, the user could power larger appliances or even run whole residential systems if need be at will with the reliability of a renewable energy source.

2.0 Project Description

This part of the project discussion will be dedicated to explaining the purpose and motivation behind developing an affordable high capacity solar powered battery system. Alongside the discussion of the motivation of the project, the project goals and objectives will be discussed. Finally, this section will include engineering specifications, a block diagram outlining the flow of the project and division of labor, and the project's house of quality..

2.1 Motivation

What happens when the power goes out, or maybe there was none to begin with? In the cases where power is lost, we lose access to many comforts and some necessities. When there is no power to begin with, life can be difficult all together. There are solutions out there, but in most cases, the price tag is too high, or the effect on the environment is detrimental. In terms of the environmental impact, imagine having to run a gas-powered generator consistently for power? This consistent burning of the fossil fuels required to power the generator would be harmful to the environment and expensive to maintain. In regards to Florida specifically, these are questions each of us must heavily consider. Due to our location or anyone living near the coast in the southeast United States, it isn't a matter of "if" you will lose your power, it is a matter of "when." Historically speaking, think back to 2004. Florida was hit with four hurricanes within a six-week span. Many families were left without power for almost the entirety of these six weeks. In 2020 the year with a record-breaking number of hurricanes, Louisiana was hit by five hurricanes. In the case of Louisiana, many people faced the same grim outcome of being without power for an extended period. Some of these people in both cases from Florida and Louisiana were fortunate enough to have generators, or even professionally installed solar power arrays for their homes. For those with generators, there was one key issue...gas. If one had not prepared ahead of time for the storm event and stocked up on gas for their generator, it was near impossible to find available gas. These unlucky individuals like those without generators or solar arrays were without power and had to endure the hardships that being powerless brought.

Imagine being in a scenario where there is no power to begin with. For example, an individual living off the grid where there is no power. This is actually more common than one might think in the United States. In this case, using a generator non-stop isn't a sustainable or environmentally friendly option. If one wants consistent and sustainable power one of the only options is a solar powered battery system. In this case the user would want a semi-portable and affordable system. Most cases when living remote do not allow for large complex solar power arrays. These two examples alongside many unmentioned ones have driven us to design and build an affordable high-capacity and user-friendly battery powered solar system to meet the needs of those who have lost power, or never had power at all.

2.2 Goals & Objectives

- The primary objective of this design is to be solar powered with high capacity storage for extended use.

- A secondary objective would be to include additional outputs so that several devices can be powered or charged simultaneously.
- The solar powered battery assembly will be semi-portable. It can be moved as needed for different environments.
- There are three key components to our project. To design and build an affordable touchscreen solar charge controller. In addition to the solar charge controller design we will be sourcing a battery whether that be prebuilt or we assemble battery cells together ourselves. Finally, we have our donated 100 watt portable solar panel to complete the solar charging assembly. In our case, the main difference between our solar charging assembly and others on the market is price, and our proposed touchscreen solar charge controller. Based on the research done, there aren't any others on the market like it.
- Our project must be safe. Due to the nature of our design, the system should pose no risk to the consumer. To accomplish this we have planned for the charge controller to monitor the temperature at all times and cut off the incoming charge alongside purchasing a BMS system to constantly monitor the batteries themselves.
- This design should be easy and intuitive to use by the consumer. From using the output ports to using the touchscreen display, it should be easy for the consumer to use the product without additional instructions.

2.3 Solar Assembly Basics

Understanding the basics behind how a solar assembly such as ours functions is key. There are three main components, the battery, solar charge controller, and finally the solar panel. Additionally a fourth optional main component which we will have in our assembly is that of an inverter. See the figure below for each component.

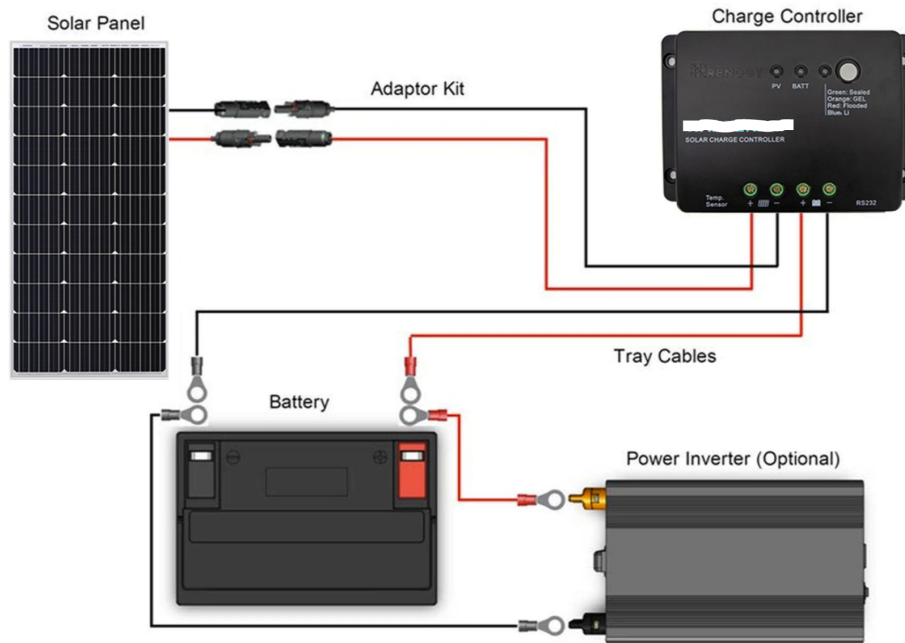


Figure 1: Basic Solar Assembly

In the assembly above, one can see the first main component is the solar panel. This doesn't need much explaining as it simply absorbs the sunlight and converts it to electrical energy. Next in line is the solar charge controller. In the case of our project, we will be designing our own as previously mentioned. The solar charge controller acts as the interface between the solar panel and the battery. It measures the amount of voltage and current coming from the solar panel into the battery. Additionally, it will cut-off incoming voltage to the battery if the battery is fully charged and convert that excess to heat. Next is the battery. In our case we are designing the solar assembly for applications such that connection to the grid isn't possible thus needing a way for the electrical energy from the solar panel to store charge to be used. The battery is directly connected to the solar charge controller. In many cases it is always wise to include a BMS system with your battery (see section 3.8 for discussion on BMS's). Many pre-built batteries used for off-grid applications like ours have built-in BMS's hence the BMS not being shown above. In regard to the battery, there are many different types of viable rechargeable batteries for solar assemblies (these battery options are discussed in detail in section 3.9). Finally as shown in the picture above, the final necessity of an off grid solar assembly is an inverter. This inverter is connected directly to the battery and converts the DC of the battery to AC. Additionally, it has an amplifying stage such that the 12V coming from the battery is converted to 120V. Inverters typically have AC outlets embedded in them. This DC to AC conversion allows connection of household devices to the previously mentioned AC outlets. There are many specifics tied to each one of these components, but they will all be discussed later in the report.

2.4 Engineering Specifications

| |
|--|
| Simple install and assembly for the customer |
| Total price estimate to be less than \$800 |
| Easy to use/understand touchscreen LCD interface |
| Weight of the assembly > 60 lbs excluding the solar panel |
| Solar panel must be rated to output 100 watts with at least 80% efficiency |
| Battery assembly must adhere to at least IP54 water resistance |
| Assembly will have 2 AC outlets |
| Battery capacity will be 200 Ah |
| The solar charge controller will have built-in polarity protection |
| Low temperature protection (See Below) |
| Built in backflow protection in the solar panel |
| Demonstrable Engineering Specifications |
| Battery and charge info on touch screen LCD display |
| Graph on LCD display in real-time displaying solar panel peak voltage values over time |
| Battery discharge high temperature cut-off |
| Solar panel charge high temperature cut-off |
| Momentary bypass button to turn inverter on to override BMS fault error |

Table 1: Engineering Specifications

2.5 Software Specifications

| |
|---|
| The application shall route charge |
| The application shall measure the charge of the battery |
| The application shall measure the voltage from the battery |
| The application shall measure current |
| The applications shall measure ambient temperature |
| The application shall measure power consumption |
| The application shall measure the voltage from the solar panels |
| The application shall control the heat sink |
| The application shall disconnect the output from the battery based on the charge level of the battery |
| The application shall reconnect the output to the battery based on the charge level of the battery |
| The application shall display the above information on the display |

Table 2: Software Specifications

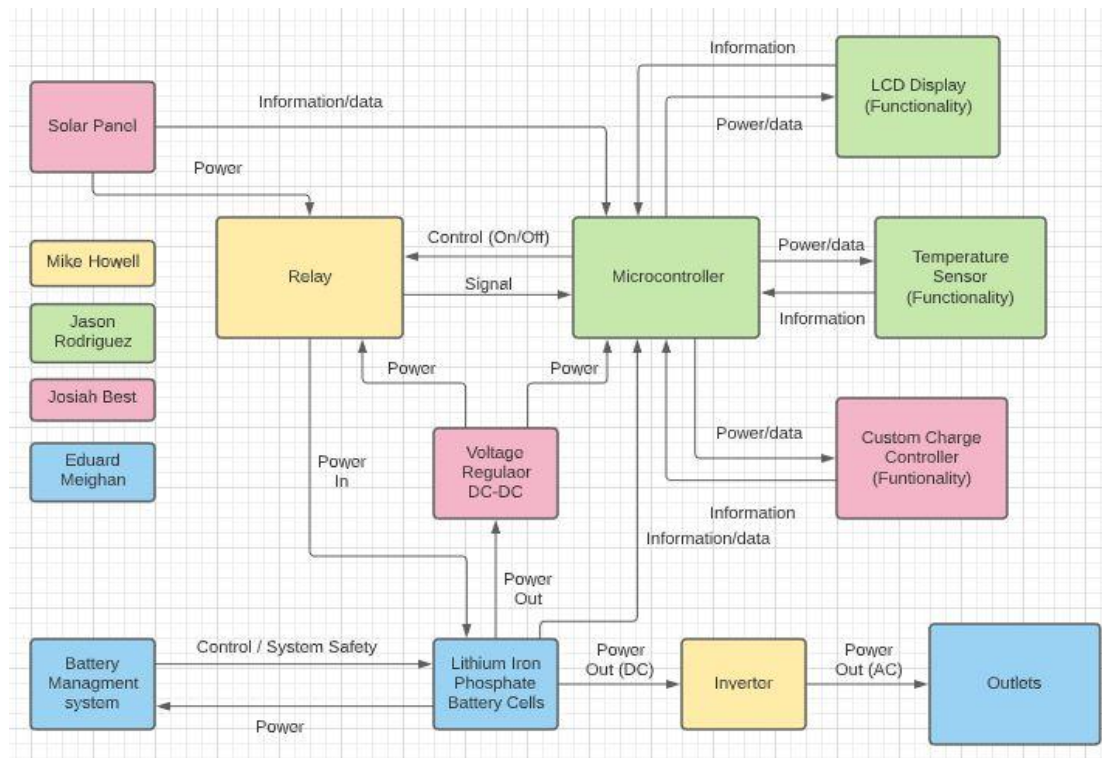
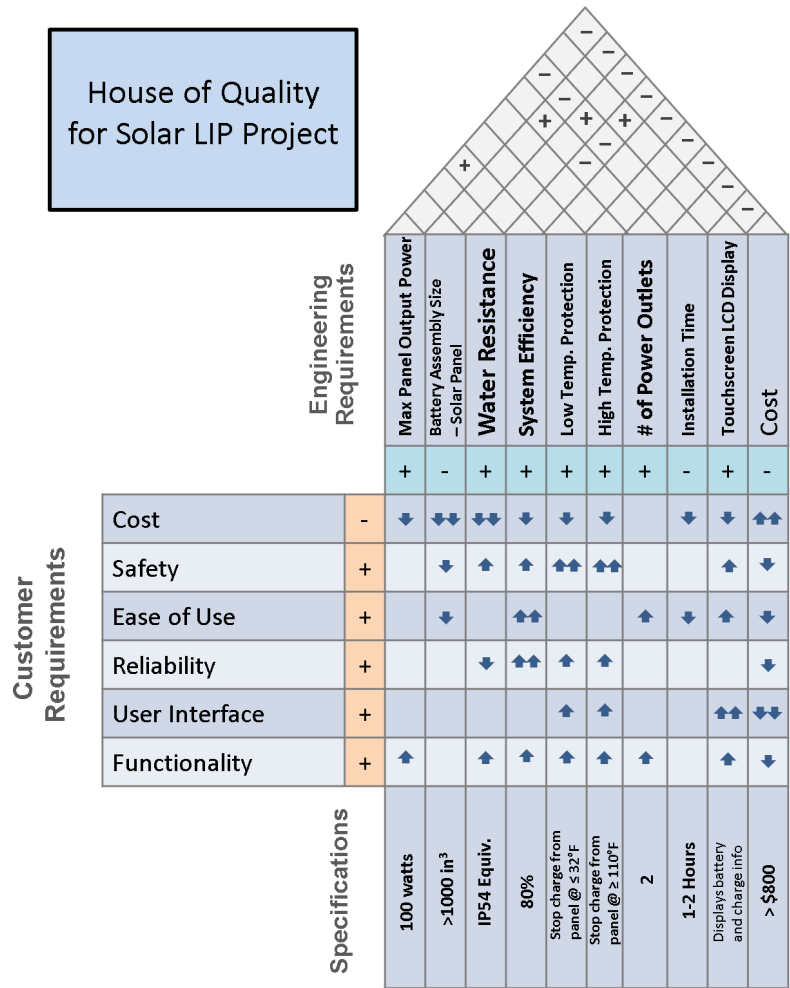


Figure 2: Block Diagram & Division of labor

From the block diagram above we have summarized our project into blocks where the flow is indicated by the arrows. To help the user to better understand how our product operates we can elaborate upon this diagram. First, the solar panel that we choose will convert the sun's solar energy into electrical energy which will then provide power to a bank of lithium iron phosphate battery cells. Before this is done, this power will have to go through a custom charge controller that will be fashioned as a PCB and will provide enough power to charge the batteries but to not have them overcharged. It will also keep the batteries from leaking current to the solar panel which would result in losses and damage. The charge controller will communicate with the microcontroller to give active status of the energy being provided and relayed to the batteries and this information will be forwarded to a touchscreen LCD display which will be powered by the microcontroller. When the charge controller detects that the battery is approaching peak capacity, it will send a signal to the relay to stop the flow of charge into the storage cells. While the relay allows or blocks power to the cells, a Battery Management System or BMS will monitor that the charging of the cells will be done equally and thus safely. The BMS provides safety for large capacity cells in a variety of ways. The first is that it will make sure that all cells charge evenly. This mitigates a problem of longevity as uneven charging can drastically shorten battery life. The BMS will be powered directly by the battery cells and will provide control for safe and efficient charging and discharging of the cells. Although we put a voltage regulator in the block diagram we know that our microcontroller has a built in regulator which will automatically convert the correct amount of power needed to run the embedded system. One other functionality that will work alongside the microcontroller will be a temperature sensor. This will provide real time system information to make certain that the system is not overheating. Proceeding from the storage cells, the power within the cells will be split between DC and AC. Power will come out of the cells in the form of DC only but will be converted into AC

through an inverter or more commonly known in the world of academia as a DC to AC converter. This will be supplied to outlets that will provide power to AC appliances. The power not used for the outlets will be fed into a voltage regulator which will accurately split and provide the correct amount of voltage to both the relay and the microcontroller. One of the most important features in our block diagram is the microcontroller. It will act as the central hub for most (if not all) structures contained within our project. The microcontroller is expected to perform the following functions: Collect information from the solar panel, collect information from the charge controller, act as a liaison between the capacity controller and the solar panel, collect information from the battery storage cells, turn on and operate effectively provided ample power from the batteries, take and provide information from and to the charge controller, power the charge controller, power the temperature sensor, take information from the temperature sensor, power the LCD display, and finally display many aspects of information from said devices to the user to inform of status, safety concerns and or possible problems within the system as a whole. Our block diagram is colored to designate tasks and assigned to specific people. Mike will be in charge of any relays and inverter tasks that we will need. He will also do any soldering and wire gauge components that we will need along with constraints. Jason will be in charge of any microcontroller operations along with the LCD display and the temperature sensor. Josiah will be in charge of the solar panels as well as the regulators and the PCB design for the custom charge controller. Eduard will be in charge of the BMS, the outlets and the battery cells. All people will intertwine for secondary tasks as this project is a team effort and we will all be relying and working with one another.

House of Quality for Solar LIP Project



Polarity:
 + Positive
 - Negative

Relationships:
 Strong Positive Correlation = ↑↑
 Positive Correlation = ↑
 Negative Correlation = ↓
 Strong Negative Correlation = ↓↓

| Table Index | |
|-------------------------------------|----------------------------------|
| ENG Requirement | Value/Feature |
| Max panel output power | 100 watts |
| Battery Assembly Size - Solar panel | > 1000 inches ³ |
| Water resistance | IP54 Equiv. |
| System efficiency | 80% |
| Low Temp. Protection | Stop charge from panel @ ≤ 32°F |
| High Temp. Protection | Stop charge from panel @ ≥ 110°F |
| Installation time | 1-2 Hours |
| # of power outlets | 2 |
| Touchscreen LCD Display | Displays battery and charge info |
| Cost | > \$800.00 |

Figure 3: House of Quality

3.0 Project Research

In this chapter, we will be exploring the technologies typically used in solar powered batteries as well as present fundamental information that will help influence our choices regarding parts, tools, and design choices. We will be comparing different products for certain applications and they will be primarily judged based on their functionality and cost. Other factors such as size, durability, documentation, and useability will also be considered but can be compromised when justified.

3.1 Microcontroller

There are many commercially available microcontrollers (MCUs or microcontroller units) that serve the need for both general or specific purposes. For the solar charge controller, an MCU that is low powered and able to drive an LCD to display a GUI is needed. This also means that the MCU needs to have a sufficient amount of memory and processing power to run the GUI in tandem with its core functionalities. Since the solar charge controller will be driven by PWMs, the MCU should be able to produce them. Different MCUs have varying amounts of pins that can provide PWM output. In addition, there should be enough digital I/O pins left over for everything else. It's better to overcompensate in this case since functionality can be added or changed depending on the circumstance. The Atmega, ARM, and MSP430 line of MCUs are our primary consideration since they are inexpensive, well documented, and have strong support from hobbyists and the engineering industries.

Compatibility is a major consideration when choosing the right MCU. There are different ways for the MCU to communicate with external peripherals, both wired and wireless. Our solar charge controller should be constantly receiving information about the battery and the solar panel, as well as be able to do certain operations whenever it is needed. A reliable connection is needed, so wireless communication will not be considered. The most common communication methods used in MCUs are Inter-Integrated Circuit (I2C), Serial Peripheral Interface (SPI), and Universal asynchronous receiver-transmitter (UART). MCUs tend to include at least one or more of these protocols. The MCU for this project should at least support I2C and SPI since many peripherals designed for microcontrollers depend on these protocols.

Another important factor is the programming environment for the MCU. Certain programming environments may be harder to use than others and there may be very useful tools or libraries that aren't available in certain environments. Worst case scenario, if our peripherals depend on libraries that don't exist on our MCU, we would need to reverse engineer the libraries and implement them in our own environment if the challenge is not too significant. To prevent this from happening, we must check the compatibility of each component such as the LCD with our chosen MCU.

There are other factors that may influence our choice such as the maximum current of each per I/O pin, maximum operating voltage, size, or operating temperatures. These factors are heavily dependent on our solar charge controller design and any potential conflicts can be rectified through circuit design. For example, if the maximum operating

voltage is 5V and the meter reads 6V, we can use a DC-DC converter or add resistors to lower the voltage.

3.1.1 Inter-Integrated Circuit

I2C is a synchronous two-wire serial communication bus invented in 1982 by NXP Semiconductors (formally known as Philips Semiconductor). It is primarily used by slower devices found in embedded systems [80]. The I2C bus requires that each slave device needs an address, which is obtained from NXP. The protocol is widely popular due to its simplicity and abundance in the MCU industry. Many devices designed for embedded systems use I2C. Figure 4 illustrates a typical I2C configuration.

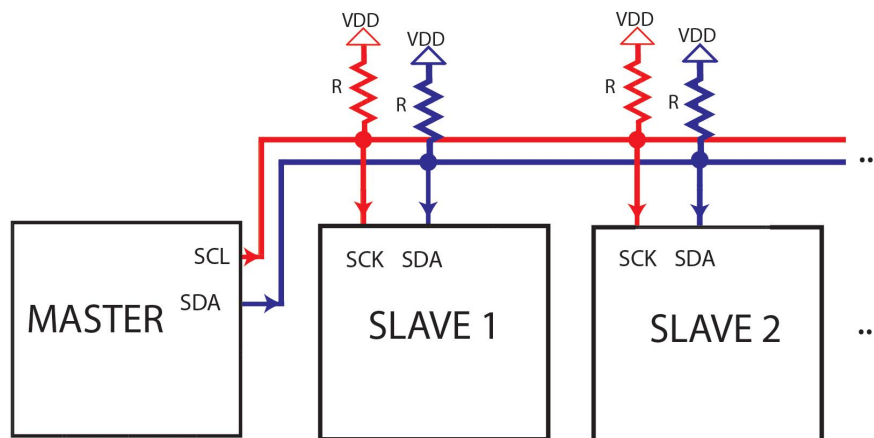


Figure 4: Typical I2C Connection

It should be noted that I2C allows for multiple different kinds of configuration such as the one illustrated in Figure 4, multiple masters existing on a single bus, or a combination of masters and slaves. Figure 4 shows that pull up resistors are connected to each wire, this is meant to set a default state for the devices, which is at high in this case. The minimum pull up resistance can be found by using this equation:

$$R_p (min) = \frac{(V_{DD} - V_{OL(max)})}{I_{OL}}, \text{ where } V_{DD} \text{ is the source shown in figure 4, } V_{OL} (max) \text{ is}$$

the maximum voltage that represents logic low and I_{OL} represents the current through the resistor. The maximum pullup resistance is limited by the bus capacitance since the I2C standard rise time may not rise to logical high before being pulled low if the resistance is too high. If the pull up resistance is too low, then the I2C pins will be unable to be driven low by the master. Most MCUs have built in pull up resistors that can be enabled or disabled.

Being that I2C is a serial communication protocol, bits are sent one at a time. The two wires in I2C are called SCL and SDA. SCL provides the clock signal to synchronize all data transfers coming from SDA. Figure 5 shows an example of transferring 8 bits of data from a slave to the master.

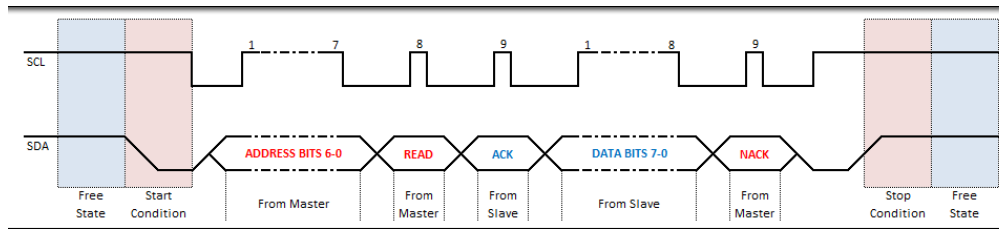


Figure 5: SCL & SDA Signals

The master will always start by sending the address bits first, then the read or write bits. The slave that has the corresponding address represented by the address bits will send an acknowledgement signal (ACK) to the master to indicate that it is ready. From figure 5, since read bits were sent, the slave is sending data to the master. After the master retrieves the data it will send a NACK signal then a stop condition to end the transfer. Figure 5 also demonstrates I2C's robustness since SCL keeps the communication between the master and slave synchronous and we also see that the master and slave let each other know when they are ready and when to stop communication. Since only one device can transmit data at a time, I2C is a half-duplex transmission mode. So we must use another protocol if we need full-duplex communication. In addition, there are some issues in regards to I2C such as the problem of sending a byte containing the 7 bit slave address and 1 bit for read and write. Some devices may need the programmer to left shift the byte by one to take account of the last bit, therefore creating confusion when the datasheet specifies the address and that address becomes a new value when it's shifted [182].

However, I2C's simplicity and ease of including additional slaves in an I2C bus makes I2C the best option to use when needing to cut down on cost and circuit complexity.

3.1.2 Serial Peripheral Interface

Like I2C, SPI is also a synchronous serial communication protocol. It was developed by Motorola in 1979, predating I2C. Unlike I2C, SPI can communicate in full duplex mode using a master device and a slave device. 3-wire and 4-wire communication can be done with SPI. A simple example of a 4-wire SPI bus is depicted in Figure 6.

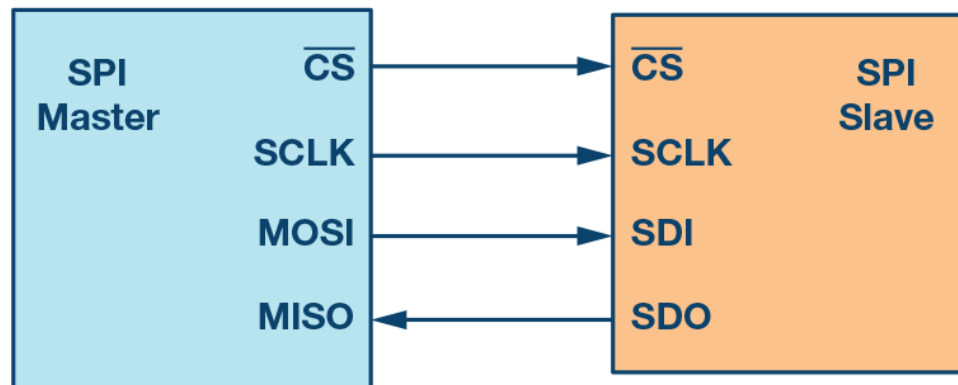


Figure 6: Typical SPI Connection

The SPI bus has four logic signals, Chip select (\overline{CS}), clock (SCLK), master out-slave in (MOSI), and master in-slave out (MISO) [52]. The \overline{CS} signal is used to select a slave device. It does not rely on using address bits to connect to a slave, rather, the \overline{CS} line uses pull-up or pull-down resistors to keep a default state then changes that state to establish the active slave. The master generates the clock signal and data transmitted between the two devices is synchronized to the generated clock SCLK.

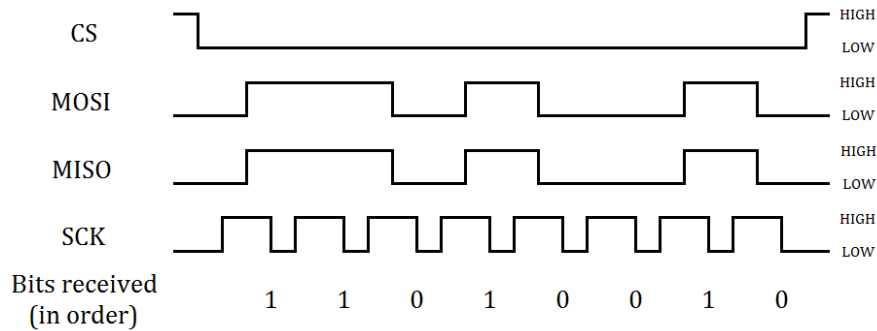


Figure 7: Example of SPI Signals

Compared to I2C, SPI devices support much higher clock frequencies [142], making it the preferable choice when speed is a consideration. MOSI and MISO are connected to the slave's serial data in (SDI) and out (SDO) lines, respectively. In I2C, one wire is used to transfer data between the master and slave. Full-duplex transmission is possible in SPI because two wires are used to transfer data between the master and slave devices.

Aside from its full-duplex capability, one of the most important aspects of SPI for this project is that SPI devices generally consume less power than I2C devices [141]. Power consumption should be minimized in the design of the charge controller, so SPI might be the best option to consider for communication at the cost of sacrificing the simplicity of I2C.

3.1.3 Universal Asynchronous Receiver-Transmitter

UART is an asynchronous serial communication circuit used by many MCUs. Depending on the definition used for "protocol," UART would not be considered a communication protocol since it is only described as being the circuit needed for transmission and receiving [Analog link, circuit basic]. There are no set rules for UART like in I2C or SPI since an external asynchronous serial protocol is needed [152]. Like I2C, it uses two wires for communication as shown in figure 8.

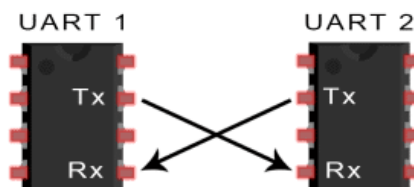


Figure 8: Typical UART Connection

However, There are actually many differences between I2C and UART despite sharing this similarity. For starters, UART supports half-duplex and full-duplex transmissions, unlike I2C which only supports half-duplex transmissions. Since UART is asynchronous, there is no clock signal to synchronous data unlike I2C. For the best compatibility, we would need to set the baud rate of the receiving and transmitting UART to be the same [124]. UART is also generally slower compared to I2C and it doesn't have flow control or data validation built in. UART relies on external protocols to do this. Circuit complexity is also low for UART, but is not suitable for connections of more than two devices [152]. Due to this, software addressing is not required unlike in I2C.

Transmission using UART involves the use of packets. Figure 9 shows what each packet consists of. The number of data bits, parity bits, and stop bits is determined by the device sending data to the UART circuits. Baud rate is also determined by the device as well.

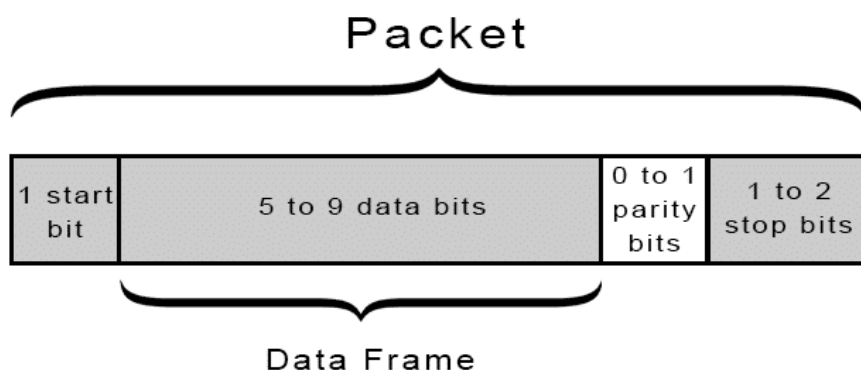


Figure 9: Contents of a UART Packet

The start bit notifies the receiving UART to start reading the bits coming from the data frame of the packet. Normally, the transmission line is held at a high voltage level. Meaning that the transmission line is pulled from high to low, similarly to how the pull up resistors operated in the I2C configuration discussed earlier. The transmission line is pulled at a low state for one clock cycle which the receiving UART will detect. The data frame contains the actual data to be sent. The number of data bits can be between 5 to 8 or 9 bits long, depending on what the parity bit is set to. The parity bit is used for error checking. While transmitting data, bits can be changed due to factors such as electromagnetic radiation, distance, or mismatched baud rates [124]. The parity bit checks the integrity of the data by counting the number of 1 bits in the data frame. If the parity was set to 0, then the receiving UART would expect an even amount of 1 bits. It would expect an odd amount of 1 bits if the parity bit was set to 1. The stop bit(s) simply signals the end of the data packet by pulling the data transmission line from low to high for one or two clock cycles.

Consideration for the use of UART will be minimal for this project. Although our MCU will most likely support it, there are already many useful peripherals that support the more reliable protocols. In addition, we would want to keep the ability to be able to scale our communication buses in the event that we need to further expand our designs.

3.1.4 Peripheral Options

Now that we have a better understanding of the communication protocols commonly used in MCUs, we can start analysing peripheral devices needed for our project that take advantage of these protocols.

Adafruit is a vendor that provides a large quantity of products specifically for MCUs. They sell many peripheral devices that range from adapters to sensors, to LCDs, and more. Adafruit primarily appeals to electronic hobbyists given that they have many tutorials and kits. This also means that their products are very affordable and are well documented. Choosing the peripherals first will give us a better understanding for what MCU we will need since we want an MCU that is compatible with the chosen parts.

3.1.4.1 1.8” TFT Display Breakout Board and Shield

One of many LCDs sold by Adafruit is a 1.8 inch thin-film-transistor display with a 128x160 screen resolution, 18-bit color depth, and two white LED backlights driven via PWM. This is technically considered a “display breakout” since an interface to communicate with the LCD is included, which uses 4-wire or 5-wire SPI. An interesting feature is that it includes a microSD card reader, so we can directly load color bitmaps from it. This feature may be helpful for designing the GUI since we can save space on the flash memory of the MCU by loading assets from the SD card instead. Only calling for those assets when needed and making memory usage efficient. In addition, we can introduce data logging features that can show helpful statistics during the debugging and testing phase of the project. In addition, the display also has a controller with its own RAM buffering so that even MCUs with low memory can drive it. According to its specifications, current draw is based on LED backlight usage, with full backlight being about 50 mA. This is reasonable enough where we can consider allowing users to adjust screen brightness directly from the GUI without worrying about severe consequences for the system in regards to power consumption and current draw.

Adafruit provided schematics for the breakout as well as EagleCAD PCBs and Arduino programming libraries that are compatible with the display. Even if we’re not using Arduino MCUs, we can port the code to different platforms. As long as our MCU has SPI, what architecture or development platform we use will not matter too much. However, it will still take some time to port the code.

3.1.4.2 2.4” TFT LCD with Touchscreen and Breakout Board w/MicroSD Socket

Another product sold by Adafruit is a 2.4 inch display that functions nearly identical to the last LCD covered. The only major difference is the touchscreen functionality. The communication method has slightly changed as well, with the breakout board being compatible with both 8-bit digital data lines or 5-wire SPI, the former being faster than 5-wire SPI.

In addition, 4 extra pins are required for the touchscreen functionality, 2 digital pins and 2 analog pins. The LCD uses a resistive touchscreen, unlike the capacitive touchscreens

that we're so used to from modern consumer touchscreen devices. This would mean that the user must apply pressure to the screen for input. How this works is that there's a flexible film layer at the very top of the screen (usually made of polyester coated with indium tin oxide) and a gap alongside another film that can create a change of voltage (which is detected by sensors) when pressure is applied as shown in figure 10.

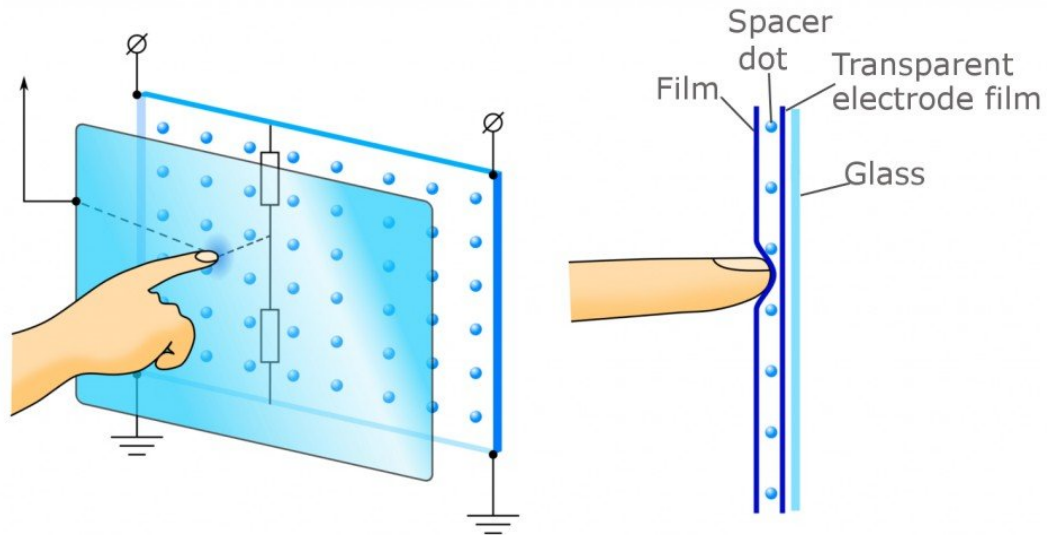


Figure 10: Resistive Touch Screen

Compared to capacitive touchscreens, resistive ones are less sensitive and are not typically designed for multi-touch sensing. They are also generally less durable compared to capacitive touchscreen and are more difficult to repair. If we were to use this for our project, the resistive touchscreens would suit our purpose just fine since our planned GUI would be simple to use and won't rely on any complicated gestures. Adafruit provides a touchscreen library for these devices and some example code to demonstrate its capabilities.

Adafruit has not given current draw specifications, but since the LCD is larger than the 1.8" inch display and also has a touchscreen, we can assume that the power consumption will be, at least, slightly higher compared to the last screen. Unfortunately, the datasheet does not contain any information about the display's power consumption. Adafruit does provide the datasheet for its TFT controller chip. According to it, the chip driver has a maximum operating voltage of 3.3V and a typical current consumption during standby mode of 100 μ A.

3.1.4.3 2.8" TFT LCD with Capacitive Touchscreen and Breakout Board w/MicroSD Socket

Yet another TFT LCD product, this 2.8" display functions just like the previous one but now has a capacitive single-touch touchscreen rather than a resistive one.

Like resistive touchscreens, there are different types of capacitive touchscreens technologies. However, they all work by taking advantage of the fact that the human body is naturally conductive.

Surface Capacitive touchscreens, for example, have four electrodes placed on each corner of the screen. When your finger comes in contact with any part of the screen, it induces current flow between the electrodes and your finger, creating a change in voltage somewhere in the screen as shown in figure 11 [54]. Sensors would detect the location of that change and interpret that input.

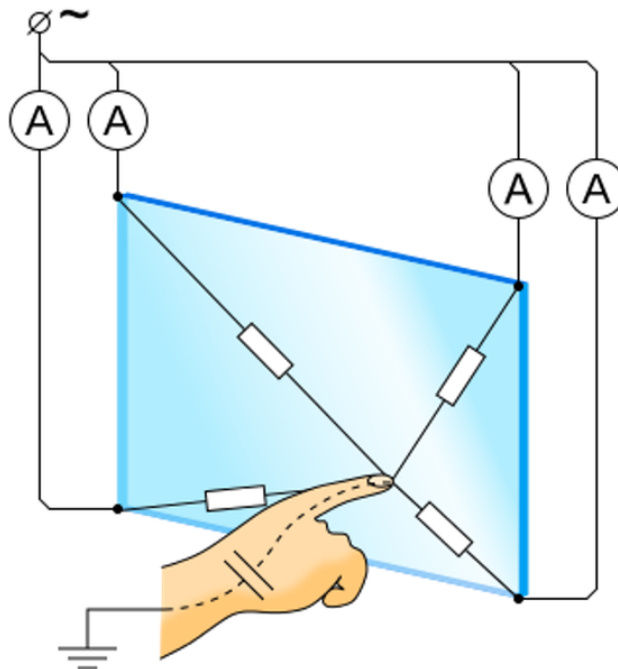


Figure 11: Capacitive Touch Screen

Capacitive touchscreens are generally more reliable, durable, and sensitive compared to resistive touchscreens. However, they do not work well when using insulators to interact with the screen, like rubber gloves. This is why you would see gloves specifically made to be used with smartphones.

Of all the LCDs covered, this one is the largest. Capacitive touchscreens usually have higher power consumption compared to their resistive counterparts. So, add the fact that this is also larger than the 2.4" touchscreen display and we have an LCD that likely has the highest power consumption. Unlike the last display, the provided datasheet is more extensive. The LCD backlight has a maximum current consumption of 80 mA and the LCD uses the same chip controller as the previous display. In addition, this LCD features a capacitive chip that is used for sensing. This chip has a maximum operating voltage of 3.6V and a typical current consumption of 2.1 mA when the operating voltage is 3.3V and the master clock is 24MHz at 25°C.

3.1.4.4 Adafruit BME280 I2C or SPI Temperature Humidity Pressure Sensor - STEMMA QT

One other peripheral that we need for our solar LIP battery is a temperature sensor. Adafruit sells many temperature sensors of varying quality and prices. Most of them have other sensors to go along with it such as a humidity sensor, altitude sensor, or pressure sensor.

Bosch's BME280 sensor is one of Adafruit's most accurate low-cost sensors for humidity, barometric pressure, and temperature. We're only interested in the product's temperature sensing capabilities, so the other sensors will be ignored. The temperature sensor is accurate within $\pm 1.0^{\circ}\text{C}$ and has an operating range of -40°C and $+85^{\circ}\text{C}$, which are good enough for our project. According to the sensor's datasheet, the typical current consumption is $1.0\mu\text{A}$ at 1 sample/second for only temperature sensing and $0.1\mu\text{A}$ when the device is in sleep mode. They didn't give any maximum current values, however, they did give us a typical current value of $350\mu\text{A}$ (or $.350\text{mA}$) when the device is at 85°C . Regardless of usage and condition, this device is very low powered.

The BME280 also supports SPI and I2C, which gives us greater flexibility in regards to wiring our devices. The sensor is mounted on the PCB with a 3.3V regulator to make it compatible with 3V or 5V input typically found in MCUs. In addition, the board is compatible with STEMMA QT connectors for easy I2C use when JST PH connectors are too large. Adafruit has provided drivers to be used with MCU's.

3.1.4.5 MCP9808 High Accuracy I2C Temperature Sensor Breakout Board

A cheaper alternative and one solely dedicated for our needs is the MCP9808 sensor. It has an operating temperature between -40°C and $+125^{\circ}\text{C}$ with a typical accuracy within $\pm 0.25^{\circ}\text{C}$. Its maximum current draw is $5\mu\text{A}$ and it can convert $0.25^{\circ}\text{C}/\text{bit}$ in 65 ms at 15 samples/sec. The sensor supports higher precision, upto $\pm 0.0625^{\circ}\text{C}$, but with slower conversion time.

It exclusively uses I2C which is a downside in terms of versatility, but it more than makes up for it by having higher precision, a smaller form factor, and a much cheaper price compared to the last sensor. Just like the last sensor, Adafruit has provided Arduino and Python/CircuitPython code for this board.

3.1.5 Pulse Width Modulation

One feature that is common amongst MCUs is the ability to generate PWMs. Since our charge controller and LCD's backlight will be driven by PWMs, we definitely need an MCU that can generate them. Most MCUs can do this, but they all vary with the number of pins that can generate PWMs. Before exploring requirements regarding PWMs, we should know more about them.

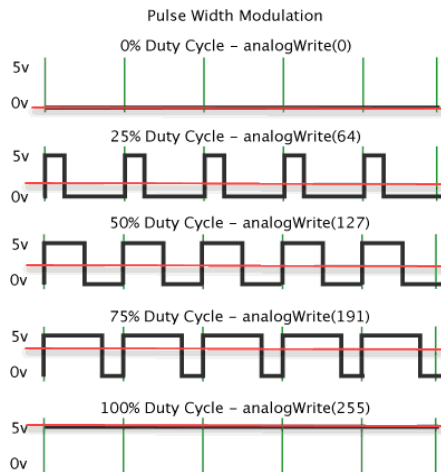


Figure 12: PWM Waveform by Duty Cycles

Figure 12 shows the waveforms of typical PWMs. Duty cycle refers to the ratio of the waveform being high to the waveform being low per period. For example, the 75% duty cycle waveform shows the wave being high 3/4th of the time per period. The most notable waveforms are the 0%, 50%, and 100% duty cycle waves. We can see that at 0% duty cycle, the wave is always low during its period and always high at 100% duty cycle. When the duty cycle is set to 50%, we see the wave being high at half a cycle and low for the other half, in other words, a square wave. A light bulb driven by PWM is constantly turning on and off, but if the rate is high enough, we wouldn't be able to notice the change that is occurring.

PWMs can be used to convert analog signals to digital signals [70]. Digital devices and analog devices often work together in many applications that require analog input to be interpreted by digital devices such as sound, radio waves, imaging, etc. Driving analog signals to digital devices can lead to unpredictable results and can even damage these devices due to issues like overheating. Digital computers are often used to process data, including those from analog sources. If we need to represent analog signals in digital devices, PWMs can be used to approximate analog signals through the process of quantization and coding [3]. Quantization is the process of mapping a large set of values into a smaller set and coding involves assigning a unique binary value to each quantization level.

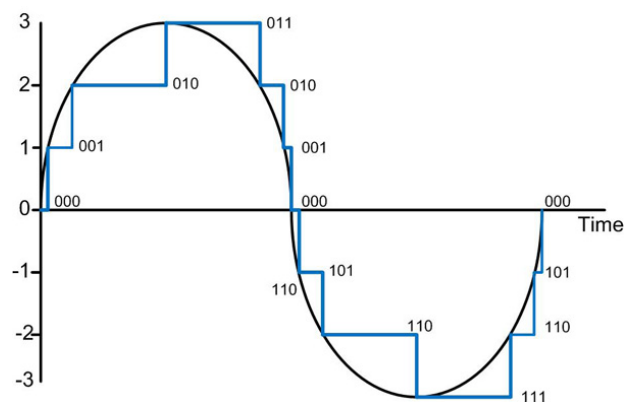


Figure 13: Analog to Digital Conversion

Obviously, the quantized signal cannot ideally represent analog signals as shown in Figure 13. The difference between the analog signal and the closest digital value at each sample is called the quantization error, which can lead to noise called quantization noise. There are ways to reduce quantization noise with some examples being oversampling and dithering.

Devices driven by PWMs will experience the average voltage of the PWM wave. The average voltage, if the trough is 0V, is calculated by multiplying the peak voltage value by the duty cycle, $V_{avg} = Duty\ Cycle * V_{pk}$. Changing the duty cycle will change the average voltage which can result in behavioral changes from the device being driven. For example, an LCD's backlight can become dimmer or brighter depending on the PWM's duty cycle, assuming voltage stays the same. Since the charge controller is driven by PWMs, this means that we can control the current going into the battery by changing the duty cycle.

3.1.6 Microcontroller Options

Now that each of the characteristics of the microcontroller we are searching for have been discussed, this section will be used to summarize characteristics of different battery options. These summarizations will be used to compare each option, and provide a basis for our microcontroller choice.

3.1.6.1 Atmega2560

The Arduino brand is known for having some of the most popular MCUs in the market. This is especially true for their Arduino UNO and because of its popularity, vendors like Adafruit sell devices meant to be used by the UNO alongside its contemporaries like the MSP430 MCUs or other Arduino boards. However, as long as the MCU has the necessary protocols to connect to the devices properly, it does not matter which MCU one uses.

Although the UNO is great for hobbyists, its 32 KB of flash memory and 2 KB of SRAM may not be enough for our planned GUI. The Arduino Mega, which uses an ATmega2560, retains the low power features of the UNO while increasing its flash memory from 32 KB to 256 KB (minus 8KB due to the bootloader) and increasing the SRAM from 2KB to 8KB. In addition, the Mega has 54 Digital I/O pins and 16 analog pins as well as SPI, UART, and TWI (Two-Wire Interface) capabilities. TWI can be used with I2C compatible devices since they are very similar. It was introduced by Atmel to avoid legal issues at the time since I2C was a registered trademark name [1]. There are only minor differences that shouldn't have an impact in the project. Interestingly, the MCU supports USART (Universal Synchronous and Asynchronous Transmitter) which supports both Asynchronous and Synchronous operations. The board is also reasonably priced at around \$40, around double the price of the UNO.

According to the MCU's datasheet, the maximum operating voltage is 6.0V, each I/O pin draws 40.0mA of DC current, and the V_{CC} (the pin that supplies power to the board) and GND pins draw 200.0mA. These are the absolute maximum ratings and, most likely,

power consumption is much lower on average. Regardless, we should be looking at the maximum ratings to anticipate the worst case scenario. The MCU has a maximum clock speed of 16 MHz, like the UNO, and can perform 16 MIPS (million instructions per second) at that clock speed.

We're also interested in looking into each MCU's low power/sleep modes since we will want to take advantage of them to save as much power as possible. Certain modes will deactivate certain modules and even the CPU. Figure 14 shows the MCU's modes as well as their active clock domains and wake-up sources, the figure is taken from the MCU's datasheet.

| Sleep Mode | Active Clock Domains | | | | | Oscillators | | Wake-up Sources | | | | | | |
|------------------------|----------------------|----------------------|-------------------|--------------------|--------------------|---------------------------|-------------------|-----------------------|-------------------|------------------|------------------|-----|---------------|-----------|
| | clk _{CPU} | clk _{FLASH} | clk _{IO} | clk _{ADC} | clk _{ASY} | Main Clock Source Enabled | Timer Osc Enabled | INT7:0 and Pin Change | TWI Address Match | Timer2 | SPM/EEPROM Ready | ADC | WDT Interrupt | Other I/O |
| Idle | | | X | X | X | X | X ⁽²⁾ | X | X | X | X | X | X | X |
| ADCNRM | | | | X | X | X | X ⁽²⁾ | X ⁽³⁾ | X | X ⁽²⁾ | X | X | X | |
| Power-down | | | | | | | | X ⁽³⁾ | X | | | | X | |
| Power-save | | | | | X | | X ⁽²⁾ | X ⁽³⁾ | X | X | | | X | |
| Standby ⁽¹⁾ | | | | | | X | | X ⁽³⁾ | X | | | | X | |
| Extended Standby | | | | | X ⁽²⁾ | X | X ⁽²⁾ | X ⁽³⁾ | X | X | | | X | |

Note: 1. Only recommended with external crystal or resonator selected as clock source.
 2. If Timer/Counter2 is running in asynchronous mode.
 3. For INT7:4, only level interrupt.

Figure 14: Sleep Modes for the Atmega2560

According to figure 14, the MCUs active clock domains are clk_{CPU}, clk_{FLASH}, clk_{IO}, clk_{ADC}, and clk_{ASY}. What this means is that during the appropriate mode, the clocks that have crosses under them are the ones that are active. The same logic also applies to the other modules in the figure, such as the timer oscillator oscillator only being active in modes that are using Timer2. In Idle mode, the MCU has everything active but the CPU and halting clk_{FLASH}. What are active in this mode are the SPI, USART, Analog Comparator, ADC, 2-wire Serial Interface, Timer/Counters, Watchdog, and the interrupt system. If we were to use this mode for our project, this would allow every part of the charge controller but the LCD to function since the devices that are connected to the MCU can, individually, operate by themselves. The low power modes should be used when only certain devices are operating at a given time so that we can deactivate parts of the MCU to save power. Unfortunately, the datasheet does not provide any statistics on the Atmega 2560's power consumption, but people have done research on this matter. When the Arduino Mega ran an infinite loop and a Fibonacci series program, separately, it had a current consumption of around 80 mA [96].

One of the biggest appeals of this MCU is the number of pins available. Its 54 digital I/O pins and 16 analog inputs can leave room for expansion or redesigning for most projects including this one. 15 of those digital I/O pins can provide PWM outputs. Unfortunately, having so many pins on one board means that it is one of the larger boards and its power

consumption is higher compared to many other MCUs. The PWM outputs can reach a maximum value of $V_{CC} + 0.5V$. This value also represents the maximum voltage on any pin except for the RESET pin according to the datasheet. Our battery and solar panels are rated much higher than V_{CC} and, somehow, our MCU needs to take these voltages as input to measure the voltage across the components. The solution for this is to use voltage dividers which will be explored further in chapter 5.0.

3.1.6.2 ATSAM21G18 ARM Cortex M0+

The Adafruit METRO M0 Express uses the 32-bit ATSAM21G18 ARM Cortex M0+ MCU. When referring to bits, it means the number of data pins that a CPU/MCU has and how wide the CPU's registers can be, in which this MCU has 32 data pins and 32-bit wide registers. In comparison, the Atmega2560 is an 8-bit CPU despite it having many more pins compared to the ATSAM21G18. The reason for this is that the Atmega2560's data pins are divided into 8-bit ports, with the exception of port G being a 6-bit I/O port. Unfortunately, with the METRO M0 Express, we do not have access to all the data pins individually since many of them are already allocated to ports such as the USB port. With the number of data pins available to the user, we can essentially think of this product as an upgraded Arduino UNO. The ATSAM21G18 is compatible with the CircuitPython programming language as well as the Arduino IDE since it uses the same MCU as the Arduino Zero. Since the METRO M0 and the Arduino Zero use the same MCU, the decision of getting one over the other will most likely boil down to availability. As of the time of this writing, the Arduino Zero is discontinued. The smaller Arduino MKR ZERO is currently available but it is more limited compared to the METRO and Zero despite having the same MCU. It supports SPI and UART like the Atmega2560 as well as the official I2C protocol which guarantees 100% compatibility with I2C devices unlike TWI. When referencing the datasheet, we're looking at figures for the 'A' variant of the devices (also known as the default variant) since those are what's on the METRO M0.

This MCU features 256KB of flash memory and 32KB of SRAM. In addition, this MCU also has a 2MB SPI flash chip which we can store data in. Compared to the previous MCU, it has four times the SRAM and retains a form factor that is similar to the Arduino UNO. The METRO Express has 25 GPIO pins, 12 of which are analog in pins. Since the MCU has a digital to analog converter, there's a pin dedicated for analog output.

According to its datasheet, the MCU requires a 3.3V power supply for every feature of the device to be operable and has a maximum absolute rating of 3.8V, unlike the Atmega's 6V. The MCU also has a maximum clock frequency of 48 MHz, which is 3 times higher compared to the previous 16 MHz clock speed that the Atmega has. The high clock speed may be beneficial for tasks that require the CPU such as drawing the GUI or datalogging, but higher frequencies will draw more power. Figure 15 shows the current consumption when the MCU is in ACTIVE mode and for different test cases.

| Mode | Conditions | T _A | Min. | Typ. | Max. | Units |
|--|--|----------------|----------------|----------------|--------------------------|--------------------------|
| ACTIVE | CPU running a While(1) algorithm | 25°C | 3.11 | 3.37 | 3.64 | mA |
| | | 85°C | 3.24 | 3.48 | 3.76 | |
| | CPU running a While(1) algorithm V _{DDIN} =1.8V, CPU is running on Flash with 3 wait states | 25°C | 3.10 | 3.36 | 3.64 | |
| | | 85°C | 3.24 | 3.48 | 3.75 | |
| | CPU running a While(1) algorithm, CPU is running on Flash with 3 wait states with GCLKIN as reference | 25°C | 60*freq + 74 | 60*freq + 136 | 62*freq + 196 | μA (with freq in MHz) |
| | | 85°C | 62*freq + 154 | 62*freq + 228 | 62*freq + 302 | |
| | CPU running a Fibonacci algorithm | 25°C | 4.12 | 4.53 | 4.92 | mA |
| | | 85°C | 4.27 | 4.63 | 4.98 | |
| | CPU running a Fibonacci algorithm V _{DDIN} =1.8V, CPU is running on flash with 3 wait states | 25°C | 4.12 | 4.53 | 4.92 | |
| | | 85°C | 4.27 | 4.63 | 4.98 | |
| | CPU running a Fibonacci algorithm, CPU is running on Flash with 3 wait states with GCLKIN as reference | 25°C | 86*freq + 76 | 88*freq + 136 | 88*freq + 196 | μA (with freq in MHz) |
| | | 85°C | 88*freq + 156 | 88*freq + 230 | 88*freq + 302 | |
| CPU running a CoreMark algorithm | 25°C | 5.78 | 6.32 | 6.80 | mA | |
| | 85°C | 5.93 | 6.47 | 7.00 | | |
| CPU running a CoreMark algorithm V _{DDIN} =1.8V, CPU is running on flash with 3 wait states | 25°C | 5.17 | 5.60 | 5.96 | | |
| | 85°C | 5.35 | 5.73 | 6.10 | | |
| CPU running a CoreMark algorithm, CPU is running on Flash with 3 wait states with GCLKIN as reference | 25°C | 106*freq + 78 | 106*freq + 136 | 108*freq + 196 | μA (with freq in MHz) | |
| | 85°C | 106*freq + 154 | 108*freq + 232 | 108*freq + 310 | | |

Figure 15: Current Consumption in ACTIVE mode

We can see from the figure that the current consumption depends on the computational complexity of an algorithm. The current consumption also varies on the frequency that the clock is set to (GCLK selects a clock source which could be the main clock source) as well as the operating voltage. In general, the figure shows the current consumption maxing out at around 7 mA. The major takeaway from the table is that the current consumption of the ATSAM21G18 is much less compared to the Atmega 2560, even when running the same Fibonacci and infinite loop algorithm.

However, the current that each I/O pin can supply will likely be less than what the Mega can supply. According to the technical specs available in the arduino website, the Arduino Zero's maximum current supply for each DC I/O pin is 7 mA. Much less compared to 40 mA current supply from the Mega. Since the Arduino Zero uses the same MCU as the METRO, the latter also having the same current supply would be a fair assumption. The ATSAM21G18 datasheet corroborates this by showing that the Output high-level current from the I/O pins maxing out at 7 mA. The I/O pins can provide either a maximum of 2mA or 7mA current, depending if the Output Driver Strength bit flag is set to 0 or 1, respectively.

There are two low power modes, Idle and Standby, but three levels within idle mode. Figure 16 is a table taken from the MCU's datasheet and it shows its sleep modes and their active components.

| Sleep Mode | CPU Clock | AHB Clock | APB Clock | Oscillators | | | | Main Clock | Regulator Mode | RAM Mode |
|------------|-----------|-----------|-----------|--------------|------------|------------------|------------------|------------|----------------|-----------|
| | | | | ONDEMAND = 0 | | ONDEMAND = 1 | | | | |
| | | | | RUNSTDBY=0 | RUNSTDBY=1 | RUNSTDBY=0 | RUNSTDBY=1 | | | |
| Idle 0 | Stop | Run | Run | Run | Run | Run if requested | Run if requested | Run | Normal | Normal |
| Idle 1 | Stop | Stop | Run | Run | Run | Run if requested | Run if requested | Run | Normal | Normal |
| Idle 2 | Stop | Stop | Stop | Run | Run | Run if requested | Run if requested | Run | Normal | Normal |
| Standby | Stop | Stop | Stop | Stop | Run | Stop | Run if requested | Stop | Low power | Low power |

Figure 16: Sleep Modes for ATSAMD21G18 ARM Cortex M0

The AHB and APB clocks refer to clock signals for the Advanced High-performance Bus and the Advanced Microcontroller Bus Architecture (AMBA) Advanced Peripheral Bus. AHB and APB are part of the de facto standards introduced by ARM. AHB is a protocol that was introduced to AMBA revision 2.0 and was made to accommodate the high performance designs that require large bandwidth. It introduced features such as split transactions, wider data bus configurations, and single-cycle bus master handover. Figure 17 shows the devices that can be interconnected with the AHB.

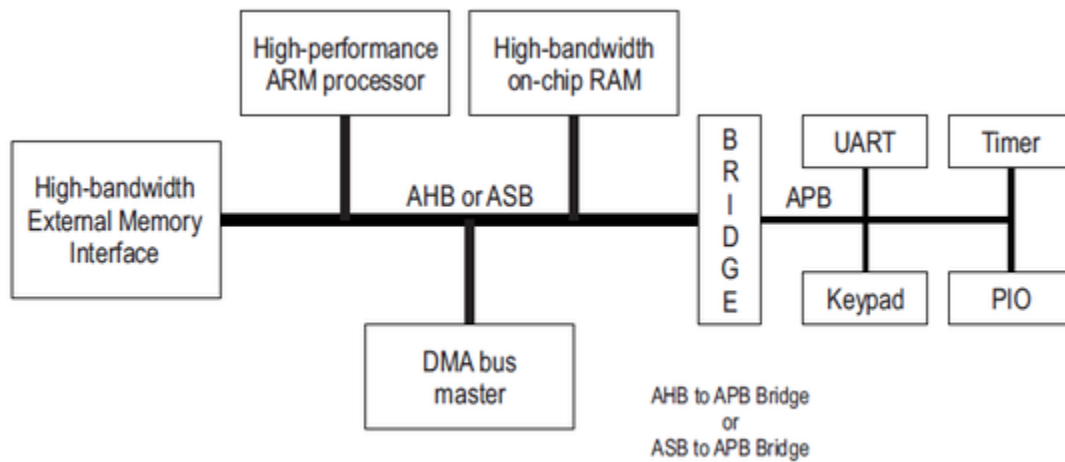


Figure 17: AHB & APB Architecture

Devices that use low bandwidth protocols such as UART, I2C, or SPI are connected to the APB [130]. The APB is optimized for minimal power consumption and reduced interface complexity. Due to the use of the AHB-APB bridge, devices in the AHB domain can communicate with the devices in the APB bridge. Since the CPU does not need to run while the AHB or APB clock is active, slave devices that are connected to those buses will be able to communicate and take advantage of the high speed benefits while in low power modes. Sleep modes Idle 0 and Idle 1 allow this to happen. This MCU also supports USART.

Although the MCU has an operating voltage of 3.3V, the METRO M0 features a 5V pin. This is because the board features onboard regulators that take the USB or DC power and convert it to 3.3V and 5V for the 3.3V pin and 5V pin. In addition, higher DC voltage can be applied and that voltage will be provided for the Vin pin. This is in the case of using a DC Jack, which can be between 6V-12V. The current draw between the 5V and 3.3V pins can be upto 800mA (if using DC Jack, 500mA if using USB) and 2A for Vin. We're not limited to just using 3.3V to power our device and the relatively large current draws will allow us to connect a good number of components and peripherals for the charge controller to our MCU.

One feature that the METRO M0 lacks is an electrically erasable programmable read-only memory (EEPROM). An EEPROM would allow us to store information even after the board shuts off, like flash memory. However, flash memory is less reliable when it comes to storing changing values compared to EEPROM since, according to the Atmega2560 MCU's datasheet, EEPROM has an endurance of at least 100,000 write/erase cycles while flash memory is 10 times less than that. Instead, as previously mentioned, the METRO M0 comes with a 2MB SPI Flash chip which is separate from its 256KB flash memory. According to Adafruit, the SPI Flash chip can be used for storage like an SD card for example. Again, it is flash memory so it is not as durable as EEPROM, but Adafruit mentioned that it is suitable for applications such as datalogging just like an SD card would be. We do get 2MB of memory, which is far more substantial than what you would typically get from a built in EEPROM. Besides, 10,000 write/erase endurance should be more than enough just for this project and there's no plans to introduce information that needs to be stored and changed while the program is running and while the MCU is shut off. The MCU also has the ability to emulate EEPROM using flash memory. There are different algorithms that exist to emulate EEPROM, but they all involve minimizing write/erase operations on specific sectors by setting up data structures to store data at different sectors at a time. For example, Patent US7058755B2 uses an EEPROM emulation method that stores data to sets of contiguous memory and calculates the location of an address by using read and write offsets and adding one of them to a base address. According to the MCU's data sheet, the EEPROM emulator uses paging for memory management. The amount of memory needed depends on certain configurations. The datasheet shows some example parameters and their results. Figure 18 shows that when the page size is 64 bytes and the available memory is 256KB, 4096 pages can be created.

| Device | Flash size | Number of pages | Page size |
|-----------|------------|-----------------|-----------|
| SAMD21x18 | 256 Kbytes | 4096 | 64 bytes |

Figure 18: Number of Pages According To Datasheet

If this feature can be used on the SPI flash chip, it would allow for more reliable data logging at the expense of some memory.

The MCU also features a 32-bit Real-Time Counter (RTC) that allows the MCU to continuously keep track of time. It can allow the programmer to use various wake up mechanisms but one of its most useful features is its clock/calendar mode. When a 1 Hz clock signal is selected and when CTRL.MODE is two, the RTC can write and read

values to the Clock Value register in a 32-bit time/date format. The time can be represented using the 12- or 24- hour format, which is configurable in the Control register. Dates can be represented using values representing the month, day, and year. The month is represented with values from 1 through 12, January through December. The day is represented using numbers from 1 through 31. The year is defined as an offset with reference to the year defined in software. 6 bits can be used to represent the year, meaning that we only have values from 0 through 63. Since the overflow flag is set when 63 rolls back to 0, we can define the year to be 2021 + year and add 64 to the reference value everytime the overflow occurs. The RTC also takes leap years into account and months ending with different days.

3.1.6.3 MSP430 LaunchPads

Texas Instruments provide their own line of low cost and low powered MCUs under the MSP430 brand. We will be focusing on their LaunchPad development kits since they provide all the necessary tools onboard for development. To expand on this, MCUs without being on a board are typically cheaper and there are more variety of MCUs to choose from as well as having more freedom when designing projects. One of the biggest issues of doing this is finding a way to flash the MCU since they wouldn't have a JTAG emulator or some other programmer interface out of the box. We would then need to set up the MCU such that we can connect the JTAG emulator to it and the PC. We would also need to buy the necessary parts and equipment to do things that are already featured on many MCU boards. Given our time constraints and the need to keep expenditures low, we're only interested in MCU's that are already on a development board such as the LaunchPad lineups.

One of their basic models is the MSP-EXP430G2ET. Given that these boards are developed by Texas Instruments, one of the largest and oldest semiconductor manufacturers in America, their documentation is extensive and they have many useful tools specifically designed for the MCUs. The LaunchPad comes with the MSP430G2553 MCU, however, users are able to swap out the MCU and replace it with a compatible MSP430G2xx2, MSP430G2xx3, or MSP430F20xx MCU due to its 14-/20-pin DIP socket. Making it one of the cheaper development boards on the market. This design gives the user extra freedom to choose the right MCU for the job. The MSP430G2553 is a 16 MHz 16-bit MCU that has 16KB of flash memory and 512B SRAM. Compared to the previous MCUs, this one has the least amount of memory. Even the Arduino UNO has more memory, 32KB of flash memory and 2KB of SRAM. The amount of memory in the MCU could be too restricting for our GUI. It is possible that we may need to upgrade the MCU, but the highest spec part, in terms of memory, that is compatible with the LaunchPad is the MSP430G2553 MCU. According to the table of supported devices in the datasheet, the MSP430G2xx3 family of MCUs contain the most memory from the list. The MSP430F2012 contains only 2KB of flash and 128B of SRAM. The 128B of SRAM is much less compared to the 32KB of SRAM available in the METRO M0 Express or the 8KB of SRAM in the Arduino Mega. The MCU supports UART, SPI, and I2C just like the previous two MCU covers.

The main appeal of the MSP430 MCUs is their power efficiency. According to the absolute maximum ratings of the MSP430G2553, the "diode current" at any device pin is

only +/- 2 mA. At 1MHz with an operating voltage of 2.2V in “active mode”, the MCU only draws around 230 μ A. At “Standby Mode” the MCU draws around 0.5 μ A. This is the lowest powered MCU covered yet and it would be an excellent MCU to use in a project involving solar energy. Figure 19 shows the low power modes available for the MCU. There are 5 low power modes, making the available options just as extensive as the Arduino Mega. According to the chart, in all low power modes the CPU is disabled, the oscillator may or may not be disabled, and certain or all of the clocks are disabled in each one. This is to be expected since the other MCUs with low power modes behave this way as well. What’s unique to the MSP430 is the enabling and disabling of the DCO and its DC generator, which allows the MCU to wake-up from low-power modes in less than 1 μ s.

| SCG1 | SCG0 | OSCOFF | CPUOFF | Mode | CPU and Clocks Status |
|------|------|--------|--------|--------|---|
| 0 | 0 | 0 | 0 | Active | CPU is active, all enabled clocks are active |
| 0 | 0 | 0 | 1 | LPM0 | CPU, MCLK are disabled, SMCLK, ACLK are active |
| 0 | 1 | 0 | 1 | LPM1 | CPU, MCLK are disabled. DCO and DC generator are disabled if the DCO is not used for SMCLK. ACLK is active. |
| 1 | 0 | 0 | 1 | LPM2 | CPU, MCLK, SMCLK, DCO are disabled. DC generator remains enabled. ACLK is active. |
| 1 | 1 | 0 | 1 | LPM3 | CPU, MCLK, SMCLK, DCO are disabled. DC generator disabled. ACLK is active. |
| 1 | 1 | 1 | 1 | LPM4 | CPU and all clocks disabled |

Figure 19: Sleep Modes for MSP430G2553

The reason as to why the LaunchPad is up for consideration is because every member of the team has some familiarity with the MSP430 MCUs due to a required class for CpE and EE majors that uses the MSP430 for lab work and studies. Using this board would only just require a refresher. However, what we know about the MSP430 MCUs can also be applicable for the other MCUs since many MCUs in the market have similar features. The Atmega MCUs also have documentation that rivals TI’s counterpart and its support in terms of libraries and tools may even surpass TI thanks to its ubiquity amongst the hobbyists. The METRO M0 uses the same MCU as the discontinued Arduino Zero and the Arduino MKR ZERO, so it also shares the same resources as those boards. In addition, it also supports CircuitPython which Adafruit provides documentation for.

3.1.7 Chosen Parts

Now that all the considered devices were covered in detail, we need to choose the most suitable parts based on our requirements and their features. To summarize, we need a low-powered MCU that is able to drive a temperature sensor, an LCD display with a GUI, and our charge controller with PWMs. We also need a high accuracy and low powered temperature sensor that utilizes the same communication protocols as our MCU and a full colored, low power LCD that can communicate with our MCU and display our GUI. Table 3 shows the decisions that were made and our reasons.

| Parts | Part Chosen | Reasons |
|---|--|---|
| <p><u>Temperature Sensors</u></p> <ol style="list-style-type: none"> 1. Adafruit BME280 I2C or SPI Temperature Humidity Pressure Sensor - STEMMA QT 2. MCP9808 High Accuracy I2C Temperature Sensor Breakout Board | MCP9808 High Accuracy I2C Temperature Sensor Breakout Board | This part has a higher accuracy compared to the Adafruit BME280, is less expensive, and is solely used for temperature sensing. The extra features, besides being able to use SPI and I2C, from the BME280 are useless for this project. |
| <p><u>Displays</u></p> <ol style="list-style-type: none"> 1. 1.8" TFT Display Breakout Board and Shield 2. 2.4" TFT LCD with Touchscreen and Breakout Board w/MicroSD Socket 3. 2.8" TFT LCD with Capacitive Touchscreen and Breakout Board w/MicroSD Socket | 2.8" TFT LCD with Capacitive Touchscreen and Breakout Board w/MicroSD Socket | We decided to use an LCD touchscreen for this project, but we had to make a decision between capacitive or resistive touch screens. We believe that a capacitive touch screen is best for this project since we want our product to feel modern. Most modern devices that use a touchscreen have capacitive touchscreens. It's about \$10 more than the resistive touchscreen and is slightly larger, but we feel that it's worth it. |
| <p><u>Microcontrollers</u></p> <ol style="list-style-type: none"> 1. Atmega 2560 (Arduino MEGA) 2. ATSAM21G18 ARM Cortex M0 (Adafruit METRO M0 Express) 3. MSP430G2553 (MSP430 LaunchPads) | ATSAMD21G18 ARM Cortex M0 (Adafruit METRO M0 Express) | This MCU is more capable than the others while also consuming less power than the Atmega 2560. It has less I/O pins than the 2560, but it already has plenty enough for this project. The MSP430 line is too restrictive in regards to memory. It also has a reasonable \$24.95 price and we can create a fairly sophisticated GUI with it. |

Table 3: Selected Parts and Reasons

3.2 Solar Panels

NOTE: We will be focusing on the three main types of solar panels, monocrystalline, polycrystalline, and amorphous. Before diving into the different types of solar panels and their functions, it is important to understand the science behind them first. A solar panel is not just one single piece. In actuality, it is many pieces acting together as one. Each of these pieces on a solar panel are called photovoltaic or solar cells. Photovoltaic simply means the ability to convert sunlight into electricity. This concept was first discovered by a French scientist known as Edmund Becquerel in 1839. He was able to realize that some materials produced energy when exposed to sunlight. With that definition, these photovoltaic cells do just that. These cells are most commonly developed with materials that are used to make semiconductors such as silicon. The reasoning behind using semiconductive materials such as silicon is due to the material's unique property of not only conducting electricity, but also its ability to simultaneously create an electric field. This ability these photovoltaic cells have to create an electric field is from the speciality treating process of the silicon wafer that the cells come from. This process is complex, and thus needs explaining. [65,72,74]

To begin, the silicon wafer first has to be cut very precisely. These cuts previously mentioned are by a method known as slurry sawing. Slurry sawing is a technique used when sawing precious materials where a high amount of precision is needed. These saws use high strength, high tension wires alongside what is known as "slurry." These wires can be as small as 250 micrometers. "Slurry" is a wet substance that is combined with particles such as diamond or silicon carbide. When turned on, the wires move back and forth at an exceptional rate over the substrate of the material being cut which creates friction between the substrate and the particles of the slurry, thus cutting the material. Slurry sawing leaves behind contaminants and imperfections on the surface of the cut material. Each of the aspects can be seen in figure 20 below. In figure 20 (a), one can see the zoomed in surface of a cut silicon wafer after slurry sawing. At this scale, it is easy to see the previously mentioned imperfections caused by slurry sawing. In figure 20 (b), the possible contaminants left behind by the slurry sawing process can be seen. After the slurry sawing has been completed and a silicon wafer has been obtained, the treatment process has to begin. [93,94,99,101]

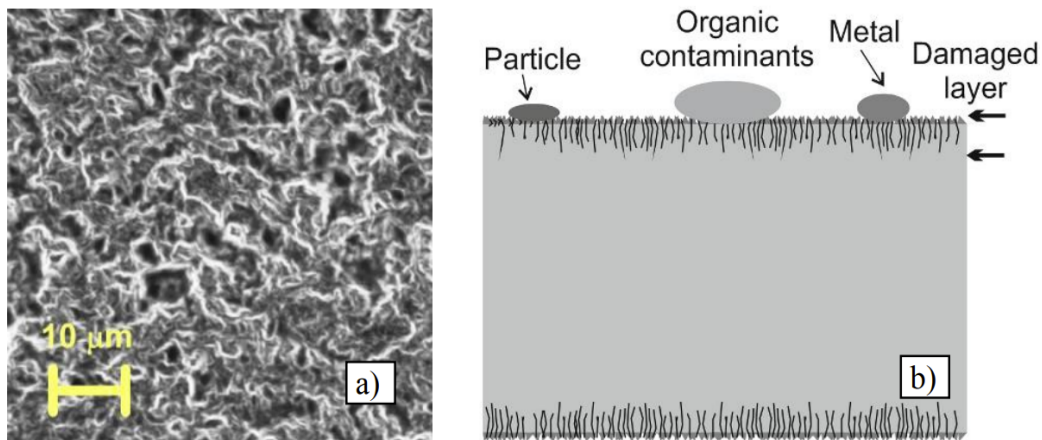


Figure 20: Silicon Wafer After Slurry Sawing

The first part of the treatment process of the silicon wafer for solar cells after it has been cut is known as texturing or etching. This process of texturing is used to remove any damaged layers on the surface of the silicon wafer from the slurry sawing process alongside creating what are known as micro pyramids (see figure 21 below for detail). These micro pyramids give the wafer texture which allows for the ability for the wafer to capture more light to increase the efficiency of the photovoltaic cell. There are many ways this texturing process can be executed. The texturing process can be physical or chemical, and either wet or dry. Alongside each of these processes, it's important to understand the difference between isotropic and anisotropic texturing. Each of these processes play an important role in physical and chemical texturing. [173]

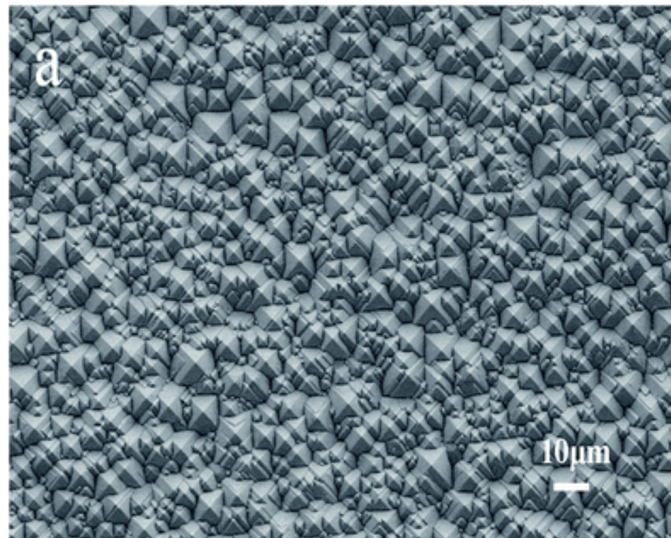


Figure 21: Textured Silicon Surface

Isotropic texturing is a process focused on removing imperfections created by the slurry sawing process, and what is known as chemical polishing. With this texturing process, the texturing rate is the same and due to its nature, this process is used in chemical texturing, and not in physical texturing. Anisotropic texturing is focused on the actual texturing of the silicon wafer to create the previously mentioned micro pyramids. Unlike isotropic texturing, this process is used alongside physical texturing as well as chemical texturing.

Physical texturing is a dry process in which the surface material of the wafer is removed by what is known as ion bombardment. This ion bombardment is delivered in the form of plasma. There are a few aspects of this method to consider. First off, this method has a low etch rate because the silicon wafer is being etched one atom at a time per each ion bombardment. Additionally, this is the only texturing process that can remove non-volatile contaminants from the substrate's surface. Due to the nature of this process, it is used in conjunction with anisotropic texturing only as discussed above.

Chemical texturing is a process that can either be wet or dry. It is performed using chemicals such as potassium hydroxide (KOH), or sodium hydroxide (NaOH) alongside additive chemicals such as isopropyl alcohol and sodium carbonate (Na₂CO₃). Other

additive chemicals include, but are not limited to potassium carbonate (K_2CO_3), sodium phosphate (Na_3PO_4) and deionized water. Of these substances/chemicals, the most commonly used in industrial solar cell texturing are sodium hydroxide, isopropyl alcohol and deionized water. Similar to physical texturing, there are a few aspects to consider with chemical texturing. Like previously mentioned, this method works alongside both isotropic and anisotropic texturing. Unlike physical texturing, chemical texturing has a very high texture rate.

Once this texturing process is finished, the other main aspect of preparing a silicon wafer to become a solar cell, is the need for an electric field to be present. Solar cells are composed of two thin layers. One layer is positively charged, and the other layer is negatively charged. Each of these layers is charged by adding an additional material to each layer. One example of an additive material that creates a negative charge by adding on to the layer of semiconductor material is phosphorus. In the opposite case, an example of an additive material that creates a positive charge when added to the layer of semiconductor material is boron. Having these opposite charges for each layer creates an electric field in between the space in the layers of the semiconductor material. As such, electrons are trapped in this electric field. When light hits the semiconductor material, the light essentially displaces the electron and frees it from the electric field. This freeing of electrons in conjunction with an electrical wire connected to the additive materials on both layers of the solar cell creates an electrical DC current by completing the circuit. From this, these solar cells are wired together thus increasing the supply of the aforementioned electrical DC current. This connection of solar cells can be used to make a standard solar panel. Additionally, anti reflective material is sometimes added to the solar cells in order to absorb more sunlight due to the apparent loss of it from light reflection.

3.2.1 Crystalline, Polycrystalline and Amorphous Solids

Before going into the different types of solar panels, it's important to first understand what crystalline, polycrystalline and amorphous solids are alongside also understanding their differences. In our case, there are crystalline, polycrystalline and amorphous solar panels. In regards to crystalline solids, they are the most common over polycrystalline and amorphous solids. As expected from a "crystal structure," they are solids that have geometric shapes with multiple flat surfaces. An obvious example of a crystalline solid would be a diamond. The atomic structure of these crystalline solids is very tight and leaves very little room for movement of the atoms. Due to this tight configuration of atoms, crystalline solids have very high melting and boiling points, thus making them particularly resistant to high temperatures. Additionally, because of this tight atomic structure, there is what is known as translational symmetry. This means that each atom is related to the atom next to it, and thus there is uniformity across the entire structure. See the first image in figure 22 below denoted as "Crystalline" for reference of the atomic structure of crystalline solids. In polycrystalline structures, there are a multitude of small crystals which can be denoted as "grains." Each of these grains are separated by what is known as a grain boundary. This boundary creates a haphazard atomic composition. The small crystals themselves have a tight atomic composition, but at the location of the grain boundaries, the atomic composition is far looser, so there is a small amount of translational symmetry. This concept can be seen in the second image in figure 22 below

denoted as “Polycrystalline” for reference of the atomic structure of polycrystalline solids. Unlike crystalline solids, polycrystalline solids do not have uniformity in atom relation due to the different grains and their boundaries. They are only periodic across each individual grain. An example of a polycrystalline solid is beryllium. Finally, amorphous solids are non-crystalline and do not have a geometric shape like crystalline and polycrystalline solids. Because of this lack of a geometric face, amorphous solids do not have edges similar to crystal and polycrystalline structures. This variation and lack of uniformity in amorphous solids is due to their atomic structure. Unlike crystalline and polycrystalline structures, the atomic composition of amorphous solids has no uniformity and therefore no translational symmetry. This structure can be seen in the third image in figure 22 below denoted as “Amorphous” for reference to the atomic structure of an amorphous solid. [53, 104,126]

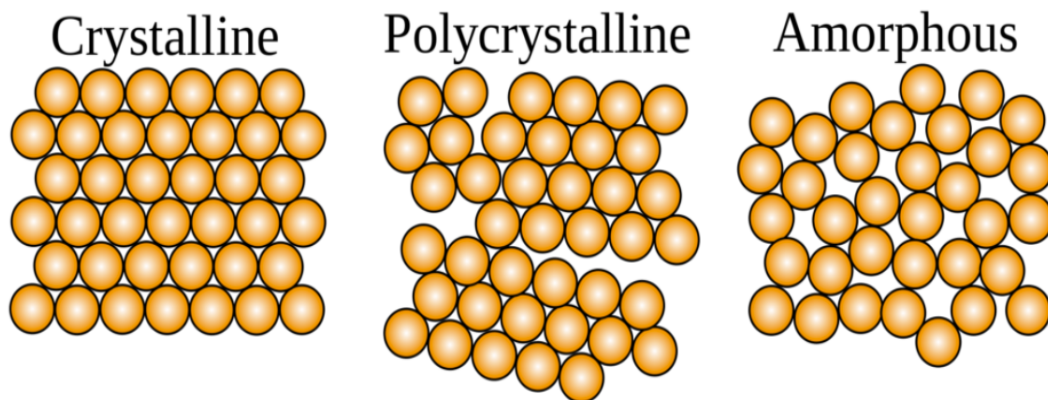


Figure 22: Atomic Structures of Crystalline, Polycrystalline, and Amorphous Solids

3.2.2 Technical Specifications of Solar Panels to Understand

Before diving into the three main types of solar panels we will be analyzing, it’s important to understand the typical specifications listed with solar panels. These specifications include, but are not limited to solar panel efficiency, open circuit voltage, and short circuit current. First is the maximum operating voltage. This is the maximum voltage that can be outputted by the solar panel when the solar panel is operating at maximum efficiency. Next, open circuit voltage is the highest amount of voltage that the solar cells on the solar panel can produce when there is no load present. No load being present means the solar panel isn’t connected to anything, and thus there is no current. The next important specification of solar panels is the maximum operating current. The maximum operating current is the amount of current that is produced when the solar panel is operating at maximum efficiency. Finally, the other important specification that is listed, is the short circuit current rating. Short circuit current is the amount of current that is being produced by the solar panel when the positive and negative contacts are connected to each other. Additionally, with this connection, the solar panel is also not connected to a load. These are the necessary basic definitions of specifications one needs to know when choosing a solar panel. There are other specifications such as size and operating temperature, but those are self explanatory, and thus do not need to be discussed. [9, 71,76] **See the figure below for a basic circuit diagram of an open circuit, and a short circuit.**

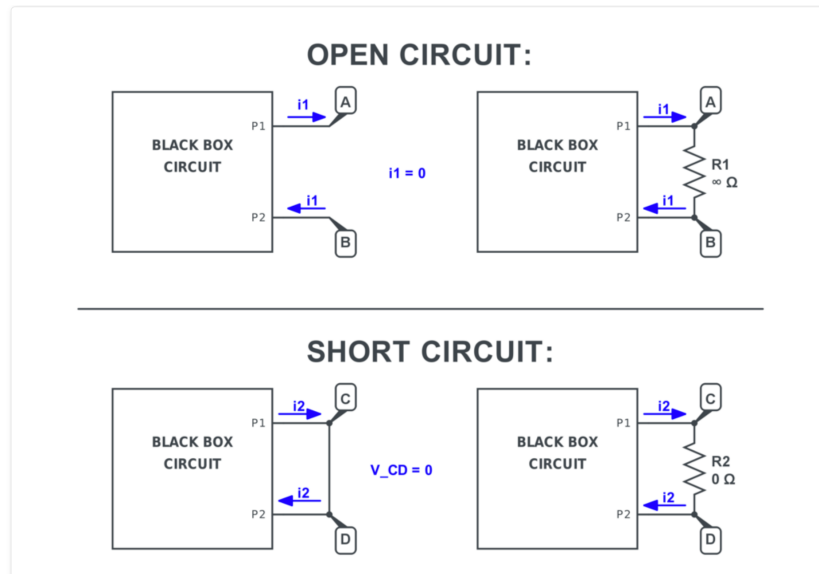


Figure 23: Open and Short Circuit Diagram

3.2.3 Solar Panel Types

In the following section different types of commonly known solar panels will be discussed. After discussing each type of solar panel below, we will outline the features each solar panel offers.

3.2.3.1 Monocrystalline Solar Panels

Crystalline or Monocrystalline solar panels are some of the most widely used solar panels today. If you have ever seen solar panel arrays on someone's roof, there's a high chance they were monocrystalline. There are multiple reasons why monocrystalline solar panels are the popular choice among consumers. First off, their appearance is a uniform matte black color that has a sleek design. The solar cells themselves have the corners sheared off which creates blank space between the cells. This blank space creates a diamond pattern which is aesthetically pleasing. Second, and most importantly is their efficiency. Out of the different types of panels that one can purchase, monocrystalline panels are the most efficient. This is due to their construction. Each monocrystalline solar cell on the panel is made from a silicon wafer that is composed of an individual silicon crystal. This crystal comes from the cut ingot created by what is known as the Czochralski method. This method starts with a "seed" crystal which is the basis of the composition and submerges it in a large container of molten silicon. From this point, the "seed" crystal is drawn up out of the vat of molten silicon thus creating an ingot. This ingot is cut into wafers which form the individual crystals that are used in the construction for monocrystalline solar cells. As discussed above, single crystalline structures have high translational symmetry, thus there is a high amount of uniformity across the crystal's atomic structure. This uniformity which allows increased electron flow is where the high efficiency of monocrystalline solar panels come from. [33, 151]

3.2.3.2 Polycrystalline Solar Panels

Polycrystalline solar panels can be recognized by their blue color unlike monocrystalline solar panels' black color. This blue color is due to their manufacturing process which will be explained later. Unlike monocrystalline solar panels, the polycrystalline solar cells do not have rounded corners, and thus fill up the entirety of the panel. Because of this blue color, many people do not find them to be aesthetically pleasing. Additionally, due to the way they are manufactured, polycrystalline solar panels are less efficient. The upside to these panels is their cost. Though aesthetically and efficiently less desirable than monocrystalline solar panels, polycrystalline solar panels offer a more cost effective option. Each of these aspects is explained by the way the polycrystalline panels are manufactured. As explained above, polycrystalline solar cells are composed of small crystals known as grains. Each cell is composed of these multiple grains which create this blue marbled pattern which can be seen on polycrystalline solar panels. This separation of crystal grains on each solar cell causes the electrons to have a more difficult time flowing due to the polycrystalline crystal's atomic structure. This is explained in section 3.2.1. [126]

3.2.3.3 Amorphous Solar Panels

Amorphous solar panels are in a class of their own. Similar to monocrystalline and polycrystalline solar panels, they are primarily composed of silicon, but there are some major differences. The first main difference is rather than being composed of crystalline silicon from solid wafers, amorphous panels are composed by using non-crystalline silicon on substrates such as glass and metal. This layer of non-crystalline silicon that makes up the amorphous panel is as thin as a micrometer. Similarly because of non-crystalline silicon being deposited on the face of a given substrate, amorphous panels' are solid black and appear as one piece conversely to monocrystalline and polycrystalline panels. Additionally because of how thin the non-crystalline silicon deposit is on the amorphous panels, they can be made flexible. This allows them to be far more versatile in how the panels can be used. Out of all the panels discussed above, amorphous solar panels are the cheapest option. Because of this economy amorphous panels are most commonly used for large scale industrial and commercial use. The drawback of these panels is their efficiency. Out of the previously listed panels, amorphous solar panels are the least efficient of the three. [60] **Amorphous panels will not be listed as an option below due to their lack of availability for non-commercial use.**

3.2.4 Solar Panel Options

Now that each of the major types of solar panels have been discussed, this section will be used to summarize characteristics of different solar panel options. These summarizations will be used to compare each option, and provide a basis for our solar panel choice.

3.2.4.1 Renogy 100W 12V Monocrystalline Foldable Suitcase Solar Panel

This first option as described above is a 100W 12V monocrystalline foldable solar panel. This portable panel is composed of (2) 50 Watt solar panels thus creating the total 100 Watts. According to the manufacturer's specifications, the maximum operating voltage of these panels is 18.0V, the open circuit voltage is 21.6V, the maximum operating current for each panel is 2.78A, and the short-circuit current for each panel is 3.08A. Additionally, the weight of the entire assembly is 27.05 lbs. This panel specifically has a 25 year efficiency rating. For this panel, this means that the panel's efficiency will not drop below 80% in the span of 25 years. Assuming this guarantee holds up, that would make this panel very reliable. Due to its portability, this solar panel set combines great efficiency and convenience. The price of this assembly is \$186.99.

Due to our project aiming to be low budget, this typically wouldn't be an option due to the portable panel's high price tag. This option is being explored because our group will be able to source a slightly used version of this same portable panel for little to no cost. If this project was reproduced and the solar panel was being bought outright, one might consider using a rigid monocrystalline solar panel of equivalent wattage due to the panel being cheaper than its portable counterpart.

3.2.4.2 Renogy 100W 12V Monocrystalline Rigid Solar Panel

The second option similar to the first, is a 100W 12V monocrystalline rigid solar panel as described above. The main difference between this panel and the portable panel assembly above, is that this solar panel is rigid and thus not foldable and portable. Additionally the portable assembly above is composed of (2) 50W solar panels to achieve the desired 100W. This rigid monocrystalline solar panel is a single 100W panel. Due to this option being rigid and composed of one panel, it is far cheaper than its portable counterpart. In this case, one sacrifices convenience for the economy. According to the manufacturers specifications, the maximum operating voltage of this panel is 18.6V, the open circuit voltage is 22.3V, the maximum operating current for the panel is 5.38A, and the short-circuit current for the panel is 5.86A. Additionally, the weight of the entire assembly is 14.3 lbs. Just like its portable counterpart, this panel has a 25 year efficiency rating. For this panel, this means that the panel's efficiency will not drop below 80% in the span of 25 years. The retail price for this panel is \$109.99.

3.2.4.3 HQST 100W 12V Monocrystalline Rigid Solar Panel

The third option is a 100W 12V monocrystalline rigid solar panel just like Renogy's panel, but this panel is made by HQST. This rigid monocrystalline solar panel is a single 100W panel. According to the manufacturers specifications, the maximum operating voltage of this panel is 18.0V, the open circuit voltage is 21.3V, the maximum operating current for the panel is 5.58A, and the short-circuit current for the panel is 5.83A. Additionally, the weight of the entire assembly is 14.3 lbs. Just like the other listed panels, this panel has a 25 year efficiency rating. For this panel, this means that the panel's efficiency will not drop below 80% in the span of 25 years. The price for this panel is \$89.99. [1]

3.2.4.4 WindyNation 100W 12V Polycrystalline Solar Panel

The fourth option that will be discussed for this project is a 100W 12V polycrystalline rigid panel. Unlike the foldable monocrystalline panel above, this solar panel is composed of a single 100W rigid panel just like the rigid monocrystalline panel discussed above. According to the manufacturers specifications, the maximum operating voltage of this panel is 17.4V, the open circuit voltage is 21.6V, the maximum operating current for the panel is 5.75A, and the short-circuit current for the panel is 6.23A. Additionally, the weight of the entire assembly is 17.6 lbs. This panel has a 25 year efficiency rating. For this panel, this means that the panel's efficiency will not drop below 80% in the span of 25 years. The price of this panel is \$77.99.

3.2.4.5 RICH SOLAR 100W 12V Polycrystalline Solar Panel

The fifth and final option that will be discussed for this project is another 100W 12V polycrystalline rigid panel. According to the manufacturers specifications, the maximum operating voltage of this panel is 18.5V, the open circuit voltage is 22.6V, the maximum operating current for the panel is 5.41A, and the short-circuit current for the panel is 5.86A. Additionally, the weight of the entire assembly is 17.5 lbs. This panel has a 25 year efficiency rating. For this panel, this means that the panel's efficiency will not drop below 80% in the span of 25 years. The price of this panel is \$81.99.

3.2.4.6 Our Solar Panel Choice

For this section, we will be briefly explaining our reasoning behind which solar panel we chose. For choosing solar panels specifically, there are few important aspects to consider. One needs to consider maximum operating voltage, maximum operating current, and of course, the cost. Below in table 4, our solar panel choices ranked in order are shown and the reasoning behind our choice is explained.

| Solar Panels | Solar Panel Choice | Reason(s) for Choice |
|--|--|--|
| Renogy 100W 12V Monocrystalline Foldable Suitcase Solar Panel | <u>First Choice (Donated)</u> Renogy 100W 12V Monocrystalline Foldable Suitcase Solar Panel | Among our first choices, each solar panel performs well as shown above. We will be using the “First Choice (Donated)” option as it has good specifications, and was free of charge for our project. Had we not been donated this, we would have used the “First Choice (No Donation)” option as its power output compares nicely to our other choices, but it is much cheaper. Our second and third choices have a comparable power output to our other choices, but are more expensive thus putting them at the bottom. |
| WindyNation 100W 12V Polycrystalline Solar Panel | <u>First Choice (No Donation)</u> WindyNation 100W 12V Polycrystalline Solar Panel | |
| Rich Solar 100W 12V Polycrystalline Solar Panel | <u>Second Choice</u> Rich Solar 100W 12V Polycrystalline Solar Panel | |
| HQST 100W 12V Monocrystalline Solar Panel | <u>Third Choice</u> HQST 100W 12V Monocrystalline Solar Panel | |

Table 4: Solar Panel Comparison

3.3 Charge Controllers

A charge controller is a device that is a mediator between the solar panel and the storage element (battery). It makes sure that the power provided by the solar panel is adequately referred to the batteries in a safe and efficient manner. It also protects the batteries from being overcharged and provides safety to both the batteries and the solar panel. It does this by regulating the amount of charge that can pass through to the batteries. As the input voltage increases the charge controller mitigates the amount of charge that can pass through to the batteries. Once the batteries are fully charged, the charge controller will no longer allow any charge to pass through. [174]

3.3.1 PWM vs MPPT

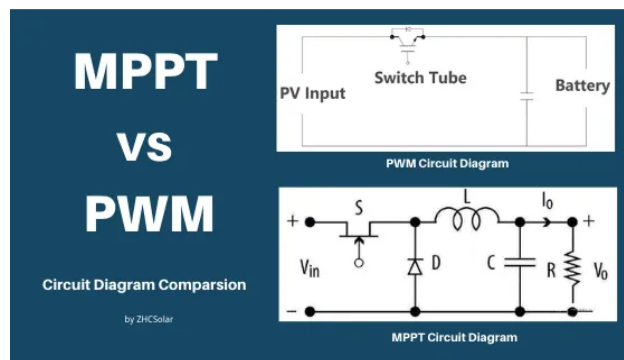


Figure 24: MPPT vs. PWM Analog Circuit

When deciding to use a charge controller one must take into account which type of controller they want to use. Figure 24 shows the two types of circuits, illustrating their respective complexities. In PWM or pulse width modulation the solar panel is connected directly to the battery with the charge controller pulling down the voltage to match the battery's desired voltage. As the battery charges up, the voltage starts to increase. As this happens, the charge controller recognizes this and limits the amount of charge that goes into the batteries. Once the batteries reach the nominal voltage, the charge controller prevents any more charge from going into the batteries. The PWM charge controller can be thought of as an electrical switch. It accomplishes the charging in three stages: Bulk, Absorb, and Float Charge. In the "bulk charge" stage, the charge controller allows the batteries to receive charge at a high current and voltage. Protections are an important aspect to keep in mind here as the voltage of the batteries should never exceed the maintenance value dictated by the charge controller. Thus, once the batteries reach the maintenance value for any reason the charge controller will not allow any more charge to pass through. In the absorb charge stage or constant voltage charging state, the battery will wait for a period of time for the voltage to fall on its own until it enters a balanced charging state. Finally the last stage known as the "float charge" is simply described as a way to maintain the voltage of the batteries by supplying a small charge current to the batteries as a constant rate. This helps alleviate the issue of batteries losing power after a complete charge due to discharge over time. As we can see in figure 25 below we need to match the battery's voltage to the solar panels voltage. Thus if you have a 12 volt solar panel, in order to minimize losses, you should use a 12 volt battery or else you increase your power loss. An example of this is shown in figure 25. If you have a 12 volt solar panel but the maximum voltage that it will operate is at 18 volts, then you will already experience losses in the PWM configuration. For a solar panel that operates at 18 Volts max power at 5.56 amps will translate to a 100 watt power output. But the battery with a 12 volt battery will likely operate at maximum around 13 volts. As a result at the same amperage it would translate to a 72 watt power output. As a result you have a 28 percent loss with these two systems as the solar panel can provide more but the battery can only intake 72 percent of what the solar panel can provide at maximum. [165,174]

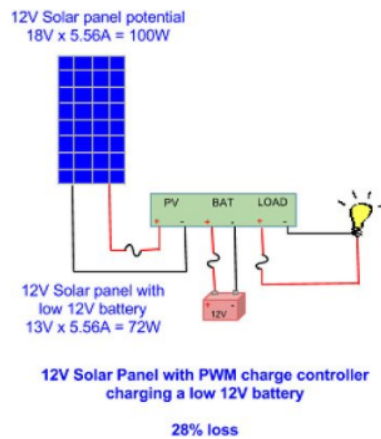


Figure 25: Losses with PWM Controller

An MPPT charge controller or Maximum Power Point Tracking will first read the V_{mp} or voltage maximum power of the solar panel and then convert it to the voltage that the battery operates at. In order to preserve the principle of continuity, the MPPT controller succeeds where the PWM does not. This is done by causing the current to be raised as it exits the MPPT charge controller since the voltage of the solar panel is higher than that of the batteries to store the charge. As a result, the device uses more available power provided by the solar panel. This makes this charge controller more efficient and creates very little losses when the energy is transferred from the panels to the batteries. The system however is more complicated and more expensive as a tradeoff. The MPPT accomplishes the charging in the following 4 stages: Bulk, Balance/Boost, absorb and float charge. In the bulk stage the mppt controller working in the voltage maximum power mode can adjust the output voltage to charge the battery but unlike the PWM controller which only can output a constant value of charge, the MPPT is able to charge at a significantly higher voltage from the solar panel when the sun is the brightest and giving the panel the most amount of insolation. This stage alone causes a significant increase in the efficiency of the MPPT charge controller as a whole. As a result, batteries are able to be charged up quicker than with the PWM method. In the balance/boost stage, the controller continuously adjusts the charging current to maintain optimal charge into the battery. In the absorb stage as the voltage increases the charging current decreases and once it reaches a certain point the constant voltage charging ends. The final stage of the charge controller is float charge. This stage is to keep the battery fully charged as the voltage will naturally decrease in time. [174] In figure 26 below we can see an example of an MPPT controller used with relation to a 12 volt solar panel and battery. We first start off with a 12 volt solar panel that can run at 18 volts at maximum power point tracking that the MPPT is designed to accomplish. Since the power into the charge controller is equivalent to power out of the charge controller, the voltage will be decreased to equal the battery voltage and as a result the current will be increased. As a result, you are able to squeeze more power out of the solar panels. This in turn creates less losses and in turn makes the MPPT controller much more efficient. In our example in the figure when we have the same solar panel that we had in our PWM configuration attached to an MPPT which relays it to the same voltage battery that we also had in the PWM, we can make a few calculations. With the solar panel outputting 18 volts max we can divide this by the maximum battery voltage of around 13 volts to obtain a unitless

value of around 1.38. When we multiply this unitless value by the same current to show that the current will increase as a result of the reduced voltage, we get 1.38×5.56 amps which gives around 7.7 amps of current. As a result of this, when our solar panel can output 100 watts max, our battery will be able to intake $13 \text{ volts} \times 7.7 \text{ amps}$ to give around 100 watts. This means that using the MPPT controller we have virtually little to no losses. [165]

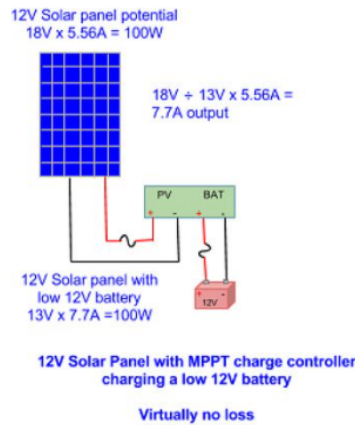


Figure 26: Losses with MPPT Controller

3.3.2 Which type of charge controller to use?

When deciding which type of charge controller to use many questions need to be raised. Some of these may be one of the following: What do you want to power? Is cost a concern? How efficient do I want my system to be? As a result, finding the functionalities of each method will help determine which route to take. The next sections will outline PWM and MPPT functionalities along with solar charge controllers that are out in the market today. This will help us to put each type side by side and to see what PWM and MPPT have to offer. The following help us to decide which method we should go for as well as which will be the most viable when we build our own custom charge controller.

3.3.3 PWM Functionalities and examples

When looking at PWM charge controllers it is best to know beforehand what type of products are out on the market today. This section outlines two PWM controllers which can help to identify similar and different functionalities so that when we decide which controller to use, we will at least have a basic understanding of what to be looking for when we build our own controller from scratch. Before we look at examples, some known facts about PWM charge controllers should be noted. Some of the facts known include the following: PWM charge controllers are typically simple in design because the amount of parts used is considerably less than MPPT, they are easily deployed with respect to MPPT's and they are cost effective as compared with MPPT. Some other aspects that may come into play when looking at PWM controllers is how efficient do you want your controller to be? Typically there will be losses as the input voltage will have to match the voltage of the battery. Finally a lot of PWM systems offer less protections as a result of the simplicity of design and reduced cost. [174]

Moving on to our first example shown below is a PWM solar charge controller created by Shenzhen Olys Company in figure 27. They offer two models: the SEC10 and the SEC20. The differences between the two models is outlined below in table 3. Some things left out in the functionality table are the parameters of the lead acid and lithium ion batteries. We have already decided on the lithium iron phosphate (LiFePO₄) batteries so it will be more useful to look at parameters applying to those only. This controller uses three stage PWM charging technology to not only provide a safe charge to the battery, but to also prolong the life of the used battery in the process. One reminder that the company gives is to never connect a capacitive load to this charge controller as this controller was not meant to provide power to devices which require high amounts of current such as drills and motors. The table below comes from the data sheet located [129,138] on the Shenzhen Olys Company website. As we can see in the data contained in the table below the Max PV power is rated for 175 watts for the SEC10 model and the other model is twice that. The max charge and load currents are 10 and 20 amps respectively. The most relevant information in the table will be what type of battery that each model applied to. Both models will be useful for our application as both use lithium iron phosphate batteries.

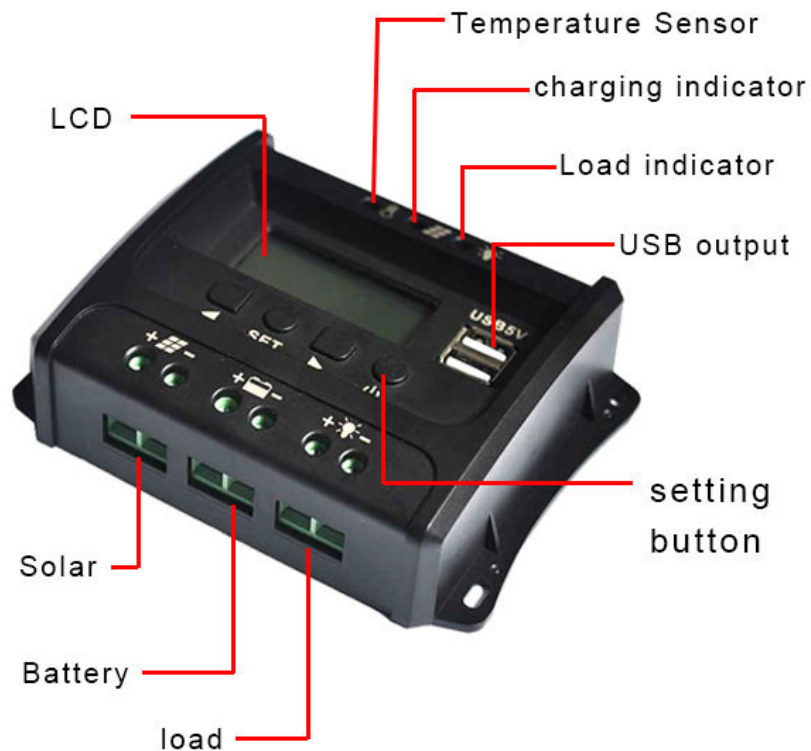


Figure 27: OLYS Solar Charge Controller

| Model | SEC10 | SEC20 |
|---------------------------|--------------------------|-----------------------------|
| Max PV Power | 175 Watts | 350 Watts |
| Max PV Voltage | 12V: 30V | 24V: 50V |
| Max Charge Current | 10 Amps | 20 Amps |
| Max Load Current | 10 Amps | 20 Amps |
| Battery types (Other) | Lead Acid | Lithium Ion (3 or 4 series) |
| Battery Type (Relevant) | LiFePO4 | LiFePO4 |
| Battery Rated Voltage | 12.8V (4 series) | 16V (5 series) |
| Over Voltage Disconnected | 16V | 19V |
| Over Voltage Off Charging | 15.5V | 18.8V |
| Boost Voltage (2 Hours) | 14.6V | 18.2V |
| Floating Voltage | 14.4V | 18V |
| Low Voltage Protection | 10.5V | 13.1V |
| Recommended Voltage | 12.5V | 15.6V |
| Battery Voltage | 12V/24V Auto recognition | |
| USB | 5V/2.1A, 2PCS | |
| Technology Used | PWM | |
| Temperature Compensation | 3mv/2V/degree C | |
| Working Temperature | -20 C to 50 C | |
| Dimension | 130*100*37mm | |
| Price | N/A | |
| Weight | N/A | |

Table 5: Technical Parameters of OLYS (Model SEC10 and SEC20) Charge Controller

In the table 5 above we also can see that the battery rated voltage given is for 4 and 5 series. For our applications the 4 series should suffice as all the parameters associated with our chosen batteries match what we would want to attain. The rated voltage, boost voltage and recommended voltage are all in line with our lithium iron phosphate battery choice. The temperature compensation and the working temperature along with the dimensions is the same for both models. Overall if we had to choose a model that would directly benefit us the most would be the SEC10 as it matches most of our design specifications for our battery.

Moving on to example two we have a solar charge controller created by Morningstar. They offer four different models and those are the PS-15, PS-15M, PS-30, and the PS-30M [102,106,117,119]. The models that end with an “M” are models that have an optional digital meter display. In figure 28 we can see the 15M model but in table 4 it includes the technical functionalities of all four models. There are a few things to note from table four. The first is that for the models that have meters (denoted by an “M”), there is an additional power consumption that applies. This power consumption given by the user manual can also vary based on how bright the screen is. At 50% brightness, the power consumption increases to 35mA and at full brightness this can go as high as 50mA. Another thing to note is that in this charge controller example there is an extra stage in the charging process. This is done in order to prolong the life of the battery that much further. Instead of the three stages where it is just bulk, absorb and float, a final stage is added and that is to equalize the remaining power into the batteries in order to increase longevity. For the PS-15 which can be found on the altE store online. We are shown that this pwm charge controller does not have a display. All the other models are shown briefly in this site however all the data sheets for this model and the other three can be found [45-48]. In table 6 we are shown all four models. To start off the first 2 models (one denoted with an “M” to indicate a display) we can see that the rated solar, load and battery current of the two models is 15 amps. The other two models with one denoted with an “M” to indicate a display, the only difference is that they are designed for 30 amp load, solar and battery currents. All four models are able to be configured to work off of either 12 or 24 volt systems with matching battery voltage of choice. As we can see the voltage accuracy of the device is quite high and the self consumption (which only applies to the models which have a display) is only around 20mA. The operating temperature is the same for all the models and the temperature compensation is constant for every model. Based on these results the best choice for our project would be the PS-15M as we would look at our system operating well below 15 amps with a 12 volt system as the batteries will nominally operate around 12.8 volts. The only setback is that it is heavier than the previous PWM controller and the dimension is a bit larger.



Figure 28: MORPROSTAR-15M Solar Charge Controller

| Model | PS-15 / PS-15M | PS-30 / PS-30M |
|--------------------------------------|---|----------------|
| Rated Solar Current | 15A | 30A |
| Rated Load Current | 15A | 30A |
| Max Battery Current | 15A | 30A |
| Load Current Rating | 15A | 30A |
| System Voltage | 12/24V | |
| Nominal Battery Voltage | 12/24V | |
| Battery Voltage Range | 10V-35V | |
| Voltage Accuracy | 0.1% +/- 50mV | |
| Max Solar Input Voltage | (12V/24V Battery): 60Voc | |
| Self Consumption* | 20mA | |
| Operating Temperature | -40 C to 60 C | |
| Meter Operating Temperature | -20 C to 60 C | |
| Storage Temperature | -40 C to 80 C | |
| Meter Resolution | 128x64 pixels | |
| Viewing Area | 5cm x 2.5cm | |
| Battery Charging | 4 stage charging: Bulk, Absorption, Float, Equalize | |
| Temperature Compensation Coefficient | -5mV/C/cell (25 C ref) | |
| Temperature Compensation Range | -30 C to 60 C | |
| Dimensions | 15.3 W x 10.5 L x 5.5 D cm | |
| Weight | 1lb/0.4kg | |
| Technology Used | PWM | |
| Price | 98.00\$ | |

Table 6: Technical Parameters of MORNINGSTAR Charge Controller (All Models)

3.3.4 MPPT Functionalities and Examples

Looking at MPPT charge controllers this section outlines two MPPT controllers which can help to identify similar and different functionalities so that when we decide which controller to build, we will at least have a basic understanding of what to be looking for when we build our own controller from scratch. Before we look at examples, some known facts about MPPT charge controllers should be noted. Some of the facts known include the following: MPPT charge controllers are typically more complex in design because the amount of parts used is considerably more than PWM, they are more expensive as compared with PWM due to not only complexity but also efficiency. Expanding upon the efficiency, MPPT controllers have an efficiency of around 99% because the battery voltage does not have to match the solar panel voltage and thus there is little to no losses when supplying power to the battery. This method squeezes every last ounce of power out of the solar panels and is able to adjust the power flow based on the intensity of the sun. Finally MPPT controllers typically have more protections in place since the device usually operates at high voltage and current ratings along with larger loads. [43,109,174]

Starting with our first MPPT solar charge controller we start with a morningstar prostar MPPT 25A solar charge controller with display in figure 29 [105]. There are a total of four models of this device and they are as follows: PS-MPPT-25, PS-MPPT-25M, PS-MPPT-40, and PS-MPPT-40M. The “M” denotes that the controller had a display for the user to see. In figure 27 we see the PS-MPPT-25M model to give us a visual representation of what the controller will look like. In table 7 we can see the different technical functionalities of all of the models of this charge controller. As we can see in table 7 below we have all four models on display. All the data sheets can be found for all four models above at [175-178] respectively. The user manual can be found [154-158].



Figure 29: PS-MPPT-25M Solar Charge Controller

| Model | PS-MPPT-25/PS-MPPT-25M | PS-MPPT-40/PS-MPPT-40M |
|------------------------------|---|------------------------|
| Max Battery Current | 25A | 40A |
| Load Current Rating | 25A | 40A |
| With 24V Battery | 700W | 1100W |
| With 12V Battery | 350W | 550W |
| Nominal Battery Voltage | 12V/24V | |
| Nominal Max. Operating Power | controller will limit and provide its rated continuous max output current into batteries. (DO NOT EXCEED Voc) | |
| Max PV Voc | 120V | |
| Current Compensation 12V | -15mV/A | |
| Current Compensation 24V | -30mV/A | |
| Peak Efficiency | 97.3% | |
| Battery Voltage Range | 10V-35V | |
| Voltage Accuracy | 0.1% +/- 50mV | |
| Self Consumption | <25mA (no meter) or <40mA (with meter) | |
| Transient Surge Protection | 4500W (solar, battery, load) | |
| Operating Temperature | -40 C to 60 C | |
| Storage Temperature | -30 C to 80 C | |
| Dimensions (standard) | 20 W x 19.4 L x 7 D cm | |
| Weight (standard) | 3.1 lb | |
| 4 Stage Charging | Bulk, Absorption, Float, Equalize | |
| Temperature Coefficient | -30mV/12V/C | |
| Resolution | 128x64 | |
| Viewing Area | 7cm x 4cm | |
| Price | 397.00\$ | |

Table 7: Technical Parameters Morningstar PS-MPPT Charge Controller (all models)

Looking above at table 7 we can decide which MPPT controller would be a more applicable one to our project. Starting with the battery current rating and the load current rating we obtain 25 amps and 40 amps for models PS-MPPT-25 and PS-MPPT-40 respectively. For our design, since the solar panel will produce around 7.7 amps maximum if we connect it to a 12 volt battery bank, the PS-MPPT-25 model is more suitable. Since the battery will be 12 volts then we will want to also use the MPPT-25 model as it will generate at maximum 350 watts which is more than enough for our design constraint of 100 watts. Both models offer nominal battery voltage of either 12 or 24 volts but we would choose the 12 volts as our nominal battery voltage on our lithium iron phosphate cells is sound 12.8 volts. As we can see from the table the peak efficiency is nearly 98% giving us very little loss in the transfer of power from the solar panels to the battery. Self consumption is an important topic to cover as we would be using the meter in our design. As a result we would take the higher end of the consumption range which would be no more than 40mA. Another good part to mention that is an advantage of an MPPT controller is that it has added protections. One of these protections is transient charge protection which is rated for 400 watts. The operating and storage temperature of all the models are within our range that we would want. The weight of the MPPT charge controller is one of its drawbacks as it weighs around 3 pounds making it bulky and cumbersome in our design. Another advantage of the MPPT is its four stage charging capability. Having four stages allows the controller to prolong the life of the batteries thus making it last longer and having a lower degradation factor. The final drawback of the MPPT overall is the cost. As compared to our previous PWM controller choices mentioned, this controller is around four times as expensive.

Moving on to the second MPPT charge controller we have the Genasun GV-10-LI-14.2V [66]. It is shown below in figure 30 below. Table 8 below outlines the data sheet [38] for this device. The user manual can be found [153] It is an ultra high speed MPPT meaning it can save you money by reducing your overall system cost. This controller is usually used in very remote areas with harsh conditions in order to extract as much power from the sun as possible. The table shows only the lithium iron phosphate model as there is also lead acid and lithium ion. A few things to note is that there is no nominal battery voltage, no temperature compensation for the battery and the charge profile is CC-CV instead of the traditional multi-stage temperature compensation. It can be seen that the efficiency is upwards of 98% in terms of providing power to the battery and also produces very little power consumption during night hours. One of the stark differences about this MPPT controller is that the weight is significantly less than the previous one mentioned at only 6.5 ounces.

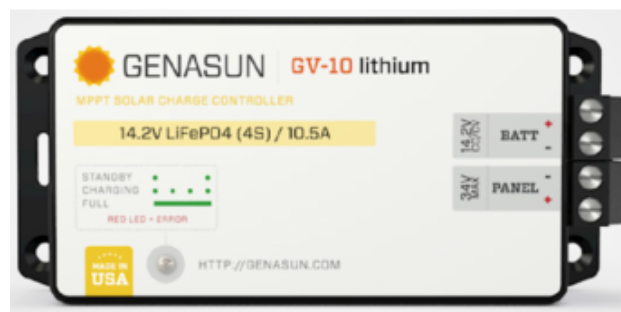


Figure 30: GV-10-LI-14.2V Solar Charge Controller

| | |
|-----------------------------------|--|
| Model | GV-10-Li-14.2V |
| Maximum Recommended Panel Power | 140W |
| Rated Battery (output) Current | 10.5A |
| Nominal Battery Voltage | N/A |
| Maximum Input Voltage | 34V |
| Recommended Max Panel Voc at STC | 27V |
| Min Battery Voltage For Operation | 8.5V |
| Input Voltage Range | 0-34V |
| Max Input Short Circuit Current | 10.5A |
| Max input Current | 19A |
| Battery Temperature Compensation | N/A |
| Operating Temperature | -40C to 85C |
| Charge Profile | CC-CV |
| CV Voltage | 14.2V |
| Electrical Efficiency | 96% to 98% |
| Tracking Efficiency | 99% |
| Night Consumption | 900uA |
| Weight | 6.5oz |
| Dimension | 14x6.5x3.1 cm |
| Connection | 4 position terminal block for 10-30 AWG wire |
| Price | 119.00\$ |

Table 8: Technical Parameters GV-10-LI-14.2V Solar Charge Controller

A few other mentions to the table above include the tracking efficiency to be almost perfect. The dimensions of this controller are relatively small and the price is significantly cheaper than our previous MPPT controller at only 119 dollars. That is almost a 400 percent difference in terms of cost. The major drawback is that it is more complicated to implement and relies on more complex algorithms and a different charging profile. As a result we would choose the Morningstar PS-MPPT-25M.

3.3.5 Which type of controller we will use and why?

For our design we will be using the PWM charge controller. We will be creating our own controller as a custom PCB and having a microcontroller drive the PWM signal through the circuit that we fashion. For the microcontroller information and PWM pertaining to the microcontroller it is outlined in more detail in **section 3.1 through 3.1.5**. We chose the PWM due to many reasons. Although we recognize that the MPPT is a better choice in terms of performance it is a roadblock in terms of cost and complexity. Also, our project is not intended to power very large external systems but to provide power to basic necessities in times of need. Table 9 below outlines our thoughts on why we will go with the PWM controller when we design our own instead of the MPPT. We first chose a controller from the two choices we showed for the PWM and we came to show the OLYS model SEC10. Next, we chose the PS-MPPT-25M from the two choices that we researched for the MPPT controllers. Putting them side by side we wanted to compare the characteristics of these two controllers with the characteristics that we were looking for in our design. We have decided to go with the PWM controller due to the factors listed in the table. For the max charging current we will not be needing 25 amps as our solar panel choice will only produce no more than 6 amps with a PWM configuration. For the charging stages we recognize that we would only get three stages but we could modify it when coding the microcontroller. For the battery type both types use our battery choice of lithium iron phosphate. Based on the dimension the PWM controller would be better and the weight was also the reason for this choice. The main reasons why we chose the PWM controller are for the complexity and cost. When we planned to design our own, we wanted to make sure that we could actually accomplish the design so we wanted to go with a less complex option. For cost we realize that complexity is directly related to cost. As a result we wanted to also go with a cost effective option. That is why we ultimately decided to go with the PWM option when we build our PCB charge controller.

| Model | OLYS SEC10 | PS-MPPT-25M |
|--------------------|---------------|---------------|
| Max Charge Current | 10A | 25A |
| Charging Stages | 3 | 4 |
| Battery Type | LiFePO4 | LiFePO4 |
| Dimension | 130*100*37 mm | 200*194*70 mm |
| Price | ~100\$ | 397.00\$ |
| Complexity | Low | High |
| Weight | ~1lb | 3.1lb |
| Efficiency | <80% | <97.3% |

Table 9: Comparing PWM vs MPPT Controllers

3.4 Relays

A relay is a simple electrically operated switch that is used as a means of interrupting or opening a circuit. More specifically, they are operated by using an electromagnet that will change the switch over when a current is applied to the relay coil. Relays can be operated by electronic circuits or by switch circuits. A switch circuit is where the switch cannot take the high current of the electrical relay.

The basic parts of a relay include the frame, coil, armature, and contacts. The frame is mechanical in nature and is used to hold the rest of the components in place. The coil is typically wound around an iron core, which causes increased magnetic attraction. This causes the electromagnetic field to be created as the current switches on, thus causing the armature to attract. The armature itself is the part of the relay that moves to open and close the contacts. It is made of a ferromagnetic metal and is attracted by the electromagnet in the relay. When it is not attracted by the electromagnet it has a spring that is attached and will allow it to return to its original position.

The symbol for a relay can differ from circuit to circuit, but the symbol that is most widely used shows the relay coil as a box and has both the “normally closed” and “normally open” contacts. This symbol can be seen below in Figure 31: Basic Relay Diagram:

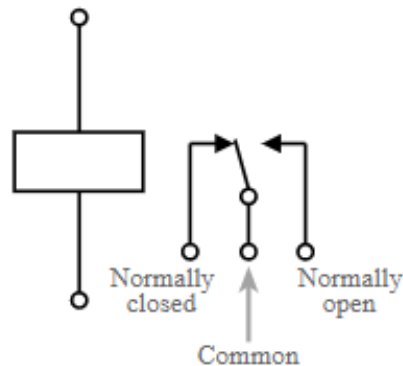


Figure 31: Basic Relay Diagram

With electromechanical relays, they are referred to in terms of break, poles, and throws. A break is designated as a single break or a double break. With a single break the contacts will break in only one spot, and they are typically used in low power applications. A double break is exactly as it sounds and will break in two places, but is typically used in high power applications. In our design, the microcontroller employs an “e-switch”, for the purpose of our project this electronic switch will be referred to as a relay. This relay is considered lower power and should be a single break. Poles are the number of sets of contacts contained in the relay. Like a break there are single poles and double poles, similarly a single pole will switch one circuit and a double pole will switch two different circuits. A relay is not limited to one or two poles, and can have several poles to switch between multiple circuits. Throws will relate to the amount of positions that a circuit has available. Typically there are only one or two throws in a relay. A single

throw is designed to both make and break a circuit while a double throw is essentially a connection from the endpoint of a circuit to another.

3.4.1 Types of Relays

Relays come in many different sizes and types. Two of the most common types of relays are electromechanical relays and solid state relays. Electromechanical relays are devices that are mechanical in nature but powered by electricity. These are considered older technology now and have been widely replaced by solid state relays. Solid state relays are powered by semiconductor technology like transistors, diodes, and integrated circuits.

Electromechanical relays are simply boiled down to electrically operated switches. These relays are most commonly used in low power circuits or when a circuit can be controlled by a single signal. These relays are typically made up of an electromagnet or magnet, the armature, the part that is controlled to open or close, and the spring that returns the armature to the original position.

Solid state relays are built differently than their electromechanical counterparts. These relays are built with coils, springs, and mechanical contacts that operate using magnetic fields to switch. Unlike electromechanical relays, these relays do not utilize any moving parts. Instead they use solid state semiconductors to achieve their functions. Due to their lack of moving parts, many see this as a major advantage of solid state relays over electromechanical relays.

3.4.2 Our Relay

Our design contains a relay which will be controlled via the graphics user interface on the charge controller. This will be done as a safety feature, so that we can prevent the charge controller from overcharging the battery. The relay can be placed before the charge controller or it can be placed after the charge controller, but it will function in the same manner regardless. For our design, the location will be placed after the charge controller and we will be using the ICStation 1CH DV 3 volt relay power switch module that contains a optocoupler high level trigger for the ESP8266 Arduino board.

3.5 LCD Display & GUI

In this section, the single touch capacitive LCD screen will be thoroughly investigated to create a suitable GUI for this project. The basic properties and science behind capacitive LCDs has already been covered in section 3.1.4.3. This section will be focusing on the specific features of the Adafruit 2.8" TFT LCD with Capacitive Touchscreen. In addition, we will be exploring the requirements for our GUI as well as looking at a graphical library that is made to simplify the GUI design process for embedded systems called Adafruit GFX Library.

3.5.1 Researching The 2.8" TFT LCD with Capacitive Touchscreen

According to the LCD's datasheet, the screen is a full colored 320x240 display with four white LEDs in Parallel for backlighting. The datasheet also mentions that it has a viewing

direction of 6 o'clock. The viewing angle of a display is "the direction from which the display will have the maximum contrast and readability" and the viewing direction is given in terms of clock positions [183]. The viewing angles, as shown in figure 32, is in respect to the normal of the center position of the screen.

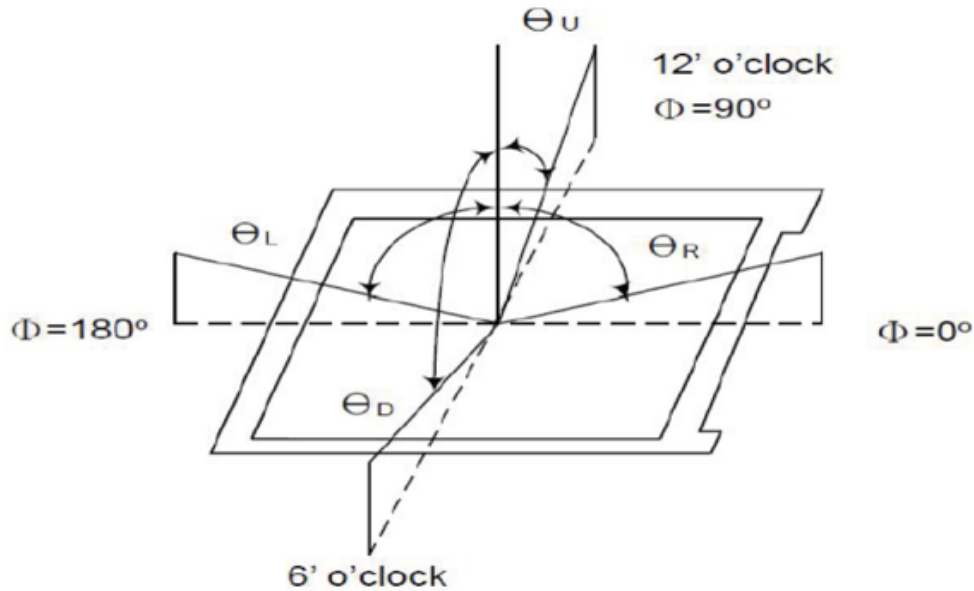


Figure 32: Viewing Angles of a Screen

If the viewing direction is 6' o'clock, then the observer needs to be below the normal of the screen to get the best possible view, figure 33 illustrates this. For the best user experience, we must keep the viewing angle of the LCD in mind when deciding the placement of the LCD in the charge controller design.

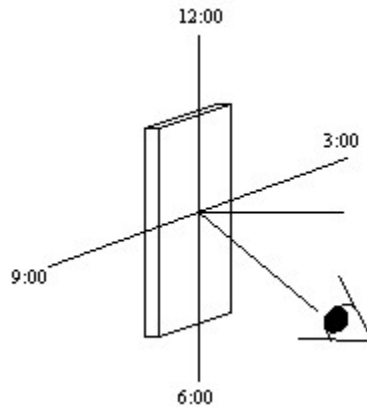


Figure 33: Observer Below Screen

Data can be sent to the LCD using SPI or via 8 bit digital data lines. For the latter, 8 pins are required to send data while an additional 4 pins are needed for the read, write, and selector pins. The 8 bit data mode is faster compared to SPI because data is sent 8 bits at a time rather than a single bit like in SPI. However, we will most likely not use this mode due to the amount of pins required. In either case, three more pins are needed for the capacitive touchscreen, which uses I2C. The SDA and SCL pins both have a 10K pullup

resistor in the breakout boards, so we don't need to provide any pull up resistors ourselves.

Since SPI is the mode being used, we are concerned with its speed. Our GUI should be quick and responsive so, to fulfill these requirements, we need to learn about how quickly data being sent in SPI mode can be displayed on the LCD. To determine that, we need to know the clock rate of the ARM M0 MCU. Let's assume that the clock rate of our MCU is 48 MHz, its highest configuration. The MCU uses the baud rate generator to generate the serial clock (SCK). According to the MCU's datasheet, "In SPI mode, the baud-rate generator is set to synchronous mode." The datasheet has provided an equation that would allow us to calculate the baud rate based on certain configurations as shown in Figure 34.

| Operating Mode | Condition | Baud Rate (Bits Per Second) |
|----------------|-----------------------------------|---|
| Synchronous | $f_{BAUD} \leq \frac{f_{ref}}{2}$ | $f_{BAUD} = \frac{f_{ref}}{2 \cdot (BAUD + 1)}$ |

Figure 34: Synchronous Baud Rate Equation

For synchronous operations, the BAUD value is 8 bits, a value between 0 to 255. Let's assume that BAUD is equal to 255. With f_{ref} as 48 MHz, we find that f_{BAUD} is 93.75 Kbits/s. Theoretically, if we wanted to draw a 250 KB image on to the display, it would take around 2.67 seconds. Normally, in terms of power consumption, setting the clock rate of an MCU to its max would be a cause for concern for power efficiency. However, as we have shown in 3.1.6.2, The MCU's power consumption is very low even at 48 MHz. Ideally, we would want assets drawn on the display at a speed that is nearly instantaneous from the perspective of the user and we will use the MCU's full capabilities in order to achieve this goal. Its sleep modes and other power saving features will still be used when possible.

According to the ILI9341 display driver datasheet, the 4-line/8-bit serial interface has two different display formats, 65k colors and 262k colors. Our LCD only supports 16 bits/pixel color, or, 65,536 colors.

3.5.2 The Graphical User Interface

The GUI is meant to show information about the battery's state to the user via an easy to understand design. The GUI should display all the current measurements on its home screen and show if the battery's output is connected or disconnected. Using the LCD's touch screen, the user will be able to pull up analytics about any particular measurements. For example, if the GUI shows a sub menu that gives the user the choice to select "Current," "Voltage," "Temperature," or "Power", the user will be able to view graphs containing peaks and troughs across certain days for those measurements. In addition, the GUI should allow users to adjust the LCD's brightness and manually connect or disconnect the battery's output. Any extra features beyond these will depend on the amount of memory leftover.

The Adafruit GFX library provides functions that can draw pixels, primitives, texts, and even images onto a display. The display can be represented as a 2 dimensional xy-Cartesian coordinate as shown in figure 35. The origin is at the top left pixel and values entered in the functions will be in terms of these coordinates.

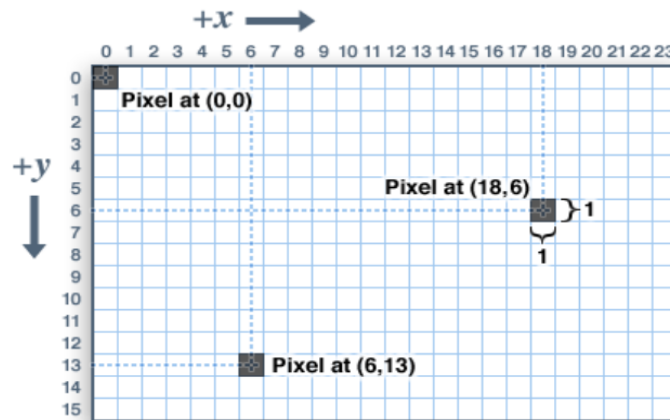


Figure 35: Screen Coordinate

Our display has a resolution of 320x240, meaning that there are 76,800 pixels in the screen or 76,800 coordinates. Colors are represented using unsigned 16-bit values in the library. Starting from the most significant bit, 5 bits are used to convey red, 6 bits for green, and the least 5 significant bits for blue as shown in figure 36. We can use hexadecimal notation to represent colors. For example, if we wanted a pixel to be fully red, its color value would be 0xF800. Each hexadecimal represents 4 bits and, just like in figure 36, the 5 most significant byte is red, hence the value.

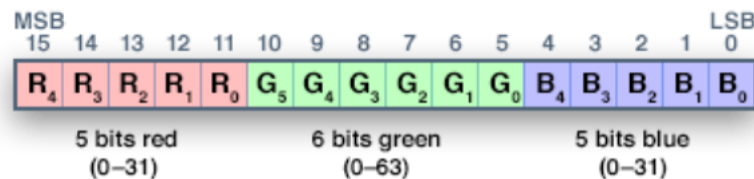


Figure 36: Color Representation In 16-Bits

We will not cover all the extensive functions found in the graphics library, but we should note some notable ones. Drawing anything complex on the screen would be a laborious task if done manually, pixel by pixel. That is why we have functions that allow us to draw shapes and images. Even so, we would still want to retain the option of drawing individual pixels especially if we're writing programs like a CPU emulator that returns pixel location and color to draw something on the screen or plotting graphs or other sinusoidal/non-euclidean figures. The most basic function allows programmers to draw individual pixels called drawpixel. We'll definitely need to use this if we want to draw graphs in our GUI. Text can also be drawn on the screen using the drawChar() function. However, this only prints one character on the screen for every function call. If the programmer wants to print many words at once, then some of the functions shown in figure 37 needs to be called before invoking the print() function.

```

void setCursor(uint16_t x0, uint16_t y0);
void setTextColor(uint16_t color);
void setTextColor(uint16_t color, uint16_t backgroundColor);
void setTextSize(uint8_t size);
void setTextWrap(boolean w);

```

Figure 37: Setter Functions

SetCursor() places the cursor at the top left corner of the text and draws each text with their attribute set by setTextColor and setTextSize as shown in figure 38. setTextSize is self explanatory, and there are two setTextColor() functions. The first setTextColor, again, is self explanatory. The second setTextColor takes an extra parameter that sets the background color of the text, which appears like a rectangle was drawn under the text. Background color cannot be set using this function for text that uses custom font.

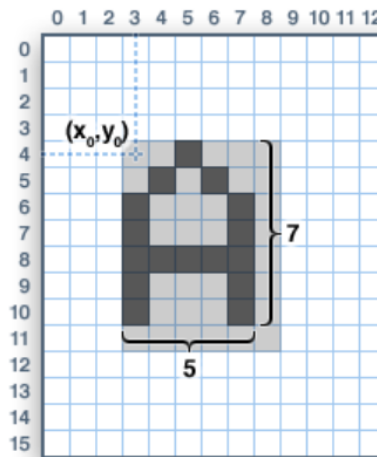


Figure 38: Drawing Text

The setTextWrap() function simply takes a boolean value that activates or deactivates text wrapping. Without text wrapping, text that is drawn beyond the screen will not be displayed in a new line.

Finally, another important aspect of the library is the ability to draw bitmaps including .BMP images. In regards to drawing images, an addon for the library is needed to be installed called Adafruit ImageReader. The details won't be covered in this paper since the API documentation goes through great detail on how to load the images from an SD card or RAM. But once the setting up process is done, the programmer can load .BMP images by using the drawBMP() function. For just drawing bitmaps, not .BMP images, there's the drawBitmap() function, shown in figure 39.

```

void drawBitmap(int16_t x, int16_t y, uint8_t *bitmap, int16_t w, int16_t h, uint16_t color);

```

Figure 39: drawBitmap() Function and its Parameters

This drawing function is one of the more complicated ones because data needs to be stored in flash memory instead of RAM. For Arduino based boards (which may also encompass the METRO M0 since it uses the same MCU as the Arduino Zero), bitmap

data needs to be loaded into flash memory using the PROGMEM utility. In addition, since bitmaps consist of contiguous blocks of 8 bit data, the data needs to be assigned to a pointer. Having a function that allows us to draw bitmaps gives us the ability to create simple animations. One application of this creating a battery icon that is filled with the amount of charge reflected by the charge controller. It would deplete or increase as the battery is charging.

3.6 Temperature Sensor

The MCP9808 temperature sensor will measure the ambient temperature at a sufficient rate to prevent damage for the battery. Although, as previously mentioned before, it is unlikely for LiFePO4 batteries to undergo thermal runaway, we would still want our charge controller to cut-off charge to the batteries if the surrounding reaches certain extreme temperatures. In addition, we would want to keep a datalog of temperature peaks for at least the past couple of days to monitor for consistency. This would require the use of a storage medium, which we have some options to choose from. More specifically, there's the SD card reader from the LCD's breakout board or the 2MB SPI flash chip that is built into the METRO M0. We will need to choose one or the other based on speed, ease of use, and reliability. The MCU will use the Adafruit MCP9808 programming library to communicate with the sensor. The only two functions we will need to concern ourselves with are readTempC() and readTempF(). These functions will return a float value that displays the temperature in their respective temperature scales, celsius and fahrenheit.

3.7 Voltage Regulators

Voltage regulators are devices that maintain an output voltage that is set beforehand regardless of any changes to the input voltage or the load conditions, in essence they do exactly as their name suggests and they regulate. There are two types of regulators, the linear regulators and the switching regulators that will be expanded upon in the next section.

Voltage regulators are common components that can be found in many different devices that we use daily like computers, alternators, and any device that needs the voltage of a power source kept within specified limits. A feature that all voltage regulators have is that it will have a stable voltage reference provided by a zener diode. This stable voltage reference is provided by a reverse breakdown voltage. The reason why a voltage regulator is so important to us specifically is its application in direct current circuits, as it will keep the output voltage constant. Another benefit of voltage regulators is that it will keep the ripple voltage from the alternating current voltage blocked at the filter. Depending on the voltage regulator it may also include additional circuitry that protects against short circuits, thermal shutdowns, and overvoltage protection.

3.7.1 Types of Regulators

There are two types of regulators, linear regulators and switching regulators. These regulators can be connected in series or in parallel. In a series regulator the load stabilizes

the regulator's output, while in parallel you have a shunt regulator that is connected in parallel to the load and will stabilize the output voltage.

Linear voltage regulators are made with MOSFETs or BJTs that act as an active pass device, in either series or parallel, and they are controlled by a high gain differential amplifier. This allows the regulator to take the output voltage and compare it with the set reference voltage to adjust the pass device and keep a constant output voltage.

Switching voltage regulators are different from linear voltage regulators in that they convert the DC input to a switched voltage that then applies a power to a BJT or MOSFET switch. This new voltage is pushed back through the circuit which allows it to control the power to switch it on and off at times to maintain a constant output voltage even if the input voltage or the load current changes. For these types of voltage regulators there are a few topologies that are worth mentioning. The first being step down which is the most common topology that we will go over.

3.7.2 Voltage Regulators in Our Project

In our project we have found that our microcontroller, the Adafruit Metro M0 Express, contains an e-switch. This switching regulator is located in the five volt power supply of our microcontroller and has the part number EG1390. As described in the types of regulators section, 3.7.1, it applies a power to a MOSFET in the circuit. This MOSFET is DMP3098L-8, and looks to be connected to the regulator via a jumper. This e-switch has a $100\text{M}\Omega$ insulation resistance and a $70\text{m}\Omega$ contact resistance. The mechanical and electrical life cycle of it is approximately 10,000 cycles.

Along with this e-switch, we have a LDO voltage regulator also located in the five volt power supply. The part number for this LDO voltage regulator is NCP1117ST50T3G. This regulator provides an output current above one amp and a maximum dropout voltage of 1.2 volts at 800 milliamps. This component is within $\pm 1\%$ accuracy and has safe operating and thermal shutdown protection.

We also took notice of a linear regulator in our 3.3V power supply. This linear regulator has a part number of AP2112K-3.3 and is a surface mounted component. It uses CMOS technology and will deliver a guaranteed 600 milliamps of continuous load current. The accuracy of this regulator is $\pm 1.5\%$ and contains a fast loop response. This fast loop response will provide us with high performance capabilities for dealing with the line and load transients in the microcontroller. Tee AP2112K-3.3 has low power consumption which should keep our microcontroller running efficiently.

There is another component similar to a voltage regulator, but it does not have some of the drawbacks. Some of these drawbacks include energy loss as heat and shutting off at high temperatures. This component is our buck converter, the HILetgo MP2307, and it will step down the voltage from the battery to 6V for the MCU. Our MCU can tolerate voltage values between 6V and 12V going into VIN and we have considered using other buck converters such as the Pololu 9V D24V22F9 or its other variations. Table X shows the comparison between the two aforementioned buck converters. The comparison done

with the Pololu 9V converter can be applied to its 6V, 7.5V, and 12V counterpart since they're similar.

| | | |
|--------------------|----------------------------|-----------------------------------|
| Key Points | HILetgo MP2307 (10 Pieces) | Pololu 9V 2.3A D24V22F9 (1 Piece) |
| Cost | \$7.79 | \$9.95 |
| Input Voltage | 4.75V-23V | (for 2.3A) 10V-36V |
| Output Voltage | 1.0V-17V (Potentiometer) | 9V |
| Output Current | 1.8A | 1.5A-2.3A |
| Typical Efficiency | 80%-95% | 85%-95% |

Table 10: MP2307 and D24V22F9 Comparison

Although the Pololu buck converter is generally more efficient and has higher maximum specifications, the MP2307 is more suited for our application since it's cheaper and still has acceptable specifications. In addition, it also has a potentiometer that can adjust the output of the buck converter making it useful for testing. Another added bonus is that the product comes with 10 pieces, which again, is useful for testing purposes if somehow some of the converters became damaged during the process.

3.8 Battery Management System (BMS)

A battery management system, or BMS for short, is a system that manages a rechargeable battery. The BMS can be either analog or digital in nature and the way that it manages these rechargeable batteries is by monitoring, recording and calculating data, balancing it, and keeping it at the appropriate temperature. The BMS is an essential part of any system containing a battery, as it keeps the parameters of the battery, or batteries, in a reasonable set of bounds to prolong the life of the battery and the equipment that it is attached to.

The most important function of the BMS is monitoring the battery, when it does this it checks multiple metrics including: voltage, temperature, coolant flow, and current. When the BMS measures the voltage, it measures the total voltage, that of the individual cells, and that of the periodic taps. When it measures the temperature it measures the average, the coolant intake, the coolant output, or and the individual cells. When it measures the coolant flow, it checks either air or fluid cooled batteries. Lastly, when it checks for current it checks the amount coming in to or out of the battery. All of these metrics are essential for keeping the battery or batteries within safe operating parameters.

One benefit of the BMS is that it has the capability to measure each cell's voltage individually, and can inform you when one cell no longer reaches the threshold that is required. This allows for a quick response to replace the cells within a battery to keep it working as needed. Not only does the BMS measure individual cell voltage, but it also individually balances the cells. This allows for proper compensation so that the overall

health of the battery is not compromised. If a cell were to short circuit, and fail, the stability of the entire battery can be in jeopardy.

While certain types of batteries do not require a BMS, like lithium batteries, the benefits of having one far exceed the risks of not having one. Having the stability that comes with a BMS is not only a large benefit, but the capability to interface with other systems, and subsystems, in the overall product provides another layer of user interfacing that allows the product to go the extra mile.

3.8.1 What Makes Up the BMS?

The BMS architecture is typically built to include multiple functional blocks of components, typically including cutoff FETs, fuel-gauge monitor, cell-voltage monitor, cell-voltage balance, real-time clock, temperature monitor, and a state machine. [133] The basic layout of a BMS can be seen in the figure below:

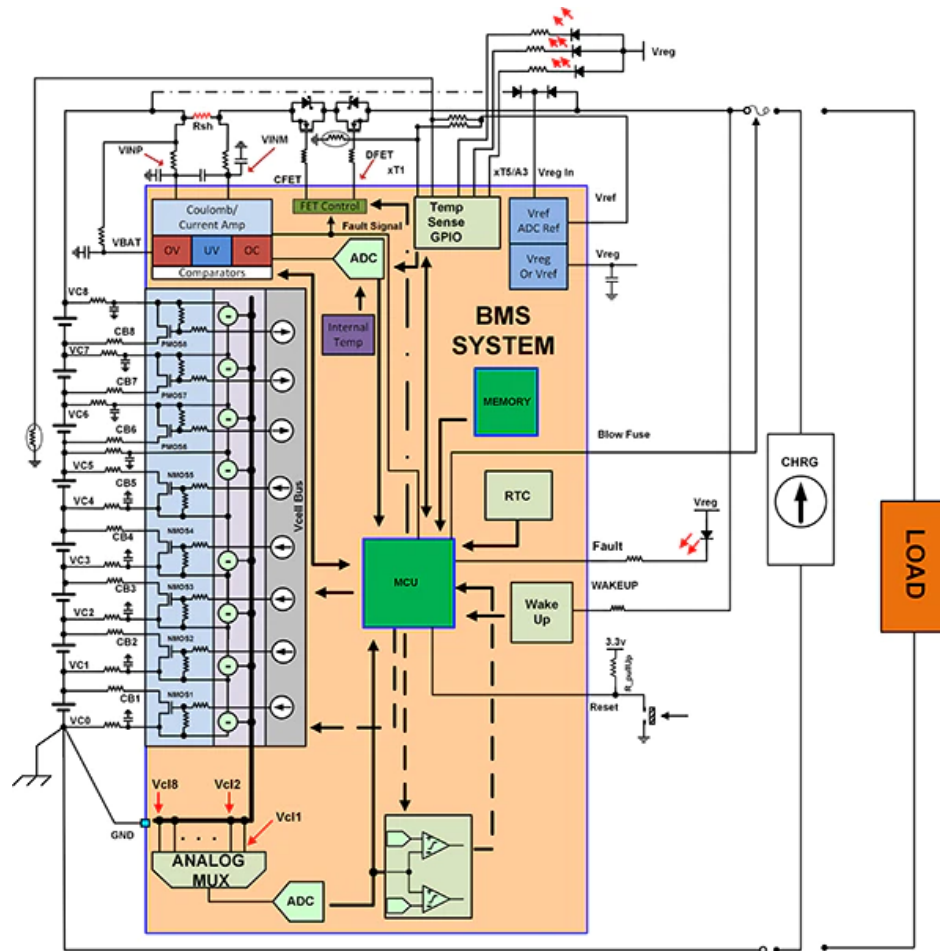


Figure 40: BMS System Diagram

The FET-driver is the section of the BMS that is responsible for the battery connection and the isolation between the load and the charger. Its behavior is affirmed from the measurements of the individual battery cell voltages, the current measurements, and the real time detection circuitry. Within the BMS setup there are two different types of

connections for the FET that are between the battery pack and the load and charger. The first setup shows the connection between the load and the charger. This can be seen in figure 41 below:

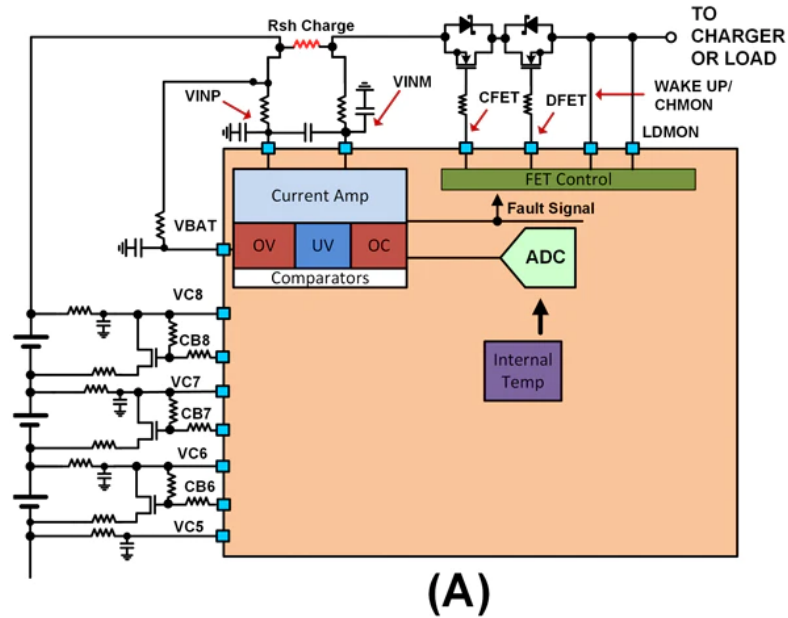


Figure 41: FET Connection Between the Load and Charger

The second setup is the one that allows for the possibility to charge and discharge at the same time. On top of this possibility, it also allows for the battery to be in use at the same time as it charges. This can be beneficial to extend the use time of the product in which it is attached to. The setup for this can be seen in figure 42 below:

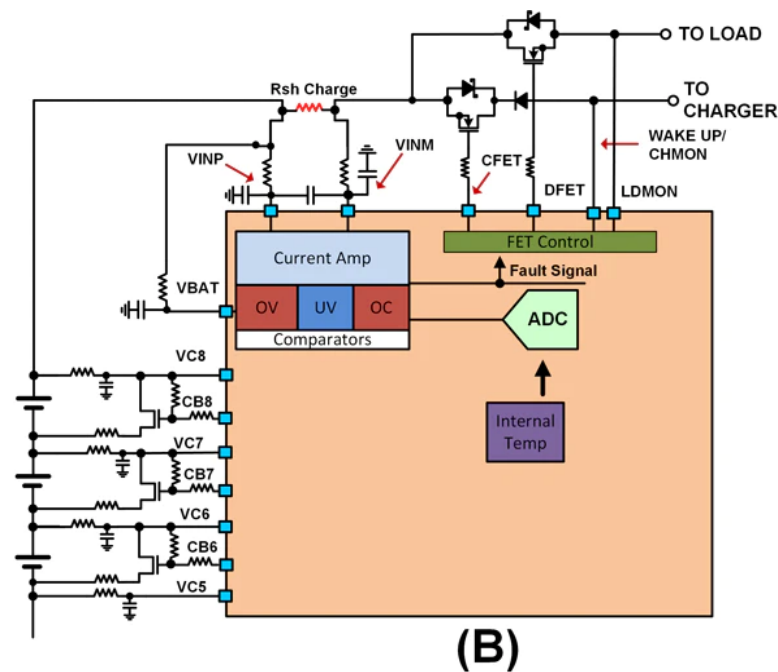


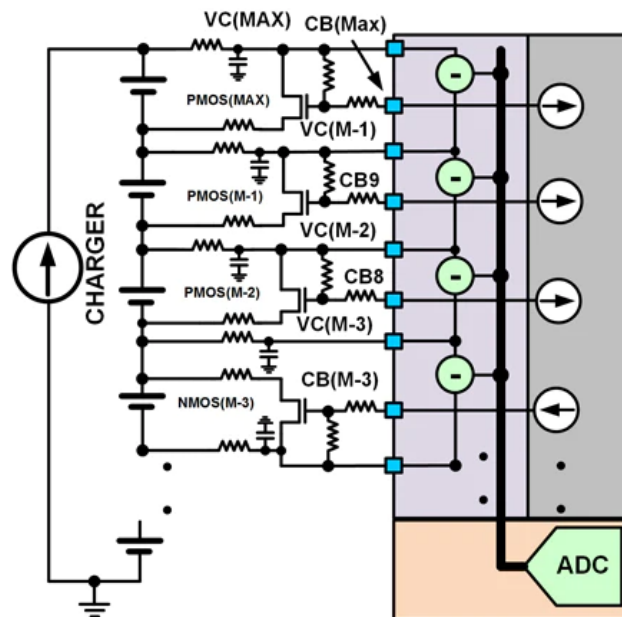
Figure 42: FET Setup of Simultaneous Charging and Discharging

The biggest benefit of the FET driver configurations is that they can be designed in a way that allows them to connect to either the low or the high side of a battery. The benefit of a low side connection to a better, is that it doesn't require the use of high voltage devices. Another benefit that is great from a business standpoint, is that this configuration can reduce the cost as it does not need a charge pump. When it comes to a high side connection, it opens the possibility of using a solid ground reference for the circuitry.

Another important function of the battery management system is monitoring the cell voltage of each individual cell. This is extremely vital as it determines the overall health of the battery, and ultimately will help the user extend the battery life. Battery cells can be connected in series or in parallel. If connected in series, it will increase the overall voltage and if connected in parallel it will increase the current drive. This is important because it will determine the cell voltage that you set for the BMS, and once you have this information the BMS can use it to determine if the battery is charged or not.

If the weakest cell reaches the charge limit first, then the rest of the cells can continue to fully charge. If the first cell reaches the set voltage limit, it will trip the battery charge limit. Unfortunately this charging set up does not allow for the maximum battery on time per charge, it actually reduces the lifetime of the battery because it requires more charge and discharge cycles.

To improve this, we slow the charge on the weakest cell which will require the connection of a bypass FET with a current limiting resistor across the cell. The result of this is that the other cells in the battery will be able to continue to progress and eventually catch up. Configurations for a bypass cell balancing FET can be seen below:



(A)

Figure 43: Bypass FET Slowing the Charge Rate

In figure 44 above, the bypass cell balancing FET slows the charge rate of the specific cell in the charge cycle.

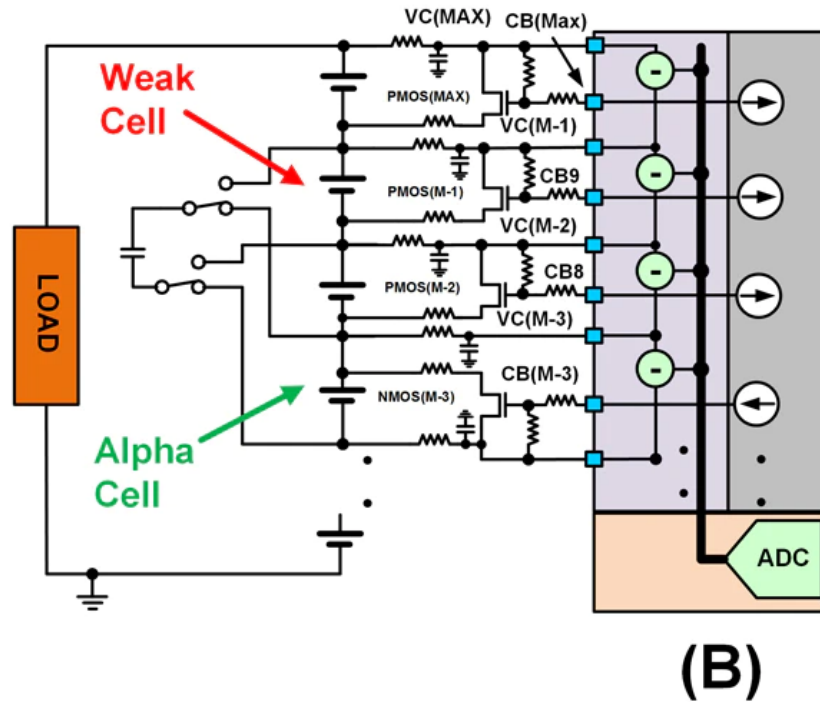


Figure 44: Active Balancing During Discharge Cycle

In figure 44 above, active balancing is used during the discharge cycle. This allows it to take the charge from a stronger cell and redirect it to a weaker cell.

The architecture for the BMS is vital to understanding how and why the BMS is such an important component of our project. The functions that the BMS is able to accomplish allows for the longevity of our battery and the individual cells as well as the longevity of the overall design. With a good BMS we can make a quality product for the consumer and still do so without exceeding a low budget.

3.8.2 Comparison of Different BMS's

After searching for many different LiFePO4 BMS's and comparing the specifications of each one, we did manage to settle on one. While comparing, I found four different BMS's that could potentially be used. The four models will have a brief summary in sub-sections of 3.8.3 with a comparison table seen below in section 3.8.2.4.

3.8.2.1 HEYO Smart BMS F4S12V60A BT

They HEYO Smart BMS is our first choice for a battery management system. The reason for this is because of the reliability it seems to have. Even though it is not the cheapest option of the four, it still has a reasonable price tag of \$45.92. A main option that we wanted to have with our battery management system is the NTC capability, and this specific battery management system has it. We also wanted to have the customization

option through the supplier that allowed us to adjust the strings in the event that we wanted to make a battery in parallel at a later date. The biggest bonus of choosing this model is the added smartphone app capability for the end user. Having this option allows the consumer to monitor the basic behavior of the battery from a distance.

3.8.2.2 DALY Waterproof LiFePO4 BMS

Our second choice was the DALY waterproof LiFePO4 battery management system because it is nearly identical to the HEYO BMS that we decided upon. The biggest differences between the two were that the DALY battery management system was not a smart system and it had to be bought in quantities of five. Even though this model is cheaper individually by a considerable margin, it was nearly double the cost to buy it in the larger quantity. A benefit that this model had over the HEYO model was the waterproofing ability, which could come in handy due to the device needing to be outside in the weather to charge.

3.8.2.3 MGod Smart LiFePO4 BMS

The third choice that we found while searching for a battery management system was the MGod Smart LiFePO4 BMS. This model had many of the same benefits found in the HEYO BMS model, but it had a longer lead time for shipping and did not have the option for customizability. We also noticed that it seemed to have a considerably lower review count than the HEYO model which led us to believe it was either less reliable or less tested in the market. This model was the cheapest to order at \$30.70 and like the HEYO BMS model, it could be ordered one piece at a time.

3.8.2.4 GFS-SP04S020 LiFePO4 Smart BMS

The GFS-SP04S020 LiFePO4 Smart BMS was our fourth, and last choice of the four different BMS models. This model did have smart system capabilities, but it did not have a case around the system and thus risked exposure to failing in a much faster period of time. This model also ended up being the most expensive model, both per piece and overall. Due to this BMS needing to be purchased as a quantity of two, and the price point of the individual piece, we placed it at the bottom of our choices.

Below is the table that was previously mentioned, it shows the comparison of each BMS for the specifications and the reasons for the order in which we placed our choices.

| Battery Management Systems | BMS Deciding Specifications | Reason(s) for Choice |
|--|---|---|
| <p><u>First Choice</u></p> <p>HEYO Smart BMS F4S12V60A BT</p> | <p><u>Rated Nominal Voltage</u></p> <ul style="list-style-type: none"> • 12 V <p><u>Rated Cell Voltage</u></p> <ul style="list-style-type: none"> • 3.2 V <p><u>Rated Amperage</u></p> <ul style="list-style-type: none"> • 60 A <p><u>Price</u></p> <ul style="list-style-type: none"> • \$45.92 | <ul style="list-style-type: none"> • Most reliable product found. • Customizable. • Smartphone App capability for the end user. • NTC Capability. |
| <p><u>Second Choice</u></p> <p>DALY Waterproof LiFePO4 BMS</p> | <p><u>Rated Nominal Voltage</u></p> <ul style="list-style-type: none"> • 12 V <p><u>Rated Cell Voltage</u></p> <ul style="list-style-type: none"> • 3.2 V <p><u>Rated Amperage</u></p> <ul style="list-style-type: none"> • 60 A <p><u>Price</u></p> <ul style="list-style-type: none"> • \$17.00 / 1 pc • \$80.00 / 5 pc | <ul style="list-style-type: none"> • Must buy in quantities of 5. • Waterproof. • Shipping time of 5-10 days. • Not a smart system. |
| <p><u>Third Choice</u></p> <p>MGod Smart LiFePO4 BMS</p> | <p><u>Rated Nominal Voltage</u></p> <ul style="list-style-type: none"> • 12 V <p><u>Rated Cell Voltage</u></p> <ul style="list-style-type: none"> • 3.2 V <p><u>Rated Amperage</u></p> <ul style="list-style-type: none"> • 60 A <p><u>Price</u></p> <ul style="list-style-type: none"> • \$30.70 | <ul style="list-style-type: none"> • Smart system. • NTC Capability • Programmable • Shipping time of 10-18 days. |
| <p><u>Fourth Choice</u></p> <p>GFS-SP04S020 LiFePO4 Smart BMS</p> | <p><u>Rated Nominal Voltage</u></p> <ul style="list-style-type: none"> • 12 V <p><u>Rated Cell Voltage</u></p> <ul style="list-style-type: none"> • 3.2 V <p><u>Rated Amperage</u></p> <ul style="list-style-type: none"> • 60 A <p><u>Price</u></p> <ul style="list-style-type: none"> • \$58.00 / 1 pc • \$116.00 / 2 pc | <ul style="list-style-type: none"> • Must buy in quantities of 2. • Does not come with a case over module. • Smart system. • Not free shipping. |

Table 11: Comparison of BMS's

3.8.3 Our Battery Management System

For our battery management system we are going to be using one that is meant specifically for a lithium iron phosphate battery. Due to our cells being connected in series as it is the preferred method for lithium cells, we will be utilizing a BMS with a single string. We have chosen the HEYO Smart BMS, in the F4S12V60A BT model. This specific BMS will allow us to monitor our cells via bluetooth with a smartphone

application. We feel that this allows for more peace of mind for the user as they do not have to be within an extremely close proximity of the device to monitor it. This specific model provides over charge protection, short circuit protection, UART function, and NTC capability. This model is also air cooled and will not require an external cooling component to prevent overheating.

This model of BMS is set up in a basic format with a positive pole labeled as B+ and a negative pole labeled as B-. The positive pole is designated as a red wire and connects to the last series of the battery pack while the negative pole is designated with a black wire and connected to the first series in the battery pack. These series' in the battery pack are then connected to a plug that will connect to the BMS. Below is the wiring diagram for the model of BMS that we will be using:

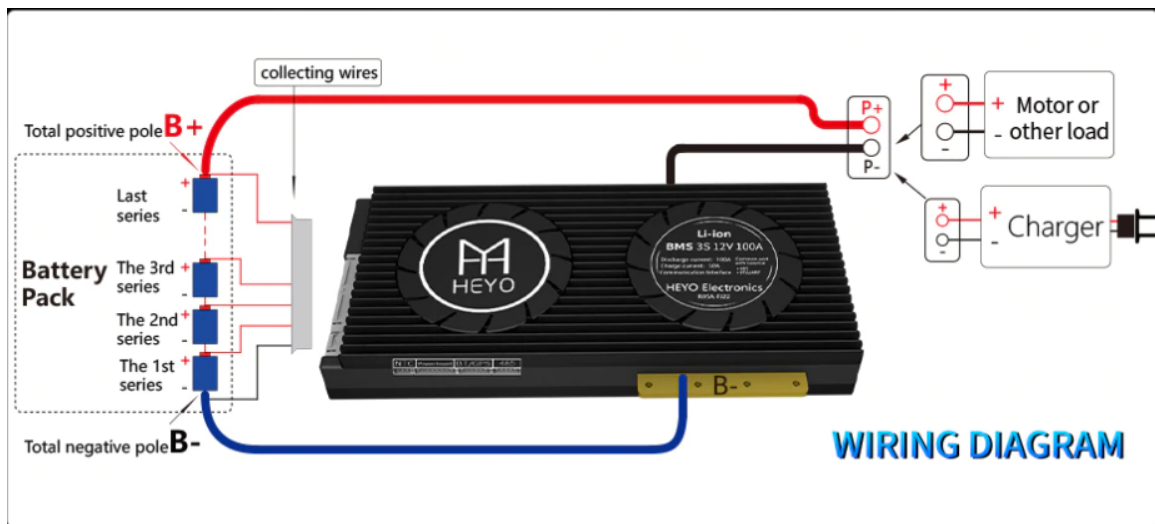


Figure 45: BMS Wiring Diagram

The next topic that will be discussed in this section is the parameters of the specific model of BMS that we have selected. This model through HEYO has the parameter list provided by the manufacturer. This parameter list goes over many different items to include: discharge, inner resistance, charge, over charge protection, balance, over discharge protection, overcurrent protection, short circuit protection, temperature protection, self consumption, working temperature, and storage temperature. These are all important parameters to know about the BMS so that when it is being operated with our device we know the limits of what it can be put under. The table will give us the description, specification, unit, and any potential remarks for each of these parameters. This table can be seen below:

| | Description | Specification | Unit | Remarks |
|----------------------------------|--|---|-------------|----------------|
| Discharge | Continue discharge current / Sparkle Current | 60 / 180 ± 30 | A / A | |
| Inner Resistance | Main circuit conduct inner resistance | ≤ 20 | mΩ | |
| Charge | Charge Voltage / Charge Current | 14.6 / 30 | V / A | |
| Over Charge Protection | Over charge detect voltage / protection delay / release voltage | 3.75 ± 0.05 / 1 / 3.65 ± 0.05 | V / S / V | Customizable |
| Balance | Balance detect voltage / release voltage / current | 3.2 / 3.2 / 30 ± 5mA | V / V / mA | |
| Over Discharge Protection | Over discharge detect voltage / detect delay / release voltage | 2.2 ± 0.05 / 1 / 2.3 ± 0.05 | V / S / V | Customizable |
| Overcurrent Protection | Over current detect voltage / detect delay | 1 / Off Load | MS | Customizable |
| Short Circuit Protection | Short circuit protection condition / detect delay / protection release condition | Short circuit of external load / 320 / Off load | μS | |
| Temperature Protection | Temperature protection | Charge: -40~65 Discharge -40~70 | °C | Customizable |
| Self Consumption | Working current / sleeping current | 20 / 200 | mA / μA | |
| Working Temperature | Temperature Range | -20~70 | °C | |
| Storage Temperature | Temperature Range | -40~80 | °C | |

Table 12: BMS Specifications Table

3.9 Rechargeable Battery

Before diving into our battery choice, it is important to understand the science behind high capacity electrolytic rechargeable batteries themselves, and the different types of high capacity electrolytic rechargeable batteries. Typically, batteries at their core are made up of multiple battery “cells” put together to achieve a desired voltage and capacity. These combined cells create chemical reactions between themselves which cause the electrons contained inside to flow, and thus create electricity. The three main components that make up a battery are the anode, the cathode, and an electrolyte. More specifically, the electrolyte which is generally an acid, is the substance inside that battery that allows the anode and the cathode to react thus creating electricity. These anodes and cathodes are composed of two different metals in order to react and create a potential difference. This is explained further below in section 3.9.1 and can be seen in figure 46 below for a better understanding of this concept. As shown in the previously mentioned figure, there is a positive terminal and a negative terminal (electrode). The anode can act as either the positive electrode, or the negative electrode as well as the cathode acting as a positive or negative electrode depending on whether the cell is a galvanic or electrolytic cell. This is explained further in sections 3.9.2. More specifically, this electricity or voltage rather, is created from the transfer of ions between the anodes/cathodes and the chosen electrolyte. One of the most basic representations that has been used for many years to explain this relationship is the lemon battery. This experiment uses a lemon, and two different types of metals, the metals being the anode and the cathode, and the lemon being acidic and thus being the electrolyte. Though very little voltage is created, the dissolving of the two different types of metals in the lemon juice creates a chemical reaction as described above, and thus creates said voltage. [79, 169]

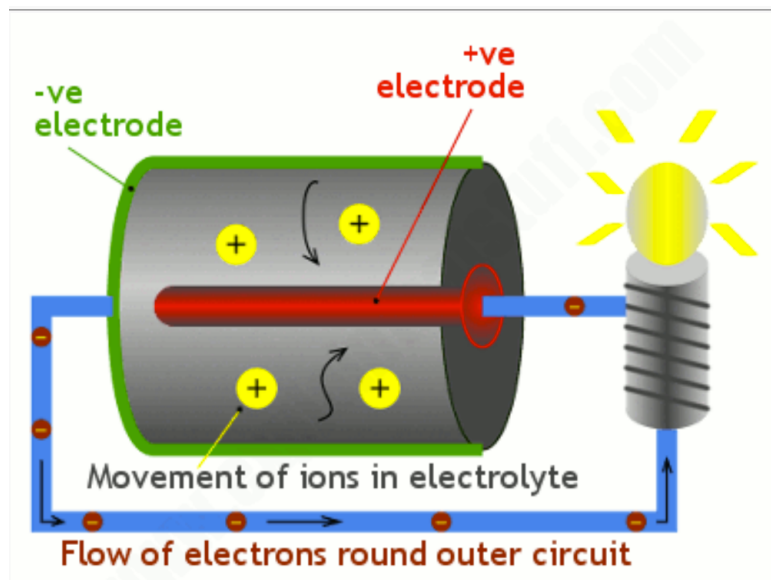


Figure 46: Potential Difference Between Two Electrodes

3.9.1 Voltage Characteristic (Redox Reactions)

Though seemingly simple, it is important to understand the voltage characteristics behind batteries. When further researched, the process for determining this voltage is far more

complex and hinges on the specific elements chosen for the anode and the cathode of the battery. The importance of these elements in terms of voltage is their individual potential values. This is where the idea of electrochemical series comes in. The electrochemical series is a list that reports the potential value of elements in increasing order. These elemental potential values are measured and listed by comparing the measured value of said elemental electrode to a hydrogen electrode. Hydrogen is used as a comparison to determine other elemental potential values due to the potential value of hydrogen being 0. [12] In this electrochemical series table, there are two main differences between the listed elements. These two main differences are whether or not the listed elements are electropositive, or electronegative. Electropositivity means that the specifically listed element is more prone to give up its electrons to the electrolytic solution it is exposed to. Conversely, an electronegative element is more prone to taking electrons from the electrolytic solution it is exposed to. This links with each element being either an oxidizing agent or a reducing agent. As previously mentioned above, in order for a battery to react with the present electrolyte and create a potential difference (electromotive force or EMF), one electrode of the battery must be an oxidizing agent, and one electrode must be a reducing agent. This is why these chemical reactions are known as oxidizing-reductions (redox) reactions. In the case of these elements, the ideal elements for an oxidizing element can be found at the top of the electrochemical series table, while the elements at the bottom of the table are ideal for reducing agents. This reaction can be characterized by the equation $E^{\circ}_{\text{cell}} = E^{\circ}_{\text{red}} + E^{\circ}_{\text{ox}}$. Taking the reverse chemical reaction into account, the equation can be rewritten as such $E^{\circ}_{\text{red}} + (- E^{\circ}_{\text{red}})$. From this equation, the previously described EMF value can be calculated thus determining the potential difference of the battery cell in question. [4, 32, 98]

3.9.2 Galvanic and Electrolytic Cells

As described above in section 3.9.2 the chemical reaction that takes place to produce a potential difference in a battery cell is called an oxidation-reduction (redox) reaction. In the case of battery cells, there are two different types of electrochemical cells where redox reactions happen. In this section, the first type (galvanic) will be explained. See the figure below for the composition of a galvanic cell. With galvanic cells the reactions that occur inside the cell are spontaneous reactions. This spontaneous chemical reaction takes place without the presence of stored electrical energy. Additionally, galvanic cells' anode operates as the negative electrode while the cathode operates as the positive electrode. Finally, the last main feature of galvanic cells is that of their physical composition. These cells have either a salt bridge connecting the two electrodes, or half-cells that are made separate by a porous membrane. This porous membrane is what allows the cell to react spontaneously as both the oxidizing and reducing agents come in contact with each other. [58, 107, 108, 137, 149]

The second type of electrochemical cell is an electrolytic cell. See the figure below for the composition of an electrolytic cell. The chemical reactions that take place in electrolytic cells conversely to galvanic cells are not spontaneous. With electrolytic cells, in order for the chemical reaction to take place inside the cell, the cell has to be attached to a power source to receive electrical energy. For electrolytic cells, the anode operates as the positive electrode while the cathode operates as the positive electrode. Unlike galvanic cells, electrolytic cells do not have to have a salt bridge present for the reaction

to take place. In the case of electrolytic cells, the ions of the oxidizing agent migrate through the electrolyte towards the cathode to be reduced, and the ions of the reducing agent migrate through the electrolyte towards the anode to be oxidized. [64]

Now the cells described above function independently of each other, but a cell can operate as a galvanic cell and an electrolytic cell at the same time under the correct conditions. This is the science behind rechargeable batteries. See section 3.9.4 for further discussion on this.

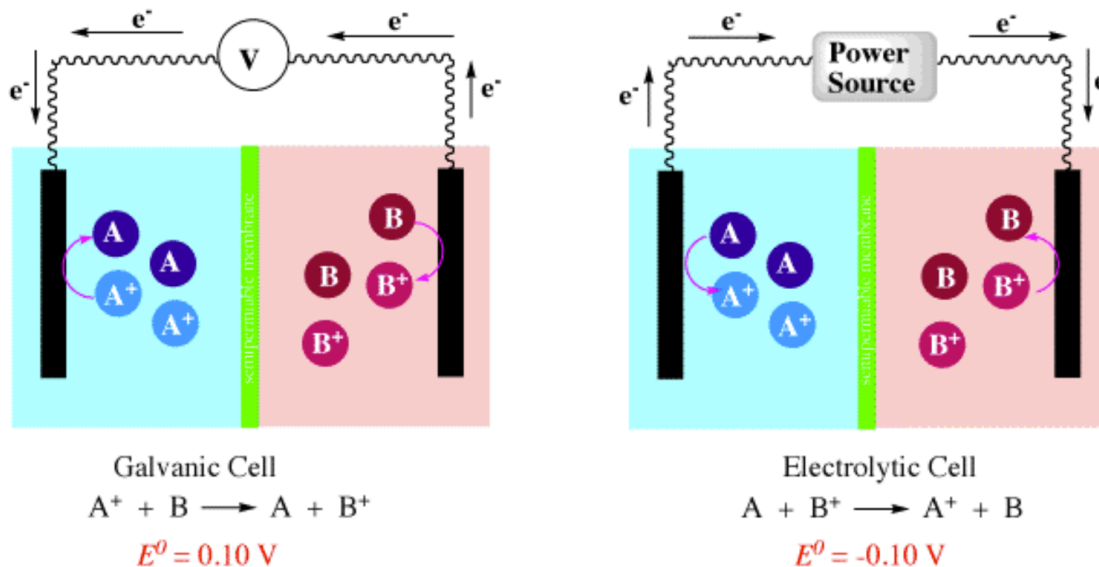


Figure 47: Galvanic and Electrolytic Cells

3.9.3 Rechargeable versus Non-Rechargeable

Now there are two important distinctions to make in the case of batteries. This distinction is what makes a battery rechargeable versus non-rechargeable. In the case of non-rechargeable batteries, the materials found in the anode and cathodes are used up after the previously described chemical reaction takes place enough times. Once this happens, the battery becomes dead, and is no longer usable. This type of battery is known as a primary battery. Conversely, rechargeable batteries have different chemical properties such that the chemical reactions inside the battery that discharge the battery can be reversed. This reversal of the electrochemical reaction happening inside the battery allows it to be recharged. Essentially, this reversal of the electrochemical reaction causes the electrons to flow in the opposite direction conversely to when the battery is being discharged thus charging said battery. The main aspect of a rechargeable battery that allows this process to happen is the ability for the anode and the cathode to return to their original state during the electrochemical reversal process. This is why as explained above, primary batteries cannot be recharged. Their anodes and cathodes degrade upon use, and cannot be reversed. In order to achieve this reversibility, the three main components (anode, cathode, and electrolyte) of the rechargeable batteries have to be chosen very carefully. If the wrong components are chosen, the anode and the cathode may deteriorate at a rate such that the electrochemical reaction cannot be reversed. All in all, the anode and cathode material has to be chosen such that their solubility in the chosen electrolyte isn't too high or too low. For example, take nickel cadmium

rechargeable batteries. The cadmium has two paramount features that makes it a perfect rechargeable battery electrode candidate. First off, the speed in which hydrogen forms on the cadmium electrode during the recharging process is quite slow. Next, cadmium has a low solubility rate such that it does not completely dissolve in the electrolyte solution chosen. These two aspects of cadmium allow it to hold near to the same composition upon discharge and recharge of the battery thus fulfilling that first main requirement of rechargeable batteries. This goes back to the concepts of galvanic and electrolytic cells described in section 3.9.3. In this example of the nickel cadmium battery, this explanation describes the process the cell undergoes when it is in an electrolytic state and charging the battery cell. As mentioned the oxidation rate of the cadmium from the migration of the nickel ions is quite slow, the reduction rate of the nickel from the cadmium ions is also quite slow. Because of the charge of each electrode in this process, the battery cell charges and the electrodes are maintained. From here, that same electrolytic cell can go into galvanic mode in which the electrodes' charges flip. This means the previous oxidizing agent becomes the reducing agent, and the previous reducing agent becomes the oxidizing agent. This reversal of electrode charges produces the reverse electron flow thus dispelling energy rather than taking it in. This is the power behind rechargeable batteries. [55, 150]

3.9.4 Discharge Rate (C-Rate)

With every battery, the main goal is for it to discharge energy in such a way that it can be used practically. The discharge rate is simply the rate over time in which the specified battery can discharge power. The discharge rate of a device can be modeled by what is known as a discharge curve. See the figure below for this concept.

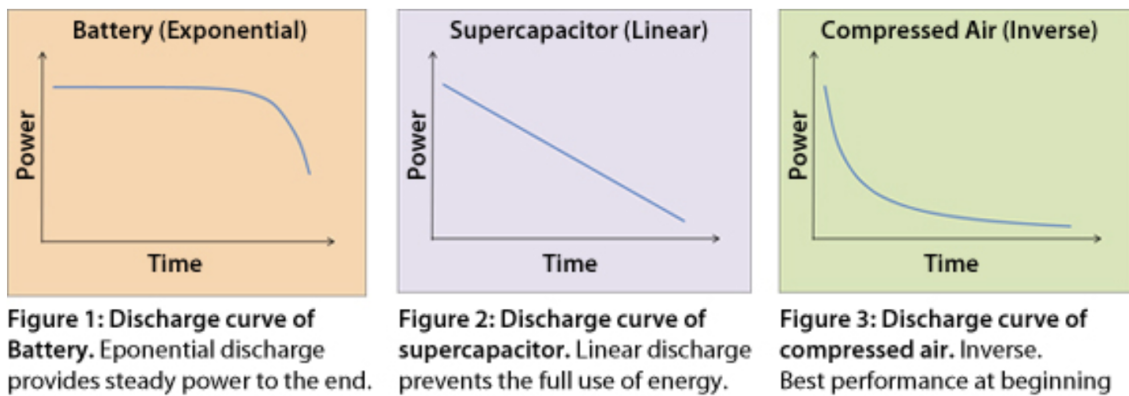


Figure 48: Discharge Curve of Battery Compared to Other Power Storage Devices

As one can see from the image above, the discharge rate of a battery provides a steady flow of power until the end in which the battery cuts off. This is what gives batteries an edge over other standard power storage devices. As seen above, other energy storage devices rapidly lose power flow as the time of discharge goes on. This can create significant problems. For example, if a device requires a steady power flow when being 3 charged by a device, out of these three options above, only a battery would work. If the other two options were chosen the battery of said device could be damaged upon charging. With this consistent discharge rate, it is important not to overstress the battery

for too long a period. If you discharge the battery at a rate it is not specified for for too long a period, it can severely damage the battery heavily reducing its efficacy. This discussed discharge rate of the battery is controlled by what is known as the C-rate. This C-rate more specifically controls the discharge rate and charging rate of a battery by scaling the power output. For example, many batteries are commonly classified as 1C batteries. This means that if said battery has a total capacity of 1Ah, the battery will discharge 1A for 1 hour. This means that this C-rate provides a one to one relationship with the discharge rate. Say the same capacity battery is instead rated as 5C. This means that the battery can discharge 5A for 12 minutes. This ability to increase discharge rate can be very useful for certain applications. For example, if one needed to fast charge their phone or their laptop, they could purchase a charger that had a higher C rating. Of course in this case, you would need to verify your device can receive battery at that rate. If you attempt to charge a battery at a discharge rate said battery is not rated for, you can severely damage it. [26]

3.9.5 Depth of Discharge/State of Charge

Depth of discharge and state of charge are very important concepts of batteries to understand. In the case of these concepts, it relates exclusively to rechargeable batteries. Though the concept is simple, it can be the difference between preserving a battery for many years and ruining it quite quickly. Depth of discharge is simply the percentage of a battery that has been discharged in relation to the remaining capacity of the battery. For example, if a battery holds 200Ah and 100Ah has been discharged, the battery's depth of discharge is 50%. This concept is very important to pay attention to when designing/purchasing a battery. In the case of depth of discharge, this value is specified by the manufacturer. Just because the capacity of your battery is 200Ah for example, does not mean you can discharge all 200Ah of battery capacity. Depending on the type of battery purchased, the manufacturer may only rate it for 85% depth of discharge. This means that a 200Ah battery should only be taken down to 30Ah of remaining capacity before recharging the battery. This concept is visually depicted in the figure below. If you continue to discharge the battery past the specified depth of discharge, it can begin to damage the battery and in the worst case scenario, render it unusable. State of charge is another important concept to understand when it comes to rechargeable batteries. This concept is essentially the opposite of depth of discharge. State of charge is the amount of remaining power in the battery compared to the amount of power discharged. This means that a battery's state of charge is 15%, the battery only has 15% capacity left. Similar to depth of discharge, some batteries can also be harmed if they are overcharged. Depending on the type of battery, the manufacturers may only rate the battery for 85% state of charge. This means the battery should not be charged over 85% of its nominally rated capacity. See the figure below for a visual representation of this concept.

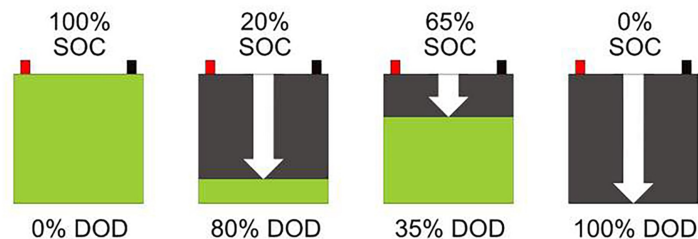


Figure 49: Depth of Discharge and State of Charge

In all cases with rechargeable batteries, the life of the battery is directly correlated with the amount one discharges the battery before charges. Even if you stay within the manufacturer's depth of discharge ratings, the life of the battery can be reduced if its capacity is being drained down to the maximum depth of discharge and recharged again. [27, 147]

3.9.6 The Effects of Ambient Temperature On Batteries

Another important factor to consider when designing/purchasing a battery is what temperatures it can handle. Naturally batteries in colder climates have reduced capacity, while batteries in higher temperature climates have a higher capacity. This is why the battery in a car will sometimes die in colder temperatures. Typically speaking, many batteries' capacity is rated when they are operating at room temperature. At freezing temperatures, a battery's capacity can be lowered as much as 20%. Conversely, at very high temperatures such as 122 degrees, a battery's capacity can be up to 12% higher. In both of these cases, these extreme temperatures can be very harmful to a battery. Specifically for extreme heat, the chemical reactions that are undergone inside the battery to produce power are increased. This increase in chemical reactions reduces the lifespan of the battery. This increase can also contribute to the thermal runaway process which is explained in section 3.9.10 below. In relation to extreme cold, the battery has to work harder to provide power and thus the lifespan of the battery is reduced. Now this effect temperature has on the battery also plays a large part when recharging a battery. Take a lead-acid battery for example. In high temperatures when charging a lead-acid battery, it can get overcharged due to the increased capacity mentioned previously. This increased charging can lead to what is known as gassing. Gassing is when one of the electrodes in a battery produces gas due to the chemical decomposition of water during the discharge or charging process. Conversely, when charging a lead-acid battery in low temperatures, it may be undercharged and then undergo what is known as sulfation. Sulfation is when a lead-acid battery does not contain enough charge such that large sulfate crystals form on the electrodes of the battery and reduce its efficacy. Though temperature needs to be considered for every type of battery, some batteries handle extreme temperatures better than others. In many cases, rechargeable batteries have built in battery management systems or (BMS) to provide high or low temperature protection such that the battery will not charge in extreme temperatures. More information on the BMS can be found in section 3.8. [16, 28, 62, 127, 146]

3.9.7 Deep Cycle Versus Non-Deep Cycle Batteries

When choosing a battery for a solar assembly, it's important to understand the difference between deep cycle and non-deep cycle batteries. A deep cycle battery is a battery designed to be able to produce steady amounts of power over a long period of time. Additionally, deep cycle batteries are designed to provide consistent power output with a high depth of discharge hence "deep" in deep cycle (See section 3.9.5 for more discussion on depth of discharge). In the case of deep cycle batteries, they can still produce a quick surge of power if needed, but not of the same magnitude of non-deep cycle batteries. Conversely an example of a non-deep cycle battery would be a car battery. A non-deep cycle battery is designed specifically to discharge a large amount of

power in short increments. For example starting your vehicle initially requires a large amount of power. With non-deep cycle batteries, they typically will not discharge more than 20 percent of their overall capacity. Because they are most commonly used in larger engine applications, the alternator in said engines provides the power once the engine is started by the battery. This is the ideal application for a non-deep cycle battery in order to increase its longevity. Non-deep cycle batteries are generally characterised by two ratings, cold cranking amps, and reserve capacity. Cold cranking amps are the amount of amps that can be produced by a battery at 0 degrees celsius for 30 seconds. Reserve capacity is the amount of amps a battery can deliver without being fully discharged. Deep cycle batteries perform well in terms of reserve capacity, but not as well in cold cranking amps. Conversely, non-deep cycle batteries perform well in terms of cold cranking amps, but not as well in reserve capacity. Deep cycle and non-deep cycle batteries both have the same exact chemistry when looking at equivalent battery types. The difference between the two is their plate thicknesses. A deep cycle battery has thicker plates in order for less current to flow and thus deliver a smaller amount of power over a longer period of time. A non-deep cycle battery has thinner plates in order for more current to flow thus delivering more power in a shorter period of time. In the case of our design, our lithium iron phosphate battery that we will choose needs to be a deep cycle battery. Since it is a part of a solar assembly, the battery will need to deliver consistent amounts of power for a longer period of time. Additionally, it will be discharged deeper depending on what the battery is charging. With these two constraints, it is clear why we need a deep cycle battery. [17, 166]

3.9.8 Battery Energy Density

Another important factor when choosing a battery is energy density. Energy is the amount of electrical energy that a battery holds proportional to its weight. Because of this relationship, the measurement for this function is given as Watt-hours per pound or (Wh/lb). Part of the methodology of achieving a higher energy density is linked with the amount of material inside the battery. Batteries with a higher energy density have a higher quantity of active material packed inside them. It's important to note that energy density should not be confused with power density. Power density is the rate in which electrical energy can be discharged, whereas energy density relates to the battery's capacity as stated above. Having a battery with a high energy density is preferable for many reasons, but one of the main reasons is due to the run time of the battery in relation to its size. The higher the energy density of a battery, the smaller the battery needs to be in order to output an equivalent amount of power to that of a larger battery with a lower energy density. This opens up a wide range of possibilities when it comes to batteries. In the case of our design, we want our solar assembly to be semi-portable. If we chose a 200Ah battery like in our design with a low energy density, its size would greatly inhibit its portability. Because of this, for our design, it's important that we focus on battery types that have a high energy density in order to fulfill our self-imposed requirement of portability. It's important to note that it can be dangerous if a battery's energy density is too high. As previously explained above, higher energy density batteries have more active material packed inside them. Because of this, higher energy density batteries are more prone to thermal runaway which was explained in section 3.9.10 below. [17]

3.9.9 Thermal Runaway

Thermal runaway is a concept that is crucial to understand when designing a battery assembly. As explained above in order to achieve a higher energy density, manufacturers/designers of batteries have packed them full of more active material. This higher amount of active material causes rechargeable batteries to be more prone to thermal runaway. With all rechargeable batteries, during the charging process there is a large amount of heat generated. Typically, this heat is removed naturally by escaping the battery assembly. In some cases when the heat created by the reaction in the battery charging process can not escape at a fast enough rate, it can cause the battery to overheat and fail. More specifically, this overheating process happens from lack of cooling as previously explained, which then leads to a lower internal resistance and thus increasing the charging current and creating too much heat. This failure causes the battery cells to dry up, and even melt. In the worst cases, batteries can even explode when under these conditions for an extended period of time. This failure can lead to serious damage and expulsion of highly toxic chemicals. This is the concept of thermal runaway. Though all types of rechargeable batteries can suffer from thermal runaway, as previously mentioned above, certain types with a higher energy density are more prone to it. This higher energy density leads to more heat being created during the charging process hence the higher chance of suffering from thermal runaway. For example, lithium-ion batteries have a high energy density, and are some of the most commonly known batteries to suffer from thermal runaway. They require more extensive maintenance and cooling in order to prevent said thermal runaway. So, how can thermal runaway be prevented? The three main aspects to prevent thermal runaway are doing regular check ups on a battery's charging voltage and current, providing ample cooling to the battery during the charging process, and storing the battery in environments where the ambient temperature is not extreme. If each of these steps are followed during the battery charging process, the chances of encountering thermal runaway in a battery are quite small. [49]

3.9.10 Rechargeable Deep-Cycle Battery Types

In the following section different types of commonly known rechargeable deep cycle batteries will be discussed. After discussing each type of battery below, we will outline the features each battery offers.

3.9.10.1 Nickel Cadmium Batteries

The first type of rechargeable battery to be discussed is the nickel cadmium battery. This type of battery was the second rechargeable type of battery behind lead acid batteries to be commercially released. The two main components for the electrodes are nickel hydroxide and cadmium hence nickel cadmium. In the charged state, the nickel hydroxide acts as the positive electrode, and the cadmium acts as the negative electrode. In the case of nickel cadmium batteries, potassium hydroxide is used for the electrolyte. Nickel cadmium batteries are hardy and forgiving. One drawback to nickel cadmium batteries is that of their memory effect. With nickel cadmium batteries, they have to be fully discharged before recharging, otherwise the battery "remembers" the previous charge and

then results in a loss of capacity. Additionally, because of the low energy density of nickel cadmium batteries each cell has a voltage of only 1.2V meaning for higher capacity systems, one would need many cells. [22,73, 118]

3.9.10.2 Nickel-Metal-Hydride Batteries

The second type of rechargeable battery to be discussed is the nickel-metal-hydride battery. This battery came after nickel cadmium batteries. The two main components for this type of battery are nickel hydroxide, and metal hydride which is the hydrogen storing metal alloy. In this case, the positive electrode is the nickel hydroxide, and the negative electrode is the metal hydride. Similar to nickel cadmium batteries, the most common electrolyte used in the composition of these batteries is potassium hydroxide. Unlike nickel cadmium batteries, nickel-metal-hydride batteries are not hardy and forgiving. They are quite fragile and have a very high self discharge rate making the charging process more complicated. Conversely, they have a higher energy density than that of nickel cadmium batteries. Nickel-metal-hydride batteries also suffer from the same memory effect as nickel cadmium batteries as described above in section 3.9.11.1. [150]

3.9.10.3 Lithium-Ion Batteries

The third type of rechargeable battery to be discussed is the lithium-ion battery. In terms of application, this battery type is one of the most commonly used in everyday devices such as laptops and cell phones. In the case of these batteries, the positive electrode is composed of lithium metal oxide, and the negative electrode is composed of graphite, or carbon. The most commonly used electrolyte for lithium-ion batteries is lithium salt dissolved in an organic solvent. Due to the composition of lithium-ion batteries, during the discharge process, the lithium ions move from the negative electrode to the positive electrode, and then reverse directions during the charging process. Additionally, lithium-ion batteries do not have any actual lithium metal inside, but rather just the lithium's ions due to lithium metal's instability. Lithium-ion batteries have one of the highest energy densities of any rechargeable battery on the market. This also means that they are one of the most susceptible batteries to thermal runaway due to the high amount of active material inside them. Overall, lithium-ion batteries are quite low maintenance in comparison to nickel based batteries. This low maintenance is due to their very low self-discharge rate, and not suffering from the memory effect explained for the nickel battery types. This means that lithium-ion batteries do not need to be fully discharged before recharging. Lithium-ion battery cells typically have a nominal cell voltage of 3.6V. Another strength of lithium-ion batteries is their rated depth of discharge. Typically, manufacturers of lithium-ion batteries claim that lithium ion batteries can be taken to 100% depth of discharge. This means that these batteries can be fully discharged without having harmful long term effects or significant loss of discharge. Though manufacturers claim this, it is recommended not to go below 80% depth of discharge with these batteries to maintain better battery health. [18, 23, 34, 97]

3.9.10.4 Sealed Lead Acid Batteries (SLA)

The fourth type of rechargeable battery to be discussed is the sealed lead acid battery. In the case of these batteries, the positive electrode is composed of lead oxide, and the

negative electrode is composed of lead. In the case of the lead used for the negative electrode, small traces of other metals are added due to pure lead being too soft to use by itself. Two elements typically combined to make this lead alloy are calcium and antimony. The most commonly used electrolyte for sealed lead acid batteries is sulfuric acid. Rather than being flooded, the electrolyte is sealed inside the battery which negates the apparent maintenance needs for flooded lead acid batteries. The two main options for this sealed electrolyte are AGM and gel sealed lead acid batteries. For the gel variant, the acid is suspended in a gel that is created by combining the acid with gelling agents. Similar to nickel-metal-hydride batteries, sealed lead acid batteries are not particularly durable when being deep cycled. When fully deep cycled, the amount of rechargeable cycles falls drastically. This lack of durability for lead acid batteries is due to the corrosion caused on the positive electrode and the consistent reduction of the active material contained inside the lead acid battery. Though there are apparent negatives, sealed lead acid batteries are some of the cheapest rechargeable batteries on the market. They have a surprisingly high energy density for their price in comparison to the nickel based batteries listed in sections 3.9.11.1 and 3.9.11.2. Additionally, sealed lead acid batteries perform well in low temperatures due to their compositions whereas lithium-ion batteries do not. Just like lithium-ion batteries, sealed lead acid batteries do not suffer from the memory effect like nickel based batteries. Sealed lead acid batteries typically have a nominal cell voltage of 2V. Sealed lead acid batteries have a much different recommended depth of discharge rating than that of lithium ion batteries. Most manufacturers recommend not to take sealed lead acid batteries below 50% depth of discharge lest the battery suffer heavy capacity losses. [21, 25, 69, 162]

3.9.10.5 Lithium Iron Phosphate Batteries

The fifth and final type rechargeable battery to be discussed is the lithium iron phosphate battery. This “offshoot” of lithium-ion batteries is newer technology and has been around for a much shorter period of time than the batteries listed above. In the case of lithium iron phosphate batteries, the positive electrode is composed of lithium iron phosphate and the negative electrode is composed of graphite or carbon. Just like standard lithium-ion batteries, lithium iron phosphate batteries most commonly used electrolyte is that of lithium salt dissolved in an organic solvent. Lithium iron phosphate batteries have a lower energy density to that of their lithium-ion counterpart, but they offer increased stability because of their low resistance values. This is due to the phosphate material used in the cathode. This increased stability causes lithium iron phosphate batteries to be much safer than their standard lithium-ion battery counterparts. Compared to lithium ion batteries, lithium iron phosphate batteries the chances of thermal runaway occurring are very low. In terms of maintenance, lithium iron phosphate batteries can handle higher voltages for a longer period of time than their lithium ion counterparts, adding to their longevity. This increase in longevity makes lithium iron phosphate a titan for applications where a high cycle count is needed. A drawback to lithium iron phosphate battery cells is that they have a higher self discharge rate than that of their lithium ion phosphate counterparts. This can sometimes create issues with the balancing of each individual cell in the battery. This can be remedied with high quality cells and a good BMS (Section 3.8) system. Lithium iron phosphate batteries also do not suffer from the memory effect like nickel based batteries. Typically, lithium iron phosphate battery cells have a nominal voltage of 3.2V. Just like lithium-ion batteries, lithium iron phosphate battery

manufacturers claim that these batteries can be taken down to 100% depth of discharge. With lithium iron phosphate batteries they should only be taken to 80% depth of discharge to help maintain battery life just like their lithium-ion counterpart. Finally, unlike the previous batteries listed, lithium iron phosphate is one of the only types of batteries that offer high capacity cells that can be purchased and connected rather than buying a pre-built battery. [10,68,75]

3.9.11 Battery Options

Now that each of the major types of rechargeable batteries have been discussed, this section will be used to summarize characteristics of different battery options. These summarizations will be used to compare each option, and provide a basis for our battery choice. This decision will help us decide whether to buy a pre-built battery, or design our own using battery cells. Note: nickel cadmium and nickel-metal-hydride battery options will not be listed due to them not being viable for our project. Their discussion was used for a better understanding of rechargeable deep cycle batteries as a whole. Since we are designing a solar system that will be discharged and recharged at different rates, we need a deep cycle battery that does not suffer from the memory effect of nickel based batteries. [20]

3.9.11.1 (4) VariCore 3.2V 200Ah Lithium Iron Phosphate Battery Cells

The first option we explored was buying (4) 3.2V lithium iron phosphate cells rated for our desired capacity of 200Ah, and connecting them together in series ourselves. Copper connector plates and metal screws for the connections are also provided. [24] There are many options for high capacity lithium iron phosphate cells, but this found option provided the desired specifications alongside a good price point. We chose this as an option in order to add an extra layer of design to our project. Creating your own battery from bought cells is much cheaper than buying a pre-built battery, but there are several aspects to be considered. When ordering battery cells, there is a higher chance one or more can be damaged or faulty than ordering an already tested and assembled battery. Additionally, a BMS has to be added as this (4) cell option does not come with one. Finally, an enclosure has to be designed to seat the cells and BMS in otherwise the cells will be exposed. The maximum discharge rate when (4) of these described cells are connected in series is 3C. The maximum charging current for this assembly is rated as 1C. The nominal voltage of the assembly is $(3.2V) * 4 = 12.8V$. The maximum charging voltage for the assembly is 14.6V. The total weight of the assembly is roughly 34 lbs. Finally, the price of the assembly not including the previously mentioned BMS is \$317.04. [50]

3.9.11.2 Expert Power 12V 200Ah Lithium Iron Phosphate Battery

The second option we explored is the Expert Power 12V 200Ah lithium iron phosphate battery just like the first, but the battery is already assembled and has a built-in BMS. This option provides convenience and less room for error since we would not have to design the battery and configure a separate BMS ourselves. Additionally, this battery comes in a marine grade rated sealed enclosure meaning it can be used in more extreme conditions. The maximum discharge rate for this battery is rated at .75C. The maximum

charging current is rated at .25C. The nominal voltage rating of this battery is 12.8V, and the maximum charging voltage is 14.4V. As previously mentioned this assembly has a built in BMS (Reference section 3.8 for BMS information). The total weight of the battery assembly is 48.3 lbs. Finally, the price of the assembly is \$1349.99. [63]

3.9.11.3 LBP 12V 200Ah Lithium-Ion Battery

The third battery option explored is the LBP 12V 200Ah lithium ion battery. Just like the previous option, this battery has a built-in BMS. Unlike the previously mentioned options, this battery is lithium-ion instead of lithium iron phosphate. This battery is not marine rated, but it is rated to resist fresh water and dust. The maximum discharge rate for this battery is rated at .5C. The maximum discharge current is rated at .5C. The nominal voltage rating of this battery is 13.8V, and the maximum charging voltage is 14.4V to 14.46V. The total weight of the battery assembly is 72 lbs. Finally, the price of the assembly is \$2099.99.

3.9.11.4 Renogy 12V 200Ah AGM Battery

The fourth and final type of battery option to be explored is a 12V 200Ah AGM battery (sealed lead-acid type battery). Due to the composition of this AGM battery, a BMS would have to be externally added similar to the battery cells option discussed in section 3.9.11.1. This battery is rated to resist fresh water and dust similar to the option discussed in 3.9.11.3. The maximum discharge rate for this battery is rated at .5C. The maximum discharge current is rated at .3C. The nominal voltage rating of this battery is 12.0V, and the maximum charging voltage is 13.6V to 13.8V. The total weight of the battery assembly is 127.9 lbs. Finally, the price of the assembly is \$399.99.

3.9.12 Our Battery Choice

As shown below, we will be going with (4) VariCore 3.2V 200Ah lithium iron phosphate battery cells. First and foremost these cells were the cheapest option making them budget friendly for senior design. These cells have much higher discharge and charging rates than their already assembled competitors. Note: These rates will be governed by our chosen BMS which can be found in section 3.8 meaning each of these rates will be much lower. Nonetheless, if we upgraded our BMS we would have the ability to scale these rates up if needed. Additionally, by purchasing our own cells, we get to learn the battery cell compositions process which adds an additional design component to our project. These cells being lithium iron phosphate was another one of the main deciding factors. As described in section 3.9.10.5, lithium iron phosphate batteries are some of the safest high capacity battery types that also offer a high energy density. Additionally like all batteries in the lithium-ion family, lithium iron phosphate batteries can be taken to a very deep depth of discharge (recommended maximum of 80%).

| Battery | Battery Deciding Specifications | Reason(s) for Choice |
|---|---|--|
| <p><u>First Choice</u></p> <p>(4) VariCore 3.2V 200Ah lithium iron phosphate battery cells</p> | <p><u>Nominal voltage rating</u></p> <ul style="list-style-type: none"> • 12.8V <p><u>Max discharge rate</u></p> <ul style="list-style-type: none"> • 3C <p><u>Max charging rate</u></p> <ul style="list-style-type: none"> • 1C <p><u>Max charging voltage</u></p> <ul style="list-style-type: none"> • 14.6V <p><u>Weight</u></p> <ul style="list-style-type: none"> • 34 lbs <p><u>Price</u></p> <ul style="list-style-type: none"> • \$317.04 | <ul style="list-style-type: none"> • Lowest price out of all the listed options • Highest max discharge rate • Highest max charging rate • LiFePO4 is the safest and has the greatest depth of discharge capabilities • Self assembly =better for design project • Scalability |
| <p><u>Second Choice</u></p> <p>Renogy 12V 200Ah AGM battery</p> | <p><u>Nominal voltage rating</u></p> <ul style="list-style-type: none"> • 12.0V <p><u>Max discharge rate</u></p> <ul style="list-style-type: none"> • .5C <p><u>Max charging rate</u></p> <ul style="list-style-type: none"> • .3C <p><u>Max charging voltage</u></p> <ul style="list-style-type: none"> • 13.6-13.8V <p><u>Weight</u></p> <ul style="list-style-type: none"> • 127.9 lbs <p><u>Price</u></p> <ul style="list-style-type: none"> • \$399.99 | <ul style="list-style-type: none"> • Very good price for already being assembled and ready to use • Acceptable discharge rates for large price difference compared to other pre-assembled batteries |
| <p><u>Third Choice</u></p> <p>Expert Power 12V 200Ah lithium iron phosphate battery</p> | <p><u>Nominal voltage rating</u></p> <ul style="list-style-type: none"> • 12.8V <p><u>Max discharge rate</u></p> <ul style="list-style-type: none"> • .75C <p><u>Max charging rate</u></p> <ul style="list-style-type: none"> • .25C <p><u>Max charging voltage</u></p> <ul style="list-style-type: none"> • 14.4V <p><u>Weight</u></p> <ul style="list-style-type: none"> • 48.3 lbs <p><u>Price</u></p> <ul style="list-style-type: none"> • \$1349.99 | <ul style="list-style-type: none"> • Second best max discharge rate • LiFePO4 is the safest and has the greatest depth of discharge capabilities • Built in BMS • Marine grade rated=very durable |

Table 13: Battery Comparison

3.10 Inverters

Inverters are devices used for the conversion of DC or direct current power to AC or alternating current power. These devices are so extensively used throughout electronics that we fail to realize how vital they are to our everyday lives. Today when we use power from the grid to power our appliances at home they require an inverter to appropriately transmit the required energy supplied.

3.10.1 Power Factor and Total Harmonic Distortion

Two ways that inverters are judged in quality is by an effect called total harmonic distortion along with power factor. These effects are crucial to understanding power systems as the goal in most cases is to mitigate total harmonic distortion in order to attain a “higher power factor, lower peak currents, and higher efficiency”. In introductory AC circuits we are taught how the phase angles of voltage and current relate to power factor or expressed as an equation can be written as $\text{power factor} = \cos(\theta_v - \theta_i)$. This is a valid equation only when the current and voltage are purely sinusoidal. The equation previously is the displacement equation and the more refined definition of power factor is given to be $\text{power factor} = \frac{P_{\text{average}}}{V_{\text{rms}} * I_{\text{rms}}}$. If the load connected to the source is purely resistive then the rms (root mean squared) voltage and current can be expressed respectively as the following: $V_{\text{rms}} = \frac{V_{\text{Peak}}}{\sqrt{2}}$ and $I_{\text{rms}} = \frac{I_{\text{Peak}}}{\sqrt{2}}$. The power factor in a purely resistive circuit is 1. This is shown in figure 50 below. Notice how the current and voltage are in phase with one another. In figure 51 we can see that in an inductive load the voltage leads the current indicating a phase shift between the two. In Figure 52 we can observe that in a capacitive load the current leads the voltage also indicating a phase shift between the two. To counteract this a “compensation” of power must be added in the form of reactance or better known as power factor correction to offset the phase shift explained earlier. [92,167]

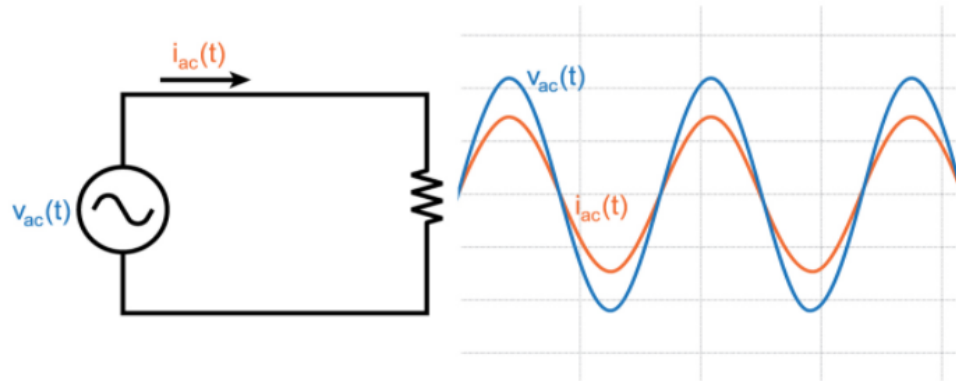


Figure 50: Purely Resistive Circuit Current and Voltage Phase

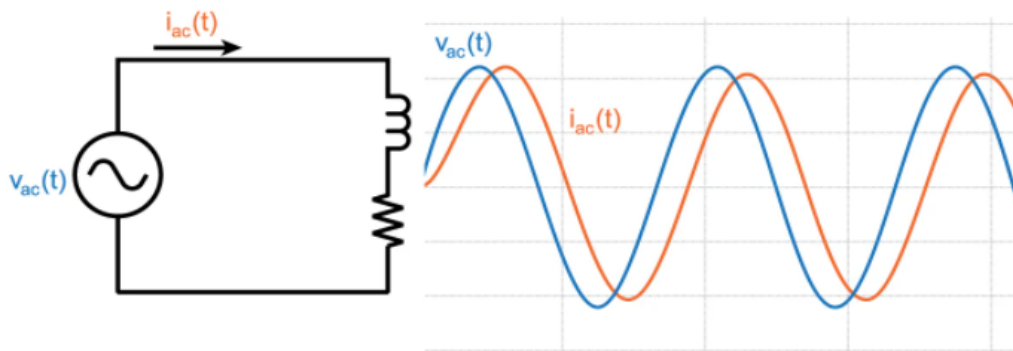


Figure 51: Inductive Circuit Current and Voltage Phase

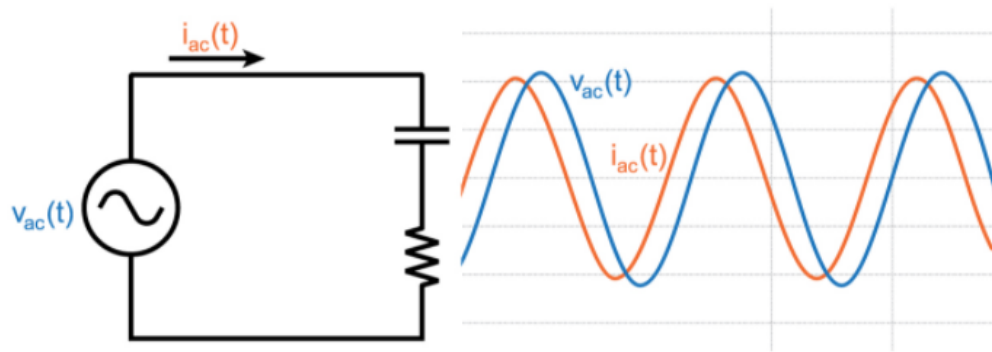


Figure 52: Capacitive Circuit Current and Voltage Phase

As a result of this power factor correction, we must alter the power factor equation to account for total harmonic distortion as some loads will not be fully resistive. In a lot of cases conversion of AC to DC or DC to AC causes the current to not be sinusoidal and this all ties back into why total harmonic distortion and power factor correction go hand in hand when choosing the correct inverter to use in our project. When we said that the current in these systems is no longer sinusoidal but is still periodic this causes the current to be able to be described in terms of harmonic distortion. Since each of the harmonics of the current has a root mean squared value, calculating the rms value of each harmonic requires a summation of all the rms values of the harmonic. Once this is obtained then the next thing to look out for is whether your output is producing real power or apparent power. Real power is produced at the fundamental frequency while apparent power is produced as a result of all of the current harmonics. [92,167]

$$PowerFactor = \frac{P_{avg}}{(V_{rms})(I_{rms})}$$

Equation 1: Power Factor in RMS

$$I_{rms} = \sqrt{I_{dc}^2 + \sum_{k=1}^{\infty} I_{k,rms}^2}$$

Equation 2: Harmonic Current

$$P_{avg} = V_{1,rms} \times I_{1,rms} \times (DisplacementFactor)$$

Equation 3: Apparent Power

$$PowerFactor = \frac{V_{1,rms} \times I_{1,rms} \times (DisplacementFactor)}{V_{1,rms} \times \sqrt{I_{dc}^2 + \sum_{k=1}^{\infty} I_{k,rms}^2}}$$

Equation 4: Revised Power Factor

$$= \frac{I_{1,rms}}{\sqrt{I_{dc}^2 + \sum_{k=1}^{\infty} I_{k,rms}^2}} \times DisplacementFactor$$

Equation 5: Simplified Power Factor

As you can see above when determining power factor we first start with the basic power equation in rms format. Then we must include the harmonics of each current (Equation 2) as well as the apparent power which already has all of the harmonics included (Equation 3). To find the power factor we must substitute these two equations into equation 1 and the resulting equation 4 is shown. With a bit of manipulation we can simplify the power factor to that of equation 5. Notice that in the first term of equation 5 we can accurately observe the distortion factor that accrues from the multiple harmonics of the current. Moving on to how the distortion factor relates to total harmonic distortion we can see that THD is related in the following way in equation 6. We can relate the distortion factor to the measurement of THD by using the equation 4 equation 5 to get the relationship between the two quantities and is shown in equation 7. The final power factor is the most correct version shown in equations 8 and 9. In our project we will have to consider total harmonic distortion as well as the displacement factor so that we can have an efficient inverter that outputs real power at an optimal rate. [92,167]

$$THD = \frac{\sqrt{\sum_{k \neq 1} I_{k,rms}^2}}{I_{1,rms}}$$

Equation 6: Total Harmonic Distortion

$$DistortionFactor = \sqrt{\frac{1}{1 + THD^2}}$$

Equation 7: Relating Distortion Factor to THD

$$PowerFactor = DisplacementFactor \times DistortionFactor$$

Equation 8: Revised Conceptual Power Factor

$$PowerFactor = \cos(\theta_v - \theta_i) \times \sqrt{\frac{1}{1 + THD^2}}$$

Equation 9: Revised Mathematical Power Factor

3.10.2 Different types of inverters

We have already established what an inverter is. It is a device that converts direct current or DC voltage into alternating current or AC voltage. The variable AC can have changing voltage magnitude, number of frequency, phases or phase difference. In sections 3.10.4 through 3.10.6 below, we classify three types of inverters based on their output characteristics: Square wave, modified sine wave, and (pure) sine wave.

3.10.3 Square wave inverters

Starting with the square wave it is by far the cheapest and least complex to understand, but the tradeoff is that it is the least used type as it offers low power quality due to total harmonic distortion of upwards of around 45 percent [134]. As a result, many if not all appliances today will not be able to run appropriately as many of these are using pure sine waves. Not only is this inverter impractical due to major losses, but it may result in damage to internal circuitry of any appliance that does not run off of the sine wave. The only thing that this inverter may be used for would be for tools which run on a universal motor. In figure 53 below we can see that a square wave is composed of a fundamental sine wave which is at the same frequency as the square wave along with the 3rd and the 5th harmonic. More odd harmonics are contained within the square wave but are not shown. As a result of these harmonics, “noise” or interference is produced which can and will damage most electronics over time. One method of producing this type of output is to use an H bridge which will turn the DC applied voltage to square wave output across an applied load. Filtering out some of the harmonics can reduce the losses output but it is still not practical to use this type of inverter for many devices today.[128,134,179]

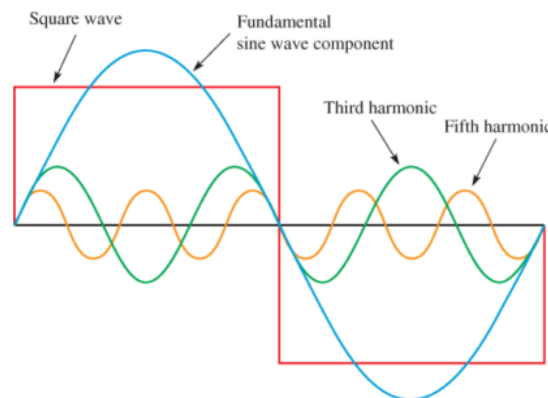


Figure 53: Harmonics of a Square Wave Inverter Output

3.10.4 Modified square wave inverters

The modified sine wave type (which are actually modified squares) provide block-like pulses with some inactive areas in around the positive and negative half cycles. These are basically constructed using two square waves. The modified square wave inverter is simpler to construct than the pure sine wave but a bit more difficult than a simple square wave inverter. They are useful and appropriate for many electronic loads but the tradeoff is a total harmonic distortion of around 24% [134]. The modified sine wave inverter is also one of the most used low cost inverters on the consumer market, most notably in car industries. In figure 54 below we can see the waveform of a modified square wave. Notice how it resembles a “sinusoid” but it is blocky and choppy in the way that it is constructed. Since the waveform is “closer” to that of a sine wave but retains its square characteristics it offers more efficiency than a square wave but not as much as a pure sine wave. A few more observations can indicate that if you wanted to reduce the THD even more you would need to use filters to block the interference that this type of inverter produces but this comes at a cost of power reduction to the load which leads to an efficiency decrease. Notice once again in figure 54 that there are three specific “levels” contained within this waveform: Peak voltage V_o , peak voltage $-V_o$, and zero. If we were to add more voltage levels we would make this inverter significantly more efficient. So much more efficient in fact that if we were to add an extra two levels we would reduce THD from 24% to around 6.5% [134]. When using a modified sine wave inverter there are a few things to keep in mind. One of the first things is to make sure that whatever load you connect to the inverter, the inverter must be able to handle the wattage that the load is drawing. The next thing is that modified sine wave inverters do not do especially well with inductive loads. This is because with a high influx of current, losses will be experienced in the transfer through heat or “buzzing” and may ultimately ruin the life or operability of the device [128,134,179].

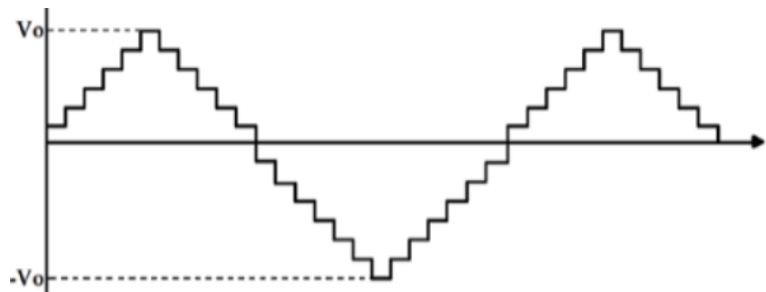


Figure 54: Waveform of a Modified Square Wave Inverter Output

3.10.5 Pure sine wave Inverters

This type of inverter is the best when it comes to the least amount of noise or interference produced. The sole advantage of this type of inverter is that it produces a very small amount of total harmonic distortion which equates to allowing most electronics to run safely and efficiently without the worry of damage or losses to the device(s). In figure 55 below we can see that a pure sine waveform is shown. Although the construction of this output can be challenging it offers the most “bang for your buck”. Another disadvantage is this type of inverter is the most expensive to construct. A few things more to note

would be that this type of inverter operates in a PWM or pulse width modulation mode. The produced frequency and voltage are controlled by altering the duty cycles of the high frequency pulses. Then the “chopped” voltage follows through a low pass filter to output a sinusoidal output that is very clean and efficient. Although the two main disadvantages are the challenge in building and cost, if you need a high quality of power, this is the best inverter to have [128,134,179].

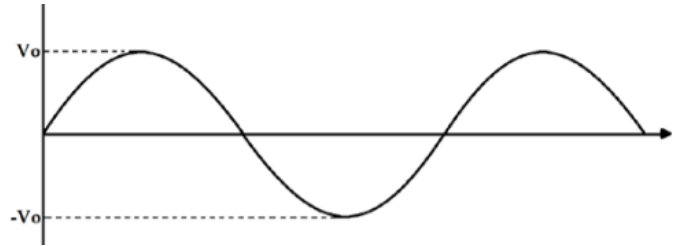


Figure 55: Waveform of a Pure Sine Wave Inverter Output

Figure 56 helps to show the entire process of the conversion of DC to AC power in a pure sine wave inverter. We start with a DC input whereby it will combine with the PWM generated by the reference sine generator at 60 Hz with a high frequency triangular wave generator which will sample the sine wave. This PWM and DC combination will go into an H bridge which will give a rough sinusoidal output. This output will then go into a low pass filter which will “clean” and smooth out the distortion and output a clean AC voltage. This then will lead to a transformer which will step up the voltage so that appliances can use the power supplied at the operating voltage those appliances were designed to run on [128,134,179].

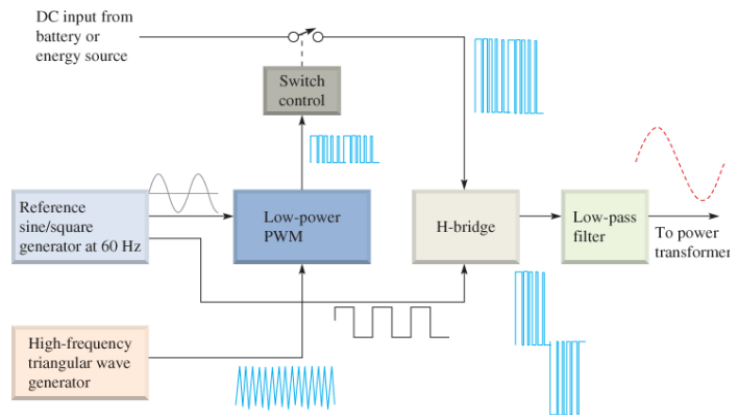


Figure 56: Sine Wave Inverter Diagram

3.10.6 Which inverter we will use and why?

For our design we will use a 3000W power inverter by EDECOA. It is a modified sine wave inverter and thus it is relatively cheap as compared to the sine wave inverter. It will help to convert the DC current coming out of the batteries into AC current to run appliances. According to Amazon this inverter is good for office equipment such as computers, printers, scanners, ect. It is also good to be used in entertainment settings such as the TV or DVD player. Household appliances and kitchen devices are also able to be

used. Ideally though, this inverter is driven for use in camping and boating. The continuous output power is around 3000W which is plenty of power for what we will be using it for. It will take an input voltage of around 12V DC and convert it to 110/120V AC. The specs state that the inverter is around 87% efficient which should be enough for our project as we are not trying to power anything too large, just to show that it can power other appliances that can only run off of AC safely and not get damaged. Figure 57 below shows the inverter along with a remote controller, a pair of cables with terminal rings, and a ground wire. Table 14 gives all of the technical information related to the inverter along with the weight and dimension. We will be using this inverter because although a pure sine wave inverter would be better in terms of efficiency, due to the cost and the scope of our project, this modified sine wave inverter should be enough to get us where we want in terms of power, efficiency and cost. Another reason that we will be using this inverter and why we will not be making any other comparisons with other products is because it is being donated to us. This will ultimately save us money for the scope of this project. Everything aside, the modified square wave inverter does have its disadvantages. The first is that since it is not a pure sine wave inverter, it will not have as efficient of a transfer from DC to AC power. Also, the inverter may heat up some due to losses within the harmonics that are created and ultimately leads to total harmonic distortion.



Figure 57: EDECOA DPM30 3000W Power Inverter

| | |
|-------------------------|----------------------------|
| Model | DPM30 |
| Continuous Output Power | 3000W |
| Max Output Power | 6000W (10ms) |
| DC Input Voltage | 12V (10-14.5V) |
| AC Output Voltage | 110V/120V |
| Frequency | 60Hz |
| Efficiency | >87% |
| No Load Current Draw | <1.7A |
| Output Waveform | Modified Sine Wave |
| Inversion Efficiency | 90% |
| Temperature Protection | 167F / 75C |
| Weight | 10.87 lbs |
| Dimension | 12.44 x 5.91 x 4.92 inches |
| Display Type | LCD |

Table 14: Specifications For DPM30 3000W Power Inverter

3.11 Soldering

Soldering is an essential skill for the development of electronics, as it is the most common way to bind or attach components. Soldering can be wire to wire in a joint, wire to component in a connection, or even component to board to secure it in place. The process of soldering is one that joins items by melting the solder and letting it re-harden in between the items. Soldering is an altogether different process than welding, as it does not require melting the items together.

There are three forms of soldering which include soft soldering, silver soldering, and brazing. When soft soldering, you would use a tin or leaded alloy to bind the items together at a temperature near 750° F. As opposed to silver soldering where the use of silver alloy would be required as well as a much higher temperature. Brazing is a similar method to silver soldering as it requires higher heat, but instead it requires the use of a brass alloy.

When soldering, flux is used to help adhere the solder to the component or wire as well as a cleaning or purifying agent for the metal. Flux can be a paste or a liquid and is typically rosin based from pine trees. It is good practice to use isopropyl alcohol to clean the solder joints as they cool, the rosin flux from pine trees can be highly corrosive when exposed to higher operating temperatures. Doing so will extend the shelf life of your solder joints

and require much less corrosion preventative maintenance over time. In our experiences, paste flux is the preferred method for wires and liquid flux is preferred for areas where it can be contained as it can become messy to handle.

There are two main classifications for soldering, miniature and micro. Micro soldering will require much more precision than miniature soldering due to the nature of the components used. Soldering at the miniature level can be done without the use of, or need for, a magnifying lens. The majority of the time that you solder will be on the miniature level. Micro soldering is done specifically with the use of a magnifying lens so that you can see the small areas that you are soldering more clearly. Micro soldering is done on very small components and circuit boards. When micro soldering it is extremely important to not apply heat from the soldering iron for an extended period of time, as overheating the components can happen easily.

3.11.1 Soldering Standards in the Industry

The authority behind soldering standards for electrical and electronic assemblies is widely regarded as the IPC J-STD-001. Other documentation for industrial standards include the following standards through IPC: A-610, A-620, A-600, 7711/21, and 6012. These standards are used for certification, performance, and testing and each one is a varying level of proficiency in soldering. Specifically the J-STD-001 standard is meant to give understanding of the materials needed, methods used, and quality assurance criteria so that you can be sure a quality product has been produced. This ensures that the entire process is controlled from beginning to end and that it is consistent across the industry when following the proper requirements.

Through IPC there are several certifications levels including: certified IPC specialist, certified standards expert, and certified IPC trainer. The certified IPC specialist, or CIS for short, is the beginner level of certification and is meant for those who plan to become proficient in learning how to solder properly. Certified standards expert, or CSE for short, is the next level of certification and deals with those who have a higher level of knowledge and understanding of the subject material. These individuals are highly proficient in soldering and have a solid foundation in IPC standards. The third and final level of certification is the certified IPC trainer, or CIT for short. This level of certification requires the individual to have superior knowledge on the IPC standards and the ability to pass this information down to other individuals.

3.11.2 Soldering in Our Project

For our project we will be soldering on the miniature level, as most of our components will come pre-soldered. We will accomplish this by using the standard soldering iron setup with a Weller WE1010NA Digital Soldering Station. This device allows us to digitally monitor the temperature of the soldering iron with a set of convenient push button arrows to adjust it.

We will be using a liquid rosin flux as well as a past rosin flux to facilitate the process of creating our solder joints. For our solder we chose to use a 60% tin 40% lead rosin core solder as it requires a lower melting temperature than silver solder, and it is easier to

utilize in our experiences. The melting point of this solder is approximately 361° F and decreases our chance of damaging components due to excessive heat exposure.

For our safety we will be soldering in open areas while utilizing portable fume extractors so that we do not inhale the smoke from the solder. Due to this solder containing lead, it can be dangerous to inhale as it is known to cause cancer with excessive exposure. When soldering we will also be utilizing safety goggles to protect our eyes from solder. We will be wearing pants and closed toed shoes as well to prevent burns, in the event that solder falls off of the component and desk.

In our project, we will be soldering components without the assistance of a magnifying glass. Our components will be soldered to our PCB with the 60/40 rosin core solder mentioned earlier. The four gauge and fourteen gauge wires that we will be using to connect various parts of our design will require the act of tinning. Tinning is where the wires typically have a small section of the rubber coat that is stripped away, the exposed wiring is then twisted tightly and covered in flux. Once the wire has been covered in flux you apply solder evenly on all sides. The reason why you properly tin these wires is to easily make solder joints and connections. These joints will have a small amount of solder applied which will adhere to the solder already connected to the wiring. This process allows the solder to seep all of the way through and make a tight and solid connection that does not risk breakage.

The final step of soldering in this project will be cleaning the solder joints and connections. Due to the flux being corrosive, we will apply seventy to ninety percent isopropyl alcohol to the connection. This will remove the flux and ensure that there is no corrosion and that there is no risk of degradation of the solder joint or connection.

3.12 Selecting Proper Gauge Wires

Selecting the proper wire gauge is very important when it comes to designing devices. The gauge of the wire is what will determine the current carrying ampacity that it possesses. The system that we will be using to measure this is the American wire gauge system that is a logarithmic stepped standardized wire gauge system that was developed by David Brown and Joseph R. Brown as well as Lucian Sharpe in 1857. The AWG system measures from thirty gauge at its smallest size to zero at its largest size. The larger the gauge of the wire, the higher the amperage allowed to pass through it. Typically the wiring that is used contains copper wire with a silicone rubber insulation covering it.

To show as a reference, there will be a wire sizing table that can be seen below. This table will show a comparison of the amps that can run through a set gauge of wire and the approximate maximum amount of length in feet that it can run through. Do note that there is a three percent voltage drop and the wire is designated as annealed copper wire at 20°C. The table can be seen below:

| Amps | One-way Wire Distance in Feet (Wire Gauge in AWG) | | | | |
|------|---|-----|-----|-----|-----|
| | 14 | 12 | 10 | 8 | 6 |
| 2 | 70 | 112 | 180 | 287 | 456 |
| 4 | 35 | 56 | 90 | 143 | 228 |
| 6 | 24 | 38 | 60 | 96 | 152 |
| 8 | 18 | 28 | 45 | 72 | 114 |
| 10 | 14 | 23 | 36 | 57 | 91 |
| 12 | 12 | 19 | 30 | 48 | 76 |
| 14 | 10 | 16 | 26 | 41 | 65 |
| 16 | 9 | 14 | 23 | 36 | 57 |
| 18 | 8 | 13 | 20 | 32 | 51 |
| 20 | 7 | 11 | 18 | 29 | 46 |

Table 15: Nominal Wire Sizing Chart

3.12.1 Wire Gauges That We Plan to Use

In our design there will be a few different wire gauges and lengths that we will be using. Due to the fact that our device will be in a localized area, and not overly large, the length of the wires that we will use won't be too long. This means that we shouldn't have to worry about when it comes to voltage loss over distance.

We will use four gauge wire in short distances from the battery management system to the battery itself. The reason why we will be using four gauge wire in this section is due to the sixty amps that will need to pass through. While six gauge wire would suffice in this situation, the safety and reliability of going up to four gauge wire will give us the peace of mind of knowing that there should be no issue. Another section of our design that will have four gauge wire is the section where the inverter connects to the battery. Again, this will be a short distance where sixty amps needs to pass through. For the same reason as the battery management system to the battery, we use four gauge in place of six gauge wire to allow us the peace of mind of knowing the current should pass through with no issue.

The other gauge of wire that we have chosen to use is fourteen gauge wire from the solar panel to the solar charge controller. At its highest, 5.58 amps, which is the maximum operating current of the solar panel, will be passing through this wire. While we could use sixteen or even eighteen gauge wire for this section, because we plan to use about seven to ten feet, the fourteen gauge wire is being donated to us. By using the donated wire, we don't have to worry about incurring extra cost to incorporate into our budget.

3.13 Transistors

In order to design our custom PCB we need to dive into reviewing some important electronic components that will be utilized in our design. To start off we need to have a solid understanding of transistors, what they are and how they work. A transistor is a component within electronics which serves to accomplish two functions: amplification or switching. When acting as an amplifier the transistor acts as a sort of current booster. It takes a small input current and produces a larger output current. When acting as a switch the transistor will have a small electric current flowing through one part of it and in turn it will cause a larger current flowing through another part whereby it will “switch” on the larger current. As opposed to diodes, a transistor has three layers (typically of silicon) instead of two. As a result we can have two different configurations: PNP or NPN. We will talk only about the NPN in this section as the PNP is just the latter configuration with everything flipped. To give names to the three different contacts on the NPN transistor we start with the emitter and collector. These two are joined to the n type silicon side as opposed to the base which is joined to the p type silicon side. Figure 58 below shows a diagram of what was explained above with the red portions indicating the n type regions and the blue portion indicating the p type region. Once you connect the transistor up to a voltage source, if we have a negative charge at the emitter, and a positive charge at the base and collector a flow of electrons will occur. The electrons are pulled from the emitter into the base so that the holes can be filled in the p type region. Once this happens, the collector then pulls the electrons out of the p type region by attracting the negatively charged electrons to the positively charged collector. As a result the transistor turns on. The small current which is at the base turns on the larger current which is the electrons flowing from the emitter to the collector. This is shown in figure 58 and 59 below [19, 36, 83, 116, 171].

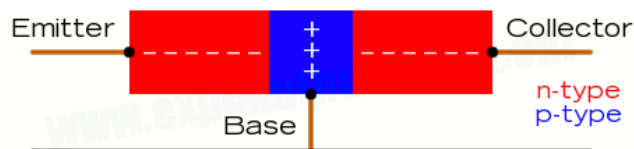


Figure 58 NPN Transistor Diagram

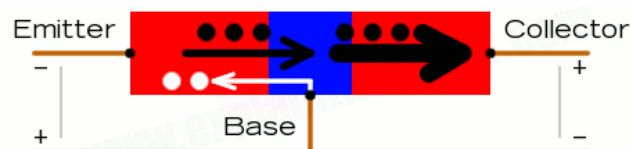


Figure 59: NPN Transistor Electron Flow

Now that we have an understanding of how transistors work on a molecular level, let's move on to labeling one on a circuit design level. Below is a figure that shows a NPN BJT (Bipolar Junction Transistor) and how you would see it in a circuit. Notice how at the top you have the collector region, bottom you have the emitter region and between you have the base region. The arrow pointing toward the emitter region indicates that when a small current is applied to the base, a larger current will flow from the collector to the emitter. How much current to be exact you ask? The answer turns out to be based on what the beta factor that the manufacturer builds into the transistor when they fabricate it.

For example, let's say that the beta factor of the transistor is 100. If we want a current of 10mA to flow through the collector into the emitter portion of the BJT then we must provide a current 100 times less than 10mA to flow through the base into the emitter. This gives the base current to be $10\text{mA}/100 = 0.1\text{mA}$ or $100\mu\text{A}$. Besides switching ON and OFF the transistor can also act as an amplifier. It can be anywhere between fully on and fully off. A small signal with little to no energy can control a transistor to make a stronger copy of that same signal in a collector-emitter or drain-source part of a transistor as shown in figure 60 below. Thereby it is able to amplify small signals [19, 36, 83, 116, 171].

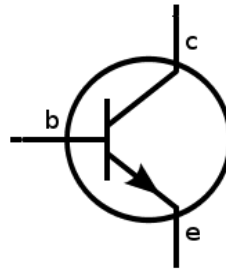


Figure 60: NPN BJT

3.14 MOSFETS

MOSFETS or known by their full name of “Metal Oxide Semiconductor Field Effect Transistor” are similar to transistors in terms of how current flows but have a major difference in how they turn on. In a transistor the current from the base into the emitter determines if a current will flow from the collector to the emitter, but in mosfets a voltage from the base (gate) to the emitter (source) determines if a current will flow from the collector (drain) to the emitter (source). Figure 61 below helps to illustrate the mosfet circuit symbol along with the direction of the current when the voltage is applied to turn the device on. One thing to note is that the mosfet shown is an N channel type. One of the best qualities about the mosfet and what it is used so much today is that it requires only one component of current as the transistor requires two. This makes mosfets typically easier to work with in terms of designing circuits and being able to find the values for the voltage and current that much easier. To turn on a mosfet, you must first find the threshold voltage of the transistor. Once you find that, you need to provide a voltage between gate and source that is HIGHER than the threshold voltage of the transistor but not go above the maximum gate source voltage limit or it can damage the mosfet. Another thing to note is that a mosfet acts like a bit of a capacitor. When you provide a voltage to the gate source region, it tends to stay there so you will have to provide a way for the extra voltage to discharge. As a result you will be able to turn OFF a mosfet [36]. Moving on to the PMOS in Figure 62 we see the circuit symbol below. The difference between the NMOS and PMOS is that the PMOS is cheaper to produce, it typically has three times higher drain resistance as compared to NMOS transistors. “The PMOS acts differently from the NMOS in that when a positive voltage is applied between the gate and source, a p type channel with opposite polarities is created between source and drain”. This as a result causes a low voltage to turn on while a high voltage at the gate turns the PMOS off. Finally the PMOS is not only cheaper but also has better immunity to interference than the NMOS [180,181].

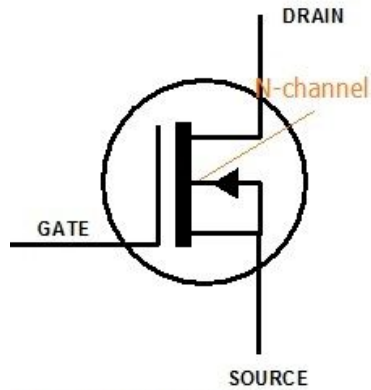


Figure 61: N Channel MOSFET

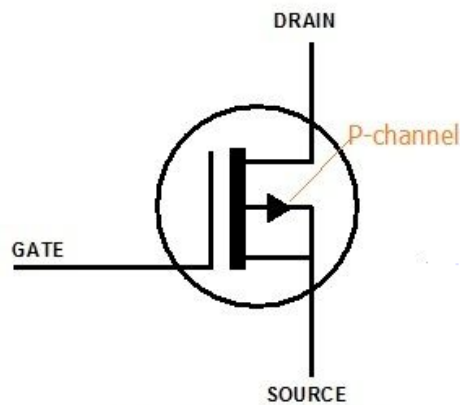


Figure 62: P Channel MOSFET

3.15 Current Sensors

The current sensor is used to read the current between two terminals and return an analog voltage that would represent the current value. An analog-to-digital converter can interpret that value since the specification of a current sensor lets us know their sensitivity. This is usually represented by a voltage value per amp. Our first choice was to use the same current sensor from opengreenenergy's schematic, ACS712 module. However, the current sensor requires 5V as its voltage source. According to its datasheet, the maximum value of V_{IOUT} can be 4.5V when supplied with current between -20A and 20A. When the current is 0A, the voltage returned is half the input voltage, 2.5V. As shown in figure 63 When the current is at the sensor's maximum range, we should expect it to return 4.5V since the sensitivity is 100 mV/A ($2.5 + .1V/A * 20A = 4.5V$). The METRO's analog pin has a maximum voltage range of around 3.3V. The current sensor may return voltage values above 3.3V, thus causing potential damage to the MCU. One solution for this problem is to use a voltage divider.

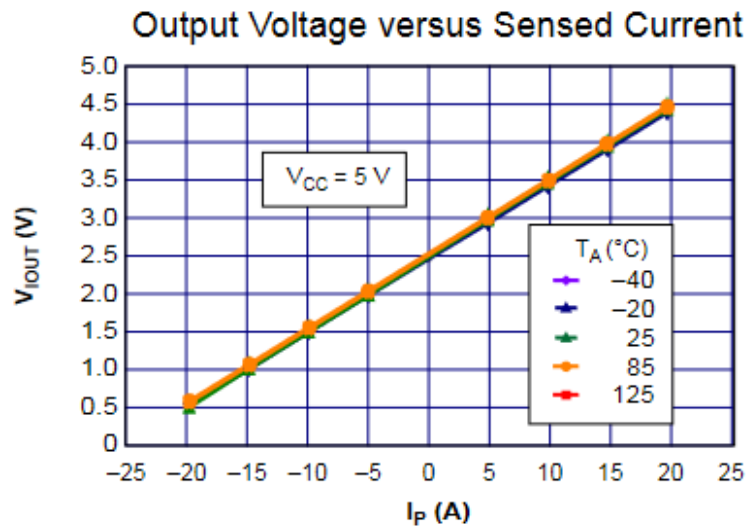
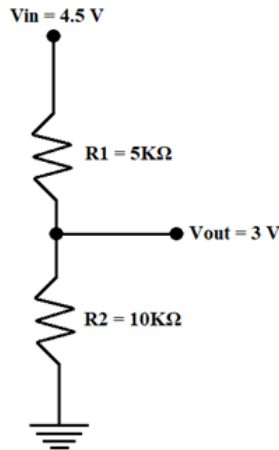
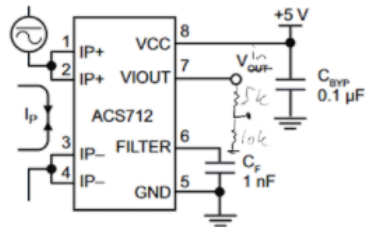


Figure 63: Relationship Between Output Voltage and Sensed Current

Figure 64 shows the process of finding the appropriate resistance value based on using a 2:3 voltage divider. We chose the 2:3 ratio since $2/3 \cdot 4.5$ is 3V and $2/3 \cdot 2.5$ is 1.67, values that are close enough to our desired range. Since the minimum R_{LOAD} value needs to be 4.7k Ω for the sensor pin, the two resistors chosen were 5k Ω and 10k Ω to form the 2:3 voltage divider. Based on this configuration, this gives us a close range between 1.67V and 3V. We need to appropriately map the current values to their corresponding voltage values since the range has changed but not the current sensor's sensitivity. Using the current sensing algorithm from the Administrator at ElectronicsHub, the code was adapted to use our 20A version of the sensor, rather than the 30A sensor [5]. The 20A sensor has a resolution of 100 mV/A sensitivity. The code's creator used an ADC converter that was 10-bits, while the METRO's ADC is 12-bits. Technically we can have better results by using the full 4096 possible values, but to keep things simple for this analysis, we will also be using the 1024 resolution. We now need to determine the scaling factor to interpret the voltage output correctly. In our algorithm, the equation was changed so that the cutoff is now 1.65 and the max is 3.30. Assuming that the sensor returned the maximum voltage, we can determine the scaling factor by setting both equations equal to each other. The result of this analysis is also shown in figure 64. Since the maximum voltage from the sensor is 4.5V, we need to determine the corresponding ADC value for both 5V and 3.3V configurations. Since the ADC returns ratiometric values, we can determine the maximum ADC value to be 920.7, or 921 since the value must be an integer [112]. Indeed, $5 \cdot 921 / 1024$ is very close to 4.50V, 4.497V to be more accurate. Although 1023 represents the reference voltage, we should still be dividing by 1024 for the final output since dividing by 1023 would cause offsetting since there are 1024 discrete steps. Using other references besides 5V can make this issue more apparent. At 2.5V, the ADC should return 512. Using the same process, the ADC values were determined for the 3.3V configuration and were used to solve for the scaling factors. Testing our new equation, we assumed that the ADC returned a random value, 900 and compared the results from the two equations. We found that the values nearly agree with each other, a 7.38% difference to be exact. At higher voltage values, the offset becomes more reasonable. However, At 2.5V, the output from our new equation becomes 0.239A. It should be 0A as shown in the 5V configuration. For these types of cases, we can add a

conditional statement that would return 0 at and below the specific pin value. In practice, there might be other errors that could be caused due to some intrinsic properties from the sensor or some other component not taken into account that can further increase differences such as the +/-1.5% accuracy from the sensor. Honing in on better scaling factors and improving our voltage divider set up during experimentation can help reduce the differences.



$$\begin{aligned} \text{At } 0 \text{ A, } V_{IN} &= 2.5 \text{ V} \\ P_{IN\ 3.3} &= \frac{5}{7} \\ P_{IN\ 5} &= \frac{5}{2} \\ \frac{\left(\frac{5}{2} \cdot \frac{5}{1024} - 2.5\right)}{.1} &= 0 \text{ A} \\ \frac{1.482 \left(\frac{5}{7} \cdot \frac{3.3}{1024} - 1.65\right)}{.1} &= .239 \text{ A} \end{aligned}$$

When $I = 0$

$$V_{in} = \frac{V_{cc}}{2} = 2.5 \text{ V}$$

| <u>IDEAL RANGE</u> | <u>APPROXIMATE RANGE</u> |
|--------------------|--------------------------|
| 1.65 V → 3.30V | 1.67 V → 3V |
| 0 A → 20 A | 0 A → 20 A |

$$\frac{2.5 \text{ V} \cdot 10 \text{ K}\Omega}{5 \text{ K}\Omega \cdot 10 \text{ K}\Omega} = 1.67 \text{ V} \quad \frac{4.5 \text{ V} \cdot 10 \text{ K}\Omega}{5 \text{ K}\Omega \cdot 10 \text{ K}\Omega} = 3 \text{ V}$$

CODE CONVERSION:

Sensitivity = 100 mVA = .1

X = Conversion Factor

Offset Voltage = 1.65 V

$$\text{Load Current} = \frac{X \left(P_{in} \cdot \frac{3.3 \text{ V}}{1024} - 1.65 \text{ V} \right)}{.100}$$

if(loadcurrent < 0)

current = 0

||conversion

let Vin = 4.5 V P_{IN 3.3} = 930

P_{IN 5} = 921

$$\frac{X \cdot (2.997 \text{ V} - 1.65 \text{ V})}{.1} = \frac{4.497 \text{ V} - 2.5 \text{ V}}{.1}$$

$$13.471 \cdot X = 19.97$$

$$\boxed{X \approx 1.482}$$

Figure 64: Voltage Division and Scale Factor for ACS712

Another option is to use a current sensor that requires only 3.3V. The best one we found that closely resembles the ACS712 is Melexis' MLX91221KDC-ABR-020-SP sensor. The main differences, besides the required voltage, from this sensor and the ACS712 module is that the former has a slightly faster response time and a much larger bandwidth. In addition, its internal conductor resistance is also slightly lower, resulting in lower losses. It's current reading results and properties are also similar to the ACS712 as shown in Figure 65. The reason why the ACS712 was considered at first was due to the

option of not having to solder the chip onto a PCB since the sensor can be brought already on a module that featured pin headers and input connectors. There are no 3.3V alternatives in stock that have around the same range as the ACS712. There are more than enough of these parts in stock and setting up the connections and soldering the sensor onto a PCB is not challenging enough to risk the possible additional losses and uncertainty from using the more popular ACS712. Table X gives a more thorough comparison between the two sensors.

| Parameter | Ratiometric Mode | Differential or Fixed Mode |
|-------------------------|--|---|
| Output Signal | $V_{OUT} [\%V_{DD}]$ Example: output is 1.65V when supply is 3.3 V → output is then 50% V_{DD} . If the supply (V_{DD}) increases with 5% to 3.465 V the sensor output will (for the same measured input current) scale ratiometrically with the supply voltage, becoming 1.733 V which is a different voltage than when the supply was 3.3 V, but as a percentage (i.e. ratiometrically seen) it remains at the same level of 50% of V_{DD} . | $V_{OUT}-V_{REF} [V]$ Example: output is 1.651 and V_{REF} is 1.651V when supply is 3.3 V. When the supply voltage is increasing to 3.4 V due to supply system variation over temperature, the sensor will still maintain the same “fixed” output values V_{OUT} and V_{REF} . |
| Offset | $V_{OUT}[0A] = 50 [\%V_{DD}]$ (programmable) | $V_{REF} = 1.65 [V]$ (Melexis programmable) $V_{OUT}[0A]-V_{REF} = 0 [V]$ |
| Offset ratiometric | Yes | No |
| Sensitivity | $[\%V_{DD}/A]$ | $[mV/A]$ |
| Sensitivity ratiometric | Yes | No |
| Measured Current | $(V_{OUT}-V_{OUT}[0A]) / \text{Sensitivity}$ | $(V_{OUT}-V_{REF}) / \text{Sensitivity}$ |

Figure 65: MLX9122 Properties

| Key Points | ACS712ELCTR-20A-T | MLX91221KDC-ABR-020-SP |
|---|--|---|
| Cost | Generally between \$3 and \$4 including the module or \$5.64 on Digikey for just the chip. | \$4.31 per chip on Mouser |
| Typical Nominal Supply Voltage | 5V | 3.3V |
| Sensor Type | Hall Effect | Hall Effect |
| Output | Ratiometric, Voltage | Ratiometric, Voltage |
| Sensitivity | 100mV/A | 62.5mV/A |
| Internal Resistance | 1.2mΩ | 0.9mΩ |
| Response Time | 5μs | 2μs |
| Bandwidth | 80kHz | 300kHz |
| Output Error (when temperature is 25°C) | +/-1.5% (when current is +/-20A) | +/-0.3% (when voltage is +/-5% V_{DD}) |
| Number of Pins | 8 | 8 |

Table 16: ACS712 & MLX9122 Comparison

Based on the table above, we can see that the MLX9122 chip is more sensitive and capable than the ACS712 while still being able to run with a 3.3V supply. It is more capable due to its lower output error difference and its higher response time, which is due to its higher bandwidth.

4.0 Design Constraints and Standards

In this section different design constraints and the necessary standards that do/may apply to our project will be discussed. Standards are important to consider when choosing/designing anything. In the case of our project, the most stringent standards are related to battery manufacturing due to the potential volatility and danger of battery manufacturing. In addition to these standards, we will be exploring the standard related to the designing/manufacturing process for the solar panel, solar charge controller, and the inverter. These standards are typically provided by the manufacturer, and if not, we will be searching on listed standards by organizations such as IEEE to find standards related to our project.

4.1 Constraints

The main constraint that may cause issues is price. Other than this, we won't know further constraints until more research is done. We would like to keep the project budget under \$800 in order to keep it affordable. This is important because our goal for this project alongside providing clean energy, is to provide an affordable solution. Most solar powered battery systems with equivalent amp hour capacity can be up to \$3000. Based upon the proposed budget we should be able to meet this, but due to shipping costs/tariffs from China, which is where a lot of the materials will come from, this may be difficult.

A secondary constraint that we may encounter during our project is time, or more specifically the lack of time. Due to the design portion of our project being limited to a two and a half month period, we need to have all of our supplies ordered before the semester begins. With this lack of time, we have elected to buy a pre-built battery management system to save us the headache and struggle of attempting to build one ourselves. With uncertain global conditions, we have ordered many of the components that we know to come from overseas, as to get ahead of potential shipping issues.

A third constraint that may give rise to issues would be the lack of experience in assembling these types of components. To deal with this, we have been advised to order multiple of each component as long as cost permits. For most of the components in our design, we have ordered up to three in the event that we inadvertently damage anything during assembly. Taking these constraints into account, we hope to have an easier road to success.

4.2 Design Standards

In this project, we must keep in mind the standards and government regulations that we must follow. Of these standards and regulations we have battery standards, IEEE standards, IPC PCB standards, and C/C++ language standards. Standards are quite possibly the most important part of our design. If we do not follow standards already set in place by industry professionals we could waste excess time on designing, assembly, re-designing, and re-assembling our project. Standards help us to remove the guesswork behind the processes that we are not familiar with. This also applies to the items and components that we implement into our design. If the manufacturers don't follow industry standards we could encounter issues with these products that potentially make

them incompatible with our design or cause them to easily malfunction and set us back in both time and money.

There are many organizations and associations which can provide standards. We will mainly focus on the standards provided by IEEE, IPC, and local and federal government standards. The institute of electrical and electronics engineers is our primary source of standards as they have a large library of information that can be narrowed down into specific topics pertaining to our design. The institute of printed circuits is our second most important source of information for standards, as the PCB is the heart of the design and the biggest requirement. IPC will allow us to get into the specifics of what is required for our printed circuit board. Lastly, local and federal government standards are important as this will dictate how, when, and with what we can ship or transport our design. If we do not abide by these standards we will encounter issues in the future for where and how our design can be used and transported.

For our programming language of C/C++, we do not have many standards to pull from but we have located a few that may apply. Primarily from sources such as Barr Group Embedded C Coding Standards. ISO/IEC 9899 and IEEE Std 1666-2011 are also C standards, but they will not be applicable. ISO/IEC 9899 is the international standard that specifies the form and establishes the interpretation of programs written in the C programming language. [86] This means that many current C programming language compilers will be compiling code based on these accepted standards. The Arduino IDE does not follow these standards, meaning that programs written in the IDE can't be compiled using those compilers. The Barr Group Embedded C Coding Standards gives us insight on how to write the code for embedded systems and the rules to follow based on their standards.

4.2.1 Battery Standards

The battery standards that we have found that apply to our design are located within the IEEE domain. Specifically, the “Low Voltage Direct Current (LVDC) Nanogrid for Home Application”. This standard is based on nanogrids, which are typically individual power grids for buildings, but it should apply for our design. Our design is twelve volts, and thus qualifies as a low voltage for this specific standard. We will also be using the Charging Module for Newest Types of Rechargeable Batteries LiFePO₄. This standard will allow us to have information on the design of the charging power module.

For the LVDC standard, we are informed that this device should power objects such as mobile phones, laptops, lights, and fans that run off of DC power. This feeds into our design and expectation of our system and allows us to know that we are already following part of this standard. The architecture of the LVDC should include subsystems such as the system controller, power switch, battery management system, solar converter, and any back up AC to DC converters. [100] For our design, the microcontroller is our “Nanogrid System Controller” as it is the main communicator between our subsystems.

The second standard that we will be using for our batteries is also from IEEE, this standard is labeled as “Charging Module for Newest Types of Rechargeable Batteries LiFePO₄”. This standards describes the batteries themselves along with the advantages

and disadvantages of using this battery. It reaffirms that the battery technology in our design is safe as it does not run the risk of thermal runaway and as such will not catch fire or explode with overcharging. [100] This standard gives us the information about higher discharge cycles than typical lead acid batteries, the higher discharge rate capability, and the considerably lower self discharge rate.

With all of this information we can maintain a data sheet of what the lifecycle of the battery, and our design, should hold. This standard also gives us the major disadvantages that we should also keep in mind with our design. Of these disadvantages, we have a higher energy density per unit weight, they have a low weight compared to its capacity when compared to other batteries, and they cannot be discharged below a certain voltage value without decreasing the battery lifetime. [100]

Along with these standards we wanted to take government standards, both local and federal, into account. The storage and transportation of these batteries must follow strict guidelines set forth by the government as to maintain the safety of everyone involved and those in the vicinity of the battery. Lithium Iron Phosphate batteries are classified as freight and dangerous goods. This means that the state of charge during transportation must be no more than 30%, and during air travel the individual cell voltage must be discharged to 2.3 volts. By discharging to this amount, the surface temperature rises only six degrees celsius and does not exhibit sparks, fumes, or fire.

4.2.2 IEEE Standards

The IEEE, or Institute of Electrical and Electronics Engineers, is the primary source of knowledge and standards for UCF students. The goal of this organization is to educate individuals on the technical advancement of electrical and electronic engineering. While there are no specific Stds through IEEE that we could find, we found multiple documents through IEEE that narrowed down to apply to our design. These documents are not Std numbered, but are referred to by their titles. Through these documents we will follow the information that it provides as if it were an industry standard.

4.2.3 IPC PCB Standards

IPC, or institute of printed circuits, is a trade association with the aim to develop trusted standards to drive the electronic industries success. These standards are implemented across the industry and help to ensure superior quality, reliability, and consistency in electronics manufacturing. [88] The standards that IPC has created are for the assembly and production side of the industry, and as such will apply to our PCB.

Commercial PCBs must abide by the standards set forth by IPC to continue to be reliable and have extended longevity in the products that they reside. This will apply to any PCB that meets the following criteria: single layer, double layer, multiple layer. Within the standards that apply, you will find general documentation, design and material specifications, and other documentation that must be followed.

As our design used a printed circuit board, we will follow the IPC standard: IPC-2221B “Generic Standard on Printed Board Design”. This standard will have the requirements

needed for the design of the PCB and for the mounting of the components. Another standard to keep in mind is the IPC-2220-FAM, which is a family of documents that contain the “Design Standards for Printed Boards”. In the IPC-2220-FAM there are many standards included that give information on various topics related to the PCB like tolerances, thickness of the conductor, requirements for the current of the traces and what it can bear, tracing and spacing between the PCB, and material properties.

It is important that we abide by these standards while designing and building our project. By doing so we should prevent many issues that can arise. A benefit of maintaining these standards during our processes is that our end product will not only be cleaner than an amateur design but it will also continue to maintain its functionality without worry of a preventable problem. Abiding by these standards will also allow other companies and the end user to have an established rule set to troubleshoot the product if there is an issue in the future. This is particularly important because it allows for everyone to be on the same pages from start to finish.

IPC standards are particularly valuable for companies as they take the guesswork out of the process. This means that employees have, in writing, the process that they must follow completely and accurately. It also takes the stress off of a company to develop these processes and allows them to integrate other devices and options that also follow the IPC standards.

The final thing that we would like to mention for the IPC standards is that the quality of product that it allows us to produce will be extremely beneficial if we intend to further produce our project upon its success. By following these standards from the beginning, we will already follow the industry standard and we will have less to worry about for product waste, delays, and reworks.

4.2.4 C/C++ Language Standards

The programming language that we’re using is a specialized version of the C++ programming language from the Arduino IDE. The Arduino IDE does not fully conform to the ISO/IEC 9899 standard for the C or C++ languages since programs written in the IDE are not compatible with them. Meaning that the code is not designed to be used with their compilers and is not very portable. There are no established standards for writing code that is agreed upon by every programmer in the industry. There are different programming standards followed by different companies or teams. However, there are numerous common programming styles and conventions for different programming languages that do exist, and for C some of those styles are K&R style or GNU. Since the programming language is very much like C/C++, many conventions and styles that are shared by those languages still apply. Michael Barr wrote a set of standards to minimize bugs in code and improve maintainability called BARR-C:2018 [11]. When applicable, we will be following this standard.

5.0 Project Design

Our project design is split into two major sections, with multiple subsections listed beneath them. These two major sections are software design and hardware design. The software design will contain topics such as the charging algorithm and the GUI. The hardware design will contain topics such as the solar charge controller, PCB and their nonlinear components or special purpose devices like the buck converter. Under hardware design, the assembly design and physical layout will also be covered.

5.1 Software Design

The software that will be loaded into the charge controller will be complex. Not only does it need to drive the circuit and interpret readings from the sensors, but it will need to display all the information on a touchscreen LCD using graphics. For this section, the charging algorithm will be covered first since this is the most important aspect of the software. The charging algorithm tells the MCU how to charge the battery and when to charge it. The performance of the entire system will depend on the algorithm, so it is important to have a solid foundation before programming it. The GUI would be the next topic to go into depth. The GUI prototype will be shown and its features will be discussed.

5.1.1 Charging Algorithm for Lithium Iron Phosphate Batteries

Ideally, when charging batteries with multi-stage chargers, they all, at the very least, go through the three-stage charging process [122]. The first stage is called the bulk stage, the second is called absorption stage, and the third is called the float stage. The stages have already been covered in section 3.3, but we need to understand what they mean for our charging algorithm. In addition, we need to interpret the research already done on lithium iron phosphate batteries to design the algorithm specifically for our battery. The purpose of this section is to present a charging algorithm for the lithium iron phosphate batteries. The charging algorithms will be based on the charging profile for the battery shown in figure 66. The figure shows a fourth stage, but we do not need to concern ourselves with this stage since it is a stage suited for batteries not charged for 6 - 12 months.

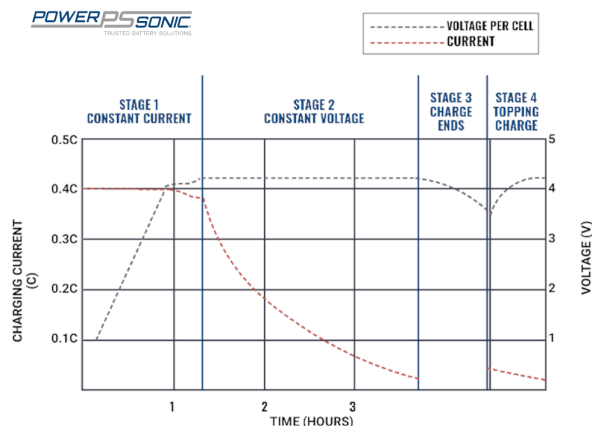


Figure 66: Charging Profile for LiFePO4

5.1.1.1 The Bulk Stage

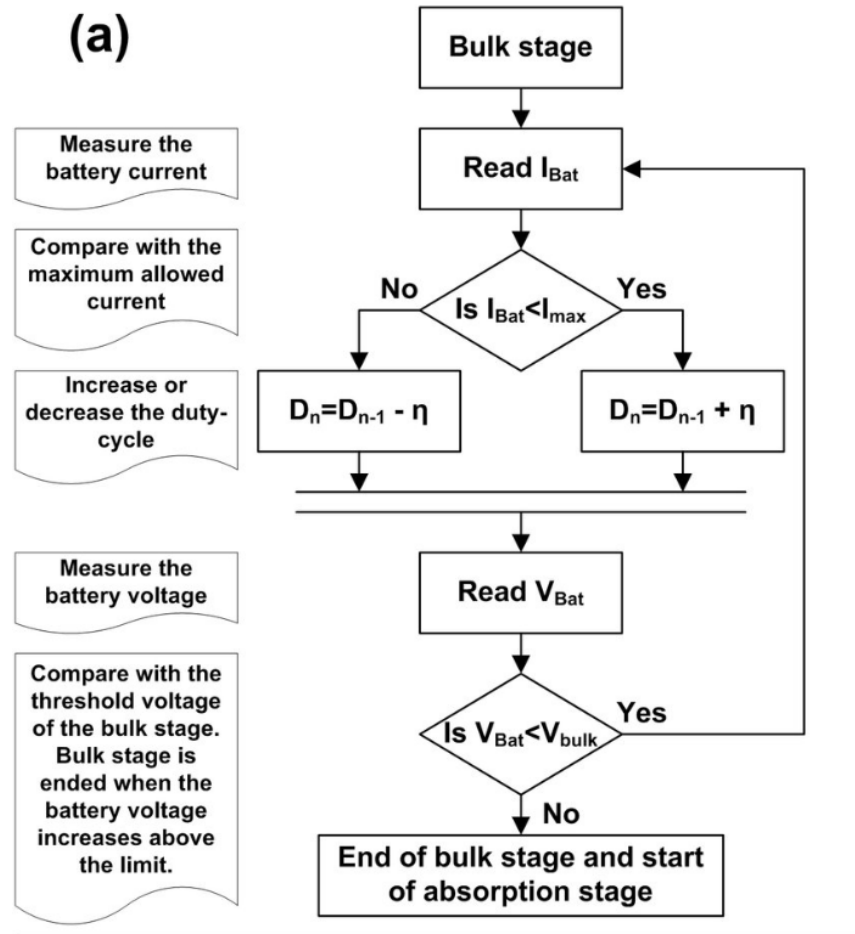


Figure 67: Bulk Stage Charging Algorithm

About 80% of the charging occurs in the bulk stage. For lithium ion phosphate batteries, the charging current can typically be 30% to 100% of the capacity rating of the battery, or 60A to 200A [78]. For our algorithm design, we do not need to worry about the current exceeding these values since the maximum operating current coming from the solar panel is 5.8A. The bulk-stage charging algorithm shown in figure 67 has a process where current is being monitored, this will be eliminated in the final design. Because the current is constant, the voltage increases with time. In order to charge the battery, we need to check if the voltage across the solar panels is greater than the voltage across the battery. In addition we need to check if our battery is below the voltage limit for the bulk stage. This limit can be determined by checking the battery's absolute charging voltage, which was determined to be 14.6V in 3.9.11.1. Assuming that the battery is less than the absolute charging voltage or V_{bulk} , the PWM duty cycle will be set to 100% since, as mentioned before, we're guaranteed for the current to be far less than what the battery is capable of in our design. However, if the user wants to scale the project such that the maximum current can exceed what the battery can handle, we will need to implement the ability to increase or decrease the duty cycle based on the current. When V_{bulk} is exceeded, the battery will enter the absorption stage.

5.1.1.2 The Absorption Stage

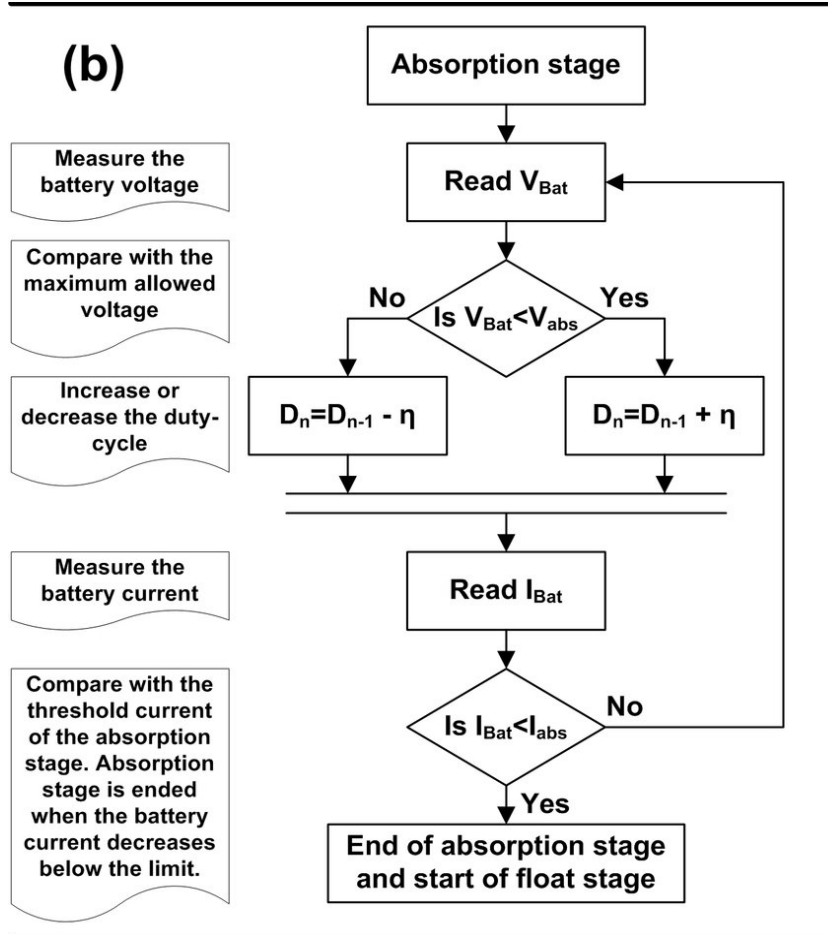


Figure 68: Absorption Stage Charging Algorithm

At this stage, the battery needs to maintain a constant 100% state of charge, which is at 14.6 V for our battery. Figure 68 shows this to be V_{abs} , but this value can be equal to V_{bulk} . Since our voltage value needs to be constant, our PWM duty cycle needs to be set such that, ideally, we keep the voltage. This is a complicated process, but the easiest way to accomplish this is to implement a proportional-integral-derivative (PID) controller. A PID controller can drive a system towards a target value [61]. The PID controller takes in an input, the desired output, and three K constants. The PID equation is shown in figure 69.

$$u(t) = K_p e(t) + K_i \int_0^t e(t') dt' + K_d \frac{de(t)}{dt}$$

Figure 69: PID Equation

The error, $e(t)$, is input minus desired output. Each term can have a weight that is determined by their K factors. K_p is the most crucial term in the equation since it is generally larger than the other K values. The integral term represents the combined error over time. The derivative term helps prevent the final $u(t)$ value from snapping back into

place too quickly due to one of the two other terms [91]. Finding the appropriate K values would require experimentation to fine tune them. The arduino library has a PID library that simplifies the process to a single function as shown in figure 70.

PID(&Input, &Output, &Setpoint, Kp, Ki, Kd, Direction)

PID(&Input, &Output, &Setpoint, Kp, Ki, Kd, POn, Direction)

Figure 70: PID Function Syntax

The direction term simply determines the direction the output will move when given an error, which is usually set to the constant DIRECT. We will not concern ourselves with POn since it is not required, nor do we need it. In this algorithm, The input will be the battery's voltage, the output is the value returned by the function, and the Setpoint parameter is the desired voltage. Since the returned value is a voltage, we will want to map it to an appropriate duty cycle value. As discussed in 3.1.5, the equation for the average output voltage is $V_{avg} = Duty\ Cycle * V_{pk}$. If we were to modify the equation to determine the duty cycle needed to maintain the setpoint voltage, $Output/V_{bulk} = Duty\ Cycle$. If we were to have 256 values, where 255 represents 100% duty cycle, then we would have to multiply the resulting duty cycle by 255. Non-integer values are truncated, this is why 127 represents 50% duty cycle.

If our voltage is constantly maintained and the battery's current is decreasing, there needs to be a point where the current is less than a certain threshold to move onto the next stage. This current is typically below 5% of the battery's rated capacity.

5.1.1.3 The Float Stage

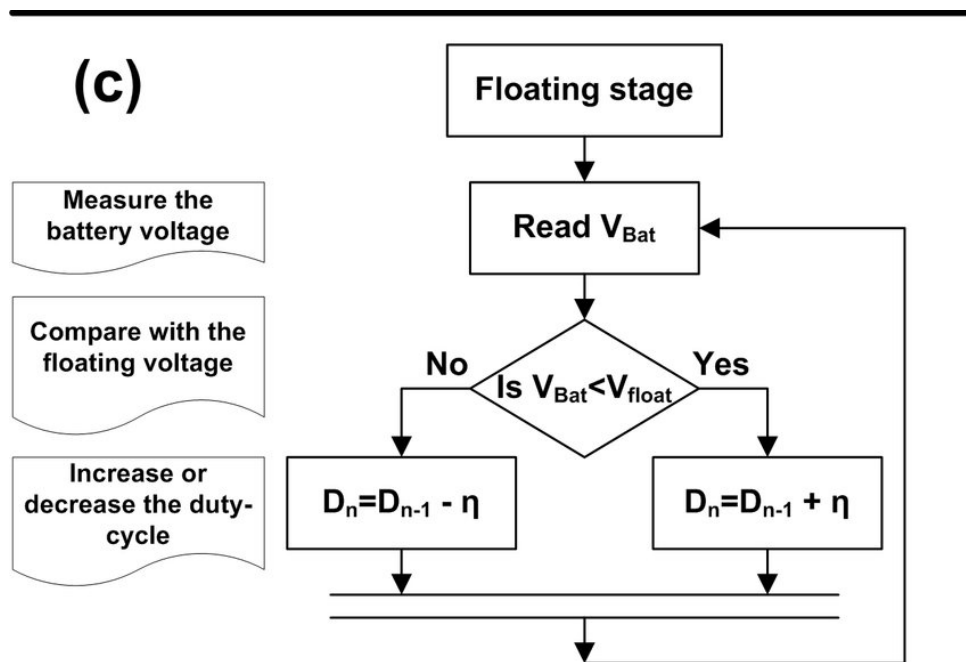


Figure 71: Float Stage Charging Algorithm

In this stage, the battery's state of charge is kept at 100%. Chargers include the float stage since battery charge level deteriorates over time when not in use. This stage keeps that battery's state of charge to a maximum at all times. This is true for most types of batteries, however, our battery does not need a float stage. As shown in Figure 71, at stage 3, the current is completely cut off. This is because LiFePO4 batteries in general cannot absorb overcharge [68, 78]. To minimize this risk, we just simply cut off the current. The self-discharge rate of lithium is very low, so low that it can deliver close to full capacity even when it has not been charged for 6 - 12 months.

5.1.1.4 The Algorithm

After going through each stage, we have prepared the charging algorithm represented in figure 72. Since there is no "end" path in the flowchart, we intended to show that the whole process is in a loop. After the battery has reached stage 3, the program would go back to the start where the bulk stage takes place again. However, if the battery is still fully charged, nothing should happen at this stage and it should go into the absorption stage. Again, if the battery is still fully charged, we should expect the current to be below the threshold, especially if the BMS is involved since it would make sure that the battery does not overcharge. After a certain period of time, when the charge level is below V_{bulk} , the charging cycle would start again. Ideally, we would want to implement a timer that would make sure that the battery wouldn't go through the charging cycle again too quickly. Since the discharge rate of the LiFePO4 battery is very low, the timer may not be needed. We can determine if the timer is needed through experimentation. Via experimentation, we can determine the discharge rate of the LiFePO4 battery and adjust the algorithm and add features that can improve the longevity of the battery. The algorithm depends on the voltage and current measurements from sensors or voltage divider circuits. Measurements that are too imprecise can lead the charging algorithm to make the charge controller do unnecessary or even potentially damaging actions. In our design we have a BMS, so the battery should be safe even if the charge controller is not working correctly. Regardless, we have done the necessary theoretical work to determine that the loss introduced into the measurements is minimal.

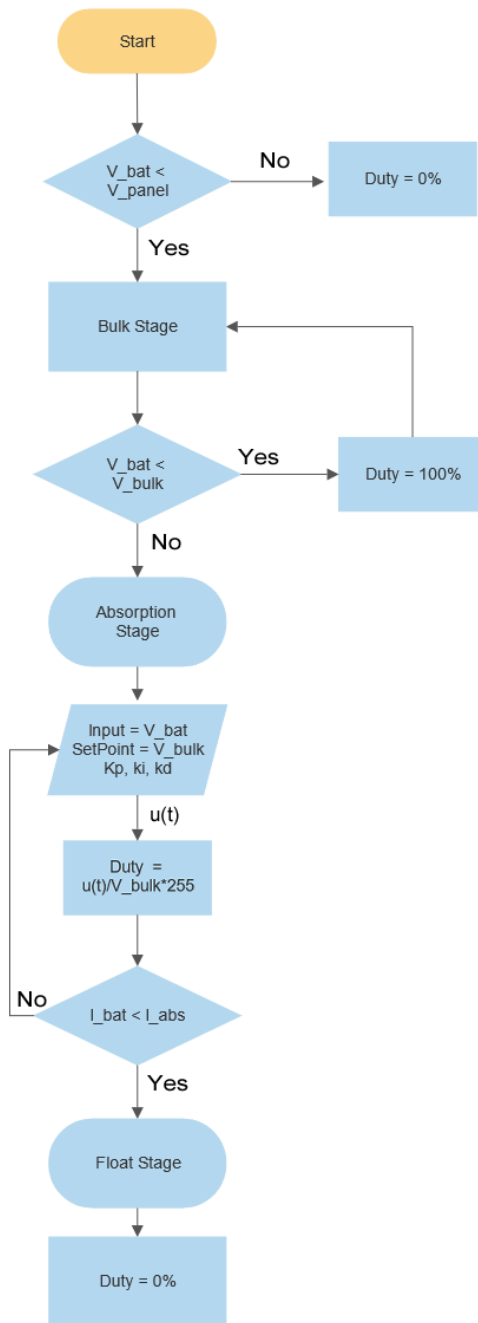


Figure 72: The Charging Algorithm

5.1.1.5 Voltage and Current Measurements

Our algorithm makes use of voltage and current information from the solar panel and battery. However, due to the limitation of the I/O pins in the METRO, voltages going to the pins cannot exceed 3.3V. Sections 3.15 and 5.2 covers the hardware that deals with these types of issues. However, because of these solutions, we will have to write code that uses some factors or equations that can convert the voltages, going into the METRO's analog pin, into their corrected values. Starting with the voltage sensors, there's a 2/11 factor that simply needs to be divided when reading voltages from the

analog pins containing the 90K and 20K resistors. For example if the voltage going into the analog pin is 200mV, then the value that should be read is $V_{out} = 200\text{mV}/(2/11) = 1.1\text{V}$. The current sensor will return voltage values with 62.5mV/A as its sensitivity. If an analog pin is reading 1.9V, then we must subtract it by the offset voltage, then divide the result by the sensitivity to get the current. There's an offset value because when the sensor is reading 0A, the output voltage is $V_{DD}/2$, which is 1.65V since $V_{DD} = 3.3\text{V}$. So for this example, $(1.9\text{V} - 1.65\text{V})/(62.5 \text{ mV/A}) = 4\text{V}$.

5.1.2 GUI Design

The GUI is meant to display information to the user in an easy to understand format using various graphical elements such as shapes or images. Our GUI is supposed to show data that the user will be interested in, which are listed in **2.4 Engineering Specifications**. The GUI should also provide basic adjustable settings to improve overall usability across many different types of users. In this subsection, the GUI prototype will be covered which consists of figure 73, figure 75, figure 76, and figure 77. The prototype shows the minimum features that we wish to employ in our final GUI.

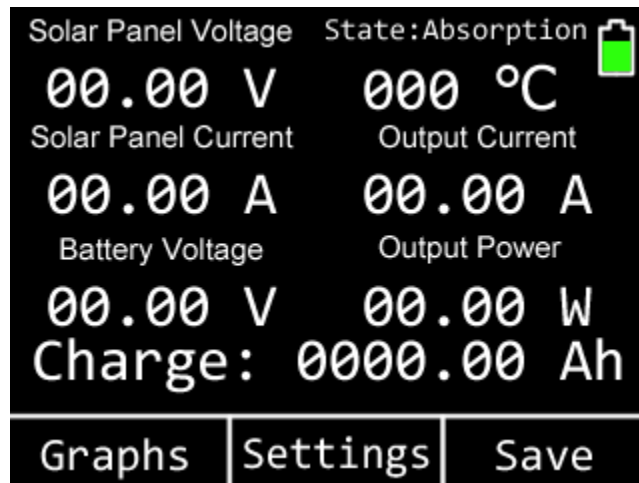


Figure 73: Main Menu Screen

Figure 73 shows the main menu. This is the first screen that the user is greeted to when the MCU boots. The screen shows the voltage across the solar panel, the current from the solar panel, the battery's voltage, the current going into the load, the ambient temperature, the load's power consumption, and the charge level of the battery. The top right corner shows the battery's charging state, the ambient temperature, and a graphical representation of the charge level. The information is displayed in a symmetrical and consistent fashion to make the screen look appealing and to make the best use of the limited space of the screen. As covered in section 3.5.2, the adafruit library can be used to create the texts and lines on the screen. The drawbitmap function can be used to create the battery icon and animate its different levels. The values and measurements would always continuously update.

The user has the ability to touch one of the three choices on the bottom of the screen. Graphs will lead the user to the screen shown in figure 77 and Settings displays a list of settings that the user is able to configure, as shown in figure 75. There's a "More" option

that will take the user to the screen shown in Figure 76 and allow the user to change the time and date, which is useful for the graph and data capture. From the main menu, the user can select “Save,” which will store the values that appear on the screen to a storage medium such as the SD card reader or the SPI chip on the MCU. The information would be saved in a text file as shown in Figure 74. By using the MCU’s RTC, we can even print the date and time of the capture. The date is displayed using the last two digits of the year, which can lead to ambiguity. However, for the purpose of demonstration, this is fine and will only serve as a minimum requirement. Using 4 digits to portray years is more complicated but if time permits, it will be added.

```
*****
State of Battery: Absorption

Solar Panel Voltage: 00.00 V
Solar Panel Current: 00.00 A
Battery Voltage: 00.00 V
Output Current: 00.00 A
Output Power: 00.00 W

Charge: 0000.00 Ah

Date: 01/01/21 Time: 00:00:00
*****
```

Figure 74: Text File Output Example

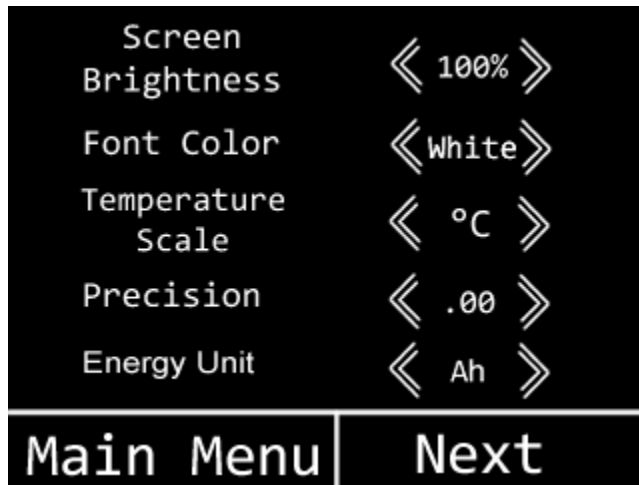


Figure 75: Settings Screen

The first of the two settings frames shows a list of parameters that can be adjusted by the user tapping on the two arrows. The first option allows the user to adjust the screen brightness, increasing or decreasing it by 5% intervals. Adjusting the screen brightness will change the duty cycle of the PWM going into the LEDs that are providing the backlight for the display. The second parameter that can be changed is the font color. This simple setting can improve the overall user experience by providing customizability. In addition, certain users might have a preferred color choice due to visibility. The user will have the ability to choose colors specifically suited for the GUI. Using darker colors with a black background will obviously hinder the user experience, so those won’t be included in the final design. The temperature scale setting allows the user to convert from celsius

to fahrenheit and vice versa. Users that don't live in the US may be more familiar with the metric system and trying to appeal to a wide audience is a hallmark of good UI design. The next setting, precision, allows the user to adjust the number of digits after the decimal from the measurements in the main screen. For certain users, the added precision may not be of much use and reducing the precision can make the GUI look more user friendly. However, leaving the precision as an option will not leave out users that would prefer the added precision. Our planned maximum precision would be to three decimal places, but it may need to be adjusted if its accuracy becomes unacceptable. Finally, the user is able to convert the charge reading from the battery from Ah to Wh and vice versa. Two choices are available to the user at the bottom of the screen, giving the choice to return to the main menu or to continue on to the next settings page.

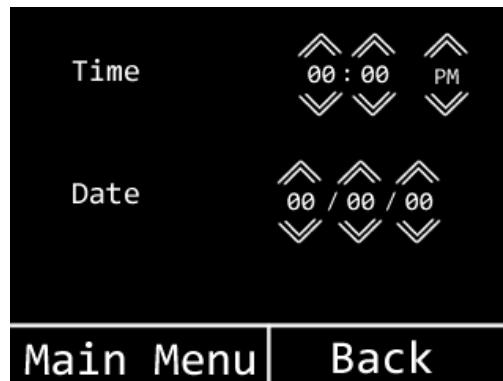


Figure 76: Time & Date Settings

Figure 76 shows more settings that the user can change. In particular, these options allow the user to change the time and date that are kept by the MCU's RTC. The time will be represented using the 24-hour and 12-hour format and, as mentioned before, the date will be represented with two digit years. There will be a setting that will allow the user to choose between the two time formats, and potentially one more for the year. The figure above shows how the 12-hour configuration should look like in the final design. The RTC has the ability to convert between 12- and 24-hour formats, which is set by using toggling CLKREP. Once this is set, we have an extra bit that gives us the information whether the time represented is AM or PM. For the same reasoning as to why we gave users the ability to convert between fahrenheit and celsius, we want to appeal to a wide demographic.

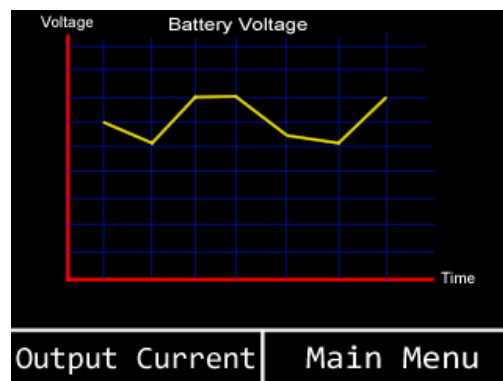


Figure 77: Graphs Screen

Finally, figure 77, shows what the graphing screen could look like. In every graph, we'll want to show the value of some function at some unit time. In this example, the voltage values were recorded per unit time for seven times. The RTC will be of immense use in this case since the unit of time can be made adjustable by the user. By unit of time, we mean from seconds to weeks or months. Depending on the selection, we'll have to limit the number of data that can be recorded and have the MCU continuously delete older data. One data structure that can be of use here is something that can organize data using a First In First Out (FIFO) scheme, more specifically, a queue. This abstract data structure will insert data into a fixed size array and process the oldest element first. In this design, whichever element is processed first will be removed from the graph.

Memory constraints, in regards to how much data can be stored, must be considered when deciding how much data can be stored and graphed. In addition, the more data displayed on the screen, the harder it is for users to observe individual points unless the ability to zoom in and out of the graph is present. We have the choice to add in a zoom feature and allow for a relatively large amount of data to be graphed or to reasonably restrict the number of points that can be graphed. The user will be able to cycle through different graphs that correspond to each measurement on the main menu. The reason why we think the graphing feature is essential is because it gives the user the ability to monitor the behavior of the battery or any other components. In addition, the use of time can help users correlate events that might have caused damage to the battery such as a stormy day.

5.2 Hardware Design

In this section, the overall hardware design components for our project will be explored and discussed. The first part of the hardware design to be discussed is that of the PCB. Each part of the schematic alongside the parts we used will be analyzed and explained. Next, the battery assembly design as a whole with the BMS included will be explained with the aid of CAD drawn schematics for reference. The last main piece of hardware being designed to be explored is the solar charge controller. Similarly to the battery assembly, the explanation of our design will be aided by custom CAD drawn schematics. This solar charge controller is the main part of our design and will include our designed PCB.

5.2.1 Solar Charge Controller PCB

In designing the PCB there are a lot of steps, math, and procedures involved. We will first start with the schematic as a whole to show all PCB components in figure 78. Next, we will break down the schematic into pieces whereby we will explain each component and its function along with why we chose it. To refresh our knowledge, the overall purpose of this PCB is to relay the correct amount of charge into the lithium iron phosphate batteries via the solar panel. That is the big picture. Contained within the PCB there are a lot of components that provide not only functionality, but also safety to the PCB itself and the solar panel and batteries [121].

that is left are the 2 negative outputs to the current sensor. These simply allow the current to pass through the current sensor and back out so these 2 terminals are just the current exiting the sensor. As you can see there are three capacitors which are connected to Vref, VDD, and Vout. The capacitor C2 going to VDD is a supply capacitor. This simply provides stability to VDD and isolates that part of the circuit from everything else thereby mitigating any signal or power disruption. The capacitors connected to Vout and Vref, C3 and C1 respectively are decoupling capacitors which simply isolate each of these respective connections from the rest of the circuit which also provides stability. We chose this current sensor for many reasons. Besides the functionality of the device we chose this as it has a primary current of 20 amps. It also has ample sensitivity along with faster reading time so that way we have an accurate up to time spec of the current value. The ratiometric property of how the current is calculated is somewhat valuable for any VDD fluctuations; although we expect to have very minimal changes to VDD as the microcontroller will be providing the power to the current sensor[121].

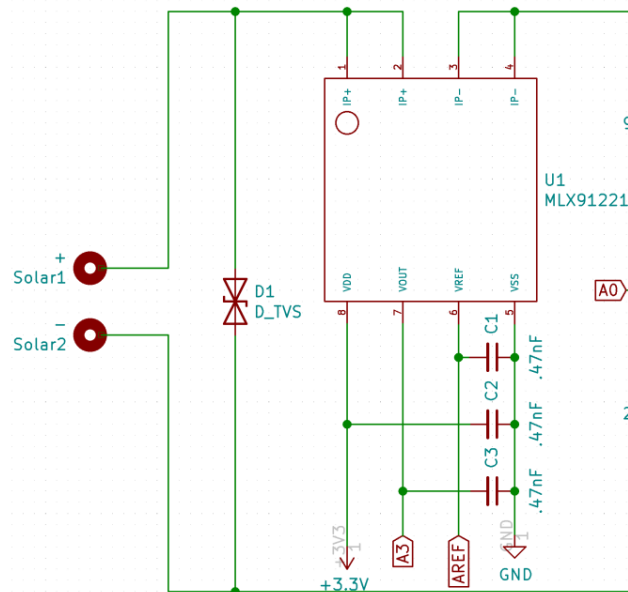


Figure 79: Schematic of Current Sensor and TVS Diode

Figure 80 below shows that once the current leaves the current sensor, the next thing that it sees will be a voltage divider consisting of a 90kΩ and a 20kΩ resistor. There are specific reasons as to the values for this voltage divider. To briefly explain the voltage divider circuit we will designate R1 to be the 90kΩ resistor and R2 to be the 20kΩ resistor. For the voltage divider to give us the correct value we are looking for, we must construct the equation in such a way that the output sees the correct input. In our case specifically, we want the microcontroller to read the voltage at the A0 pin between the resistors. A brief thing to mention here is that our microcontroller will only be able to read an input of 0 to 3.3 volts. As a result, we must use a voltage divider network in order to step down the voltage for the microcontroller so that it will be able to read an accurate voltage which has to be contained from the range of 0 to 3.3 volts. Since the analog pin A0 is between the two resistors we will want to read the voltage at R2 in order to get the correct input reading from the solar panel. The equation $V_{out} = (R2/[R1 + R2]) * V_{in}$ will suffice for our voltage divider. To prove that this equation works and that our resistor

values are $20\text{k}\Omega$ and $90\text{k}\Omega$ we start by assigning V_{out} to be the maximum voltage that the microcontroller can detect. This will give V_{out} to be 3.3V . For the V_{in} , it will be the maximum voltage that the solar panel can possibly provide at peak insolation and thus the value for V_{in} will be 18V . Given the V_{in} and V_{out} values we are able to relate R_1 and R_2 and establish a numerical ratio of what each resistor needs to be in value from one another. Through simple algebra we divide the V_{out} by the V_{in} and we are left with an equation of $0.183 = R_2/(R_1 + R_2)$ which then becomes $0.183(R_1 + R_2) = R_2$, and by simplifying gives $R_1 = 4.464R_2$. This means that for whatever value we choose R_1 to be, R_2 must be 4.464 greater than R_1 to achieve this voltage divider. As a result R_2 is chosen to be $20\text{k}\Omega$ and R_1 is $90\text{k}\Omega$. One final thing to note about the R_2 resistor is that it is a rounded value due to the resistance being calculated to be 89280Ω and thus we chose $90\text{k}\Omega$ out of simplicity. As a result there will likely be a small error associated with the reading of the voltage by the microcontroller but it will be very minimal. The capacitor that has a value denoted by $0.1\mu\text{F}$ is simply a supply capacitor which provides stability to the pin A0 so that no other elements in the circuit will affect it besides the one that it is trying to read (solar panel).

Once we have the voltage divider we move on to the 2 schottky diodes connected in parallel. These diodes are used for protection against reverse current flow and reverse polarity. Essentially it keeps the power flowing from the solar panel through the forward bias side of the diode but does not allow any current to pass through the reverse bias side thus mitigating leakage power flow which could possibly damage the solar panel [135]. Next we move onto the bipolar junction transistor which will work alongside the mosfet in our design to provide the drive to put charge into the battery. For the BJTs and the mosfets we will give tabular comparisons for each so that we can choose the best one for our application. Starting with the BJT, its role is to use a small current to drive a larger component of current. It will help to provide a large enough current to drive the mosfet to send a charge pulse to the battery thus charging it. We have found two choices for our BJT and it is outlined below in tabular format. The first one is manufactured from NXP Semiconductors which is denoted with the PMST3904 model. The other is manufactured by multcomp pro and is denoted by 2N3904. As we can see in table 17 we can see that many of the characteristics of both BJTs line up with one another. The main difference is the power dissipation of the 2nd model and the cost by a small margin. Since all the constraints below should suffice for our project, we will pick the 2N3904 model as the one we use mainly because of cost and availability at this current time. [37,44]

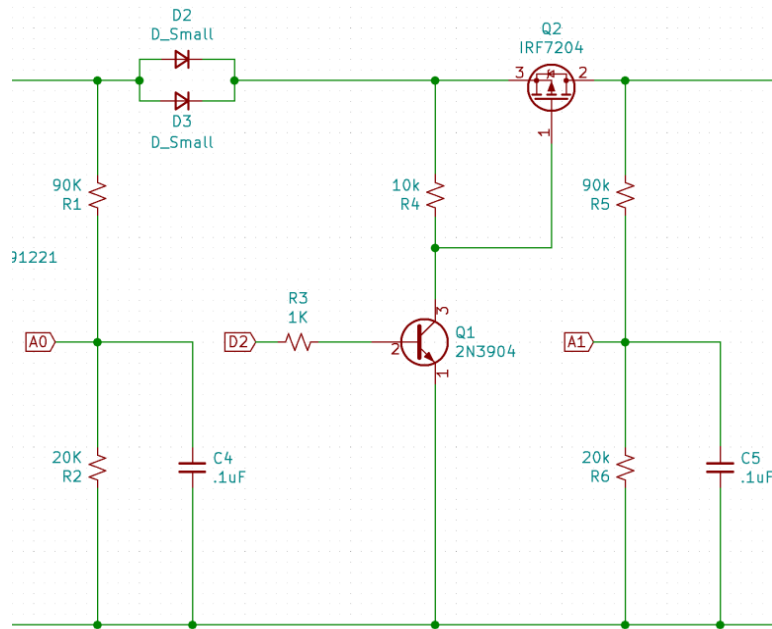


Figure 80: Schematic of Voltage Dividers, Diodes, PMOS, and NPN BJT

| Model | PMST3904 | 2N3904 |
|---------------------------------------|---|---|
| V _{ceo} | 60V | 60V |
| V _{evo} | 40V | 40V |
| V _{ebo} | 6V | 6V |
| Collector Current I _c | 200mA | 200mA |
| Total Power Dissipation | 200mW | N/a |
| Power Dissipation T _a =25C | N/a | 625mW |
| Power Dissipation T _c =25C | N/a | 1.5W |
| Storage Temperature | -65 to 150 C | -55 to 150 C |
| DC Current Gain | 300 (at I _c = 10mA) | 100-300 (I _c =10mA, I _b =1mA) |
| V _{ce(sat)} | 200mV (I _c =10mA, I _b =1mA) | <0.2V (I _c =10mA, I _b =1mA) |
| V _{be(sat)} | 650mV to 850mV (I _c =10mA, I _b =1mA) | 650mV to 850mV (I _c =50mA, I _b =5mA) |
| Noise Figure | 5db | <5db |
| Price (per 1 item) | 0.32\$ | 0.273\$ |

Table 17: BJT Comparison

Next we will discuss the mosfets that will be used within our pcb design. As the current is being driven by the BJT as it is used in the amplifying process, the mosfet will actually

allow the current to pass through as it will be switching based on how charged the battery is. The mosfet is a voltage driven device that allows the battery to be charged when the gate of the mosfet has a sufficient voltage provided to it. Once the voltage at the gate diminishes, it will allow less charge to pass into the battery. Table 18 will give the tabular comparisons of our mosfet choices. As we can see there are several differences to make note of. The first is the discrepancy between the drain currents. As we can see the 4905 version has a significantly higher drain current than the 7240 model. Along with this the pulsed drain current is much different from one another. One of the largest discrepancies is the power dissipation between the 4905 and 7240 model. There is an 80 times difference in power dissipation at a cost of increased drain current. The operating temperatures of each model are similar with the high end being given to the 4905 model. The gate to source voltage stayed the same for both models. Breakdown voltage temperature coefficient was experienced more heavily by the 4905 model and the forward transconductance was less in the 7240 model. Our choice will be the IRF7240 for two main reasons. The first is that the 7240 model is all that we would need for our PCB and secondly the cost is a lot less since we will be buying extras [39-41,89,90]

| Model | IRF4905PbF | IRF7240 |
|--|---|---|
| Id @ Tc=25C, (Vgs=-10V) | -74A (max) | N/A |
| Id @ Tc=100C,(Vgs=-10V) | -52A (max) | N/A |
| Id @ Ta=25C, (Vgs=-10V) | N/A | -10.5A (max) |
| Id @ Ta=70C,(Vgs=-10V) | N/A | -8.6A (max) |
| Idm (pulsed drain current) | -260A (max) | -43A (max) |
| Power dissipation at 25C | 200W (max) | 2.5W (max) |
| Power dissipation at 70C | N/A | 1.6W |
| Vgs | -20 to 20 (max) | -20 to 20 (max) |
| Operating junction and storage temperature range | -55 to 175C | -55 to 150C |
| V(br)Dss | -55 V (min) | -40 V (min) |
| Breakdown Voltage Temperature Coefficient | -0.05 V/C (at 25C, Id=-1mA) | -0.025 V/C (at 25C, Id=-1mA) |
| VGS(th) | -2.0 min to -4.0 max (Vds=Vgs, Id=250uA) | -1.0 min to -3.0 max (Vds=Vgs, Id=250uA) |
| Forward Transconductance | 21 S (Vds =-25V, Id=-38A) | 17 S (Vds =-10V, Id=-10.5A) |
| Price (per item) | 1.90\$ | 0.91\$ |

Table 18: MOSFET Comparison

Once the current flows out of the PMOS, the next thing that it sees will be a voltage divider consisting of a $90\text{k}\Omega$ and a $20\text{k}\Omega$ resistor. The resistors will be included so that the microcontroller will be able to recognize what the voltage is from the battery. It will then relay this through the pin A1 which will go into the microcontroller. The microcontroller will then convert the voltage to be read by the same mechanics that the first voltage divider was read but the only difference is that it will be reading the battery voltage. The values of the resistors will stay the same as the V_{out} will not go above 18 volts for the battery. Also, the microcontroller will remain 0 to 3.3 volts so the range will stay the same. The highest voltage that the battery should ever reach would be no more than 14.6. Any higher and we risk damaging the battery itself. The capacitor that has a value denoted by $0.1\mu\text{F}$ is simply a supply capacitor which provides stability to the pin A1 so that no other elements in the circuit will affect it besides the one that it is trying to read (battery bank).

Once we move past the voltage divider we will come to another protection element called a fuse in Figure 81. The fuse is an element which offers protection to our system as it will cause a break in the circuit in the event of a current spike for whatever reason. In our schematic, for whatever reason, if more than 10 amps of current goes through the fuse element it will blow and make it impossible for the current to affect any other electronics in the circuit. As there are many different varieties of fuses and that they are very simple devices we will look for one of the most cost effective one and one that is able to protect our circuit for current surges greater than 10 amps. Moving down the schematic we can also see that the battery will be connected up to the charge controller right after the fuse so that it is isolated from the rest of the circuit elements such as the current sensors, MOSFETS, BJTs and any passive elements contained within. B+ and B- give the terminal connections in the schematic and the BAT + and BAT - indicate the actual terminal connections [121].

Directly after the fuse we have another NPN transistor with a PMOS configuration. We will keep both of these devices the same as they were used previously in sending pulse charges to the actual battery. The main difference between the PMOS and NPN transistors here is that this configuration will be used to drive the charge from the battery into the load. We will use the same models for the NPN transistor and PMOS as 2N3904 and IRF7240 respectively. One thing we are likely to expect when we test this system as a whole is that in the future we may have to change certain values on the transistors and quite possibly if they do not perform as we originally thought, change the models of the transistors themselves. After the transistors will send charge to the load connected to them, a current sensor will monitor the current coming out of the MOSFET and also the current being supplied to the load where the load terminals are attached in the schematic after the current sensor. The current sensor acts the same as it did in the earlier part of the circuit. A current will be taken in the IP+ terminals where the current sensor will give a V_{out} . For the V_{out} on the current sensor we have the voltage that the current sensor sees. Once this happens the offset voltage (which is one half V_{DD}) is subtracted and then dividing that value by the sensitivity of 62.5mV/A provided by the data sheet gives the actual measured current. The capacitors C6, C7 and C8 are simply V_{ref} , V_{ss} , and V_{out} respectively are decoupling capacitors which simply isolate each of these respective connections from the rest of the circuit which also provides stability. This current sensor is the same one as we used in the earlier part of the circuit and will function the same way

but the difference will be that the load will be seeing the current and the battery will be supplying this to the load. The final connections are for the load denoted as LOAD1+ and LOAD2-. This will be what the battery actually powers. From the load the microcontroller will be powered along with a split connection going to the inverter which will convert the DC power coming out of the battery into AC power which will provide adequate charge to external devices we choose to plug into our outlets.

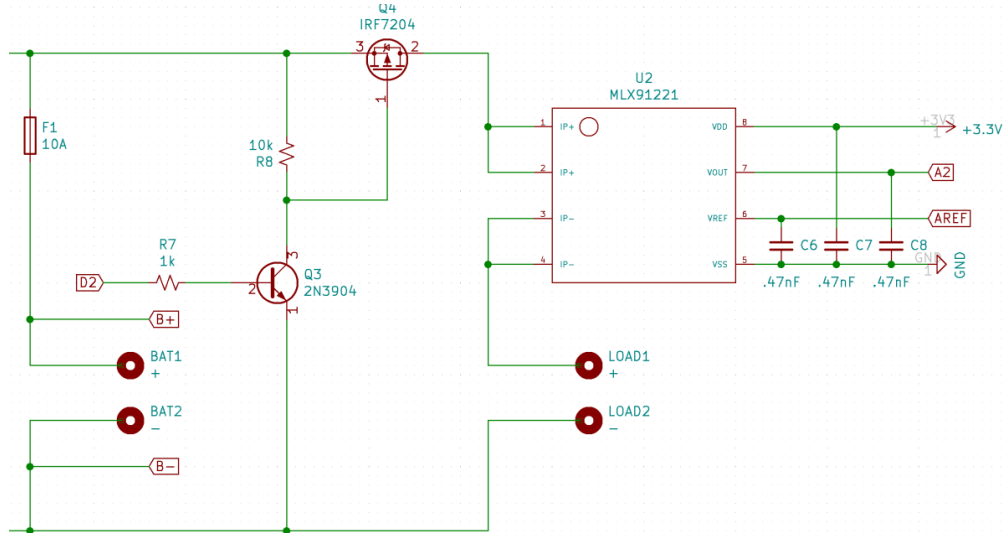


Figure 81: Schematic Focus on Fuse, Current Sensor, Battery and Load Terminals

5.2.2 Lithium Iron Phosphate Battery Assembly

As explained in section 3.8, we chose to design a battery assembly using four lithium iron phosphate battery cells in conjunction with a BMS. As described, this option was much cheaper, and added an extra layer of design to our project. At this point in the project, the battery cells have been ordered from AliExpress, but as they have to be imported from overseas, we have not received them yet. Because of this, we used custom CAD drawings we put together to simulate how our battery design will be assembled. As instructed by the manufacturer, the battery cells come in packs of four with bus bars and metallic screws for the battery contacts. Each of the cells we will be receiving is rated at 200Ah, but as mentioned in section 3.8, is only 3.2V. This means to achieve our desired 12.8V, 200Ah battery assembly, we will have to connect all four cells in series since series connections add voltage, but do not change current. Another factor we had to consider before proposing a design for connecting the cells is the potential necessity for space between the cells when they are connected. Some manufacturers recommend ordering longer bus bars to create a space between each connected cell for heat dissipation, but in the case of our ordered cells this was not the case. Each of these aforementioned design aspects discussed can be seen in figure 82 below in images 1 and 2. In figure 82, image 1, an overhead view of the connected battery cells are shown with overall dimensions. In order to establish the series connection of the cells previously mentioned, the bus bars had to be connected from positive to negative, and so on until all four cells were connected as shown in image 1 in the figure below. These bus bars will be fastened on with the provided screws and hex nuts given by the manufacturer. In image 2 of the figure below, a side view is shown with the overall dimensions.

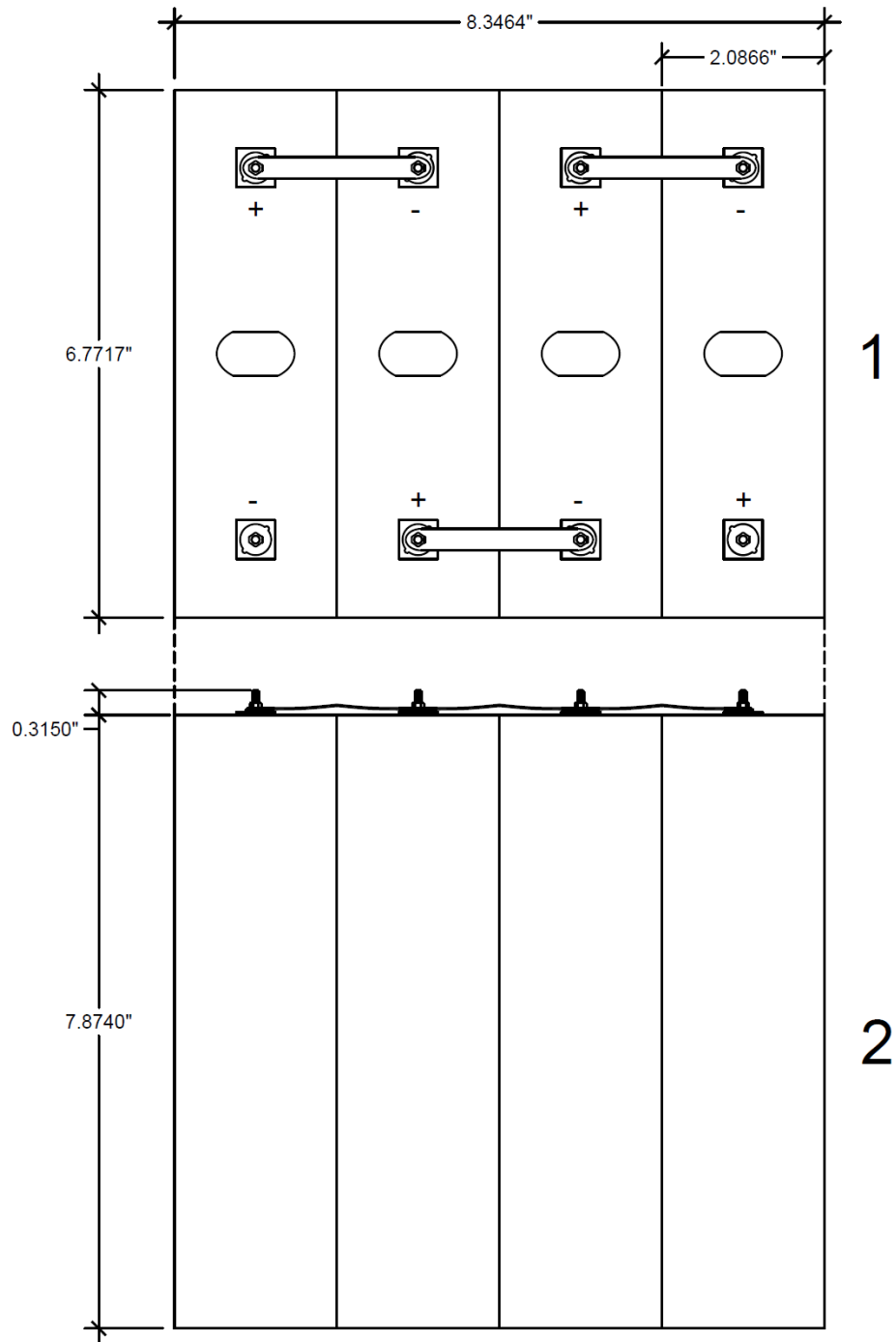


Figure 82: Battery Cell Connection With Included Bus Bars

5.2.2.1 BMS Attachment to Battery Assembly

For the next part of the battery assembly design, we need to attach the purchased BMS to the whole assembly. Though the assembly above in section 5.2.2 works without a BMS, the BMS will provide important data on the battery cells, and protection for the whole

battery assembly. A lot of research had to go into the exact attachment of the BMS to the battery in such a way that it would “play nicely” with our custom enclosure design idea. Before figuring out the attachment design, the BMS size and components had to first be considered. The dimensions of the BMS and the integral components can be seen below in figure 83 pictures 1 and 2. In image 1, the side view of the BMS is shown with the B and P cables coming out of the page. The main design component comes from picture 2 in the figure below. The first two components to consider for the design of the BMS attachment are the two cables labeled as “B” and “P.” The “B” cable is the main negative cable connected to the main negative terminal of the battery. This connection can be seen in figure 83 below in image 1 and 2. The “P” cable is used as the negative connection to the supplied load. In the case of our design we are using a modified sine wave inverter meaning the “P” cable will be attached to the negative terminal of the modified sine wave inverter. Next, the ribbon cables on the right side of image 2 in the figure below had to be implemented into the design. Because our battery assembly is four cells attached in series, it is considered a 4S assembly. The BMS shown below is rated for 4S assemblies, and thus there are five cables in the ribbon cable assembly. There are four positive cables for each positive terminal on the battery assembly, and one negative cable for the main negative terminal of the battery assembly. This connection can be seen in figure 84 below images 1 and 2. Finally, for the BMS to battery assembly connection, after all of the previous components of the BMS have been attached, a red four gauge wire will be added to the main positive terminal of the battery assembly as seen in figure 84 pictures 1 and 2. This will be the wire that extends out of the battery assembly to be connected to the load. As explained in the wire gauge we chose 4 gauge wire for the main terminals of our battery assembly to handle the 60A which our BMS is rated for. After all the wires of the BMS are connected to the battery assembly, the BMS will be attached to the side of the battery assembly as seen in figure 84 pictures 1 and 2 with a strong adhesive.

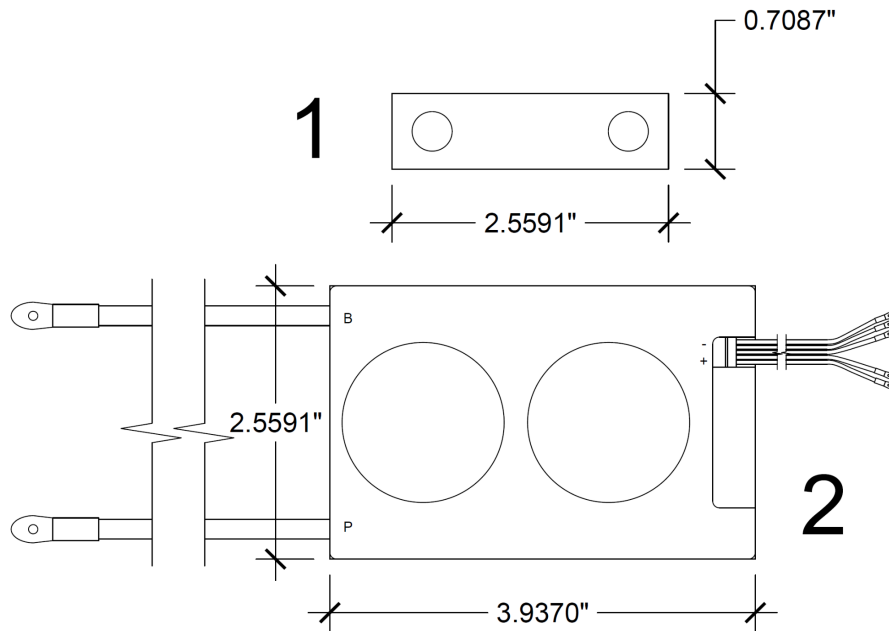


Figure 83: BMS Components and Dimensions

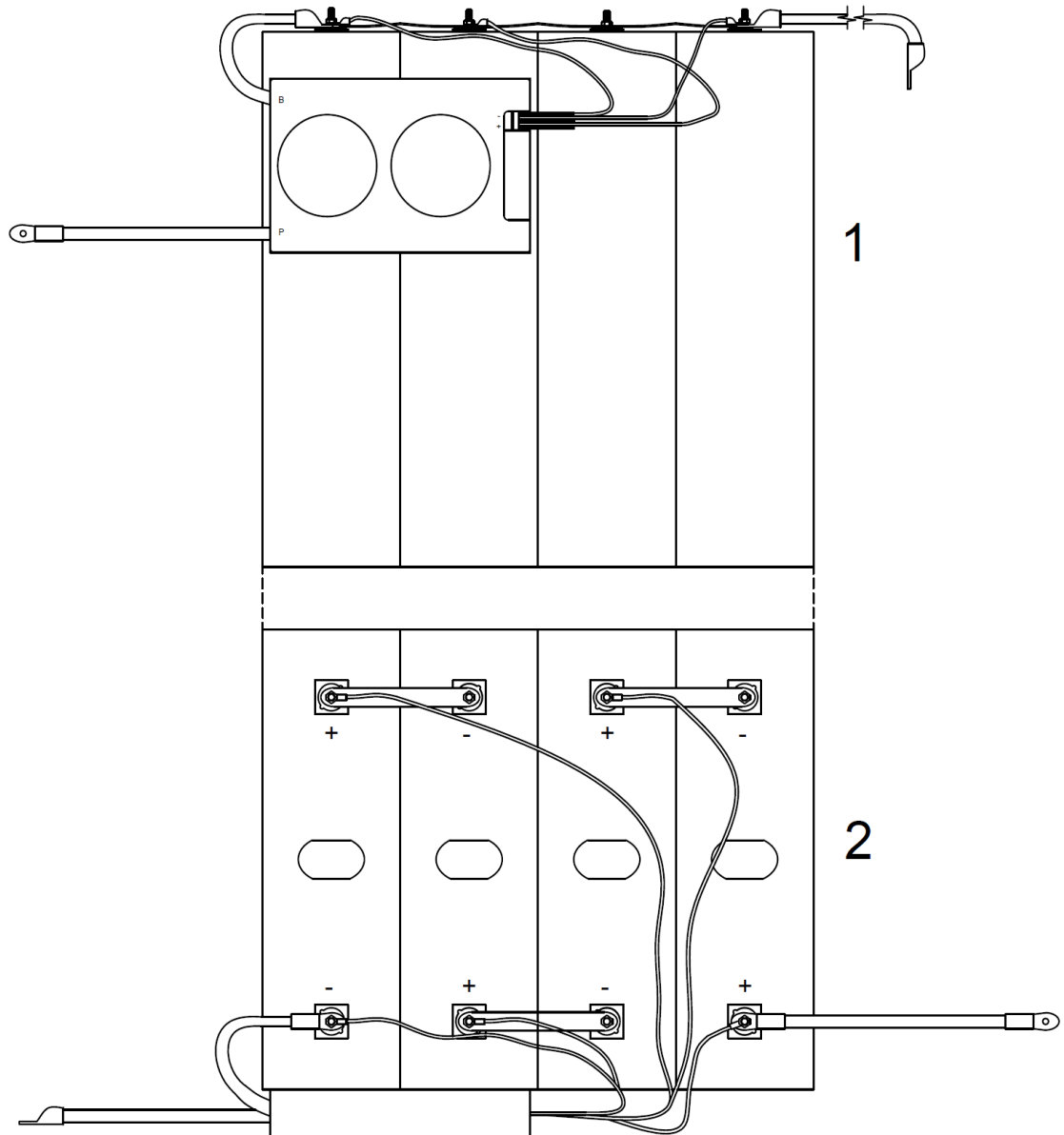


Figure 84: BMS to Battery Cells Connection

5.2.2.2 Battery Assembly Custom Enclosure Design

For the final part of our battery assembly design, we decided to design a custom enclosure to house the whole battery assembly described in the previous sections. At first we wanted to 3D print an entire enclosure, but we ended up cancelling that idea due to no longer having availability to a 3D printer that could print a housing to the scale we need. After much thought, a plexiglass design was proposed. Not only is plexiglass non-conductive, but it is also water resistant and relatively durable. Additionally, it's easy to obtain, and the whole battery assembly can be seen through the plexiglass. Our design can be seen below in figure 85 image 1 and 2.

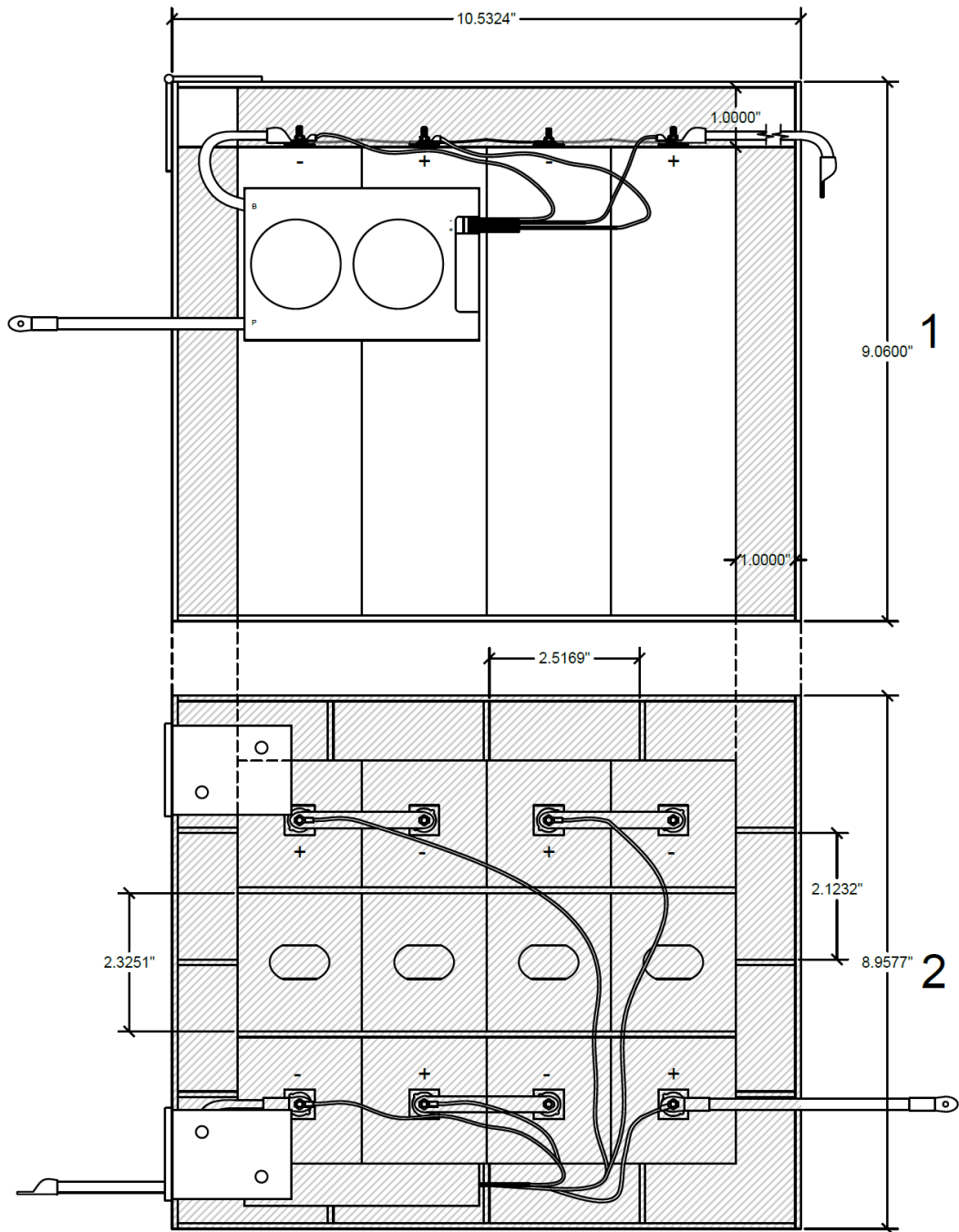


Figure 85: Custom Plexiglass Battery Assembly Enclosure

As previously explained, the above design is our custom plexiglass battery assembly enclosure. The first step for our design will be a plexiglass shell with the specified dimensions shown in the figure above in pictures 1 and 2. Next, we will be using vertical pieces of plexiglass with the shown dimensions in the figure above in pictures 1 and 2. They will be placed around the entire enclosure spaced with specified spacing. This will help hold the battery cells in place, stabilize the plexiglass shell, and allow for a greater

amount of heat dissipation. Finally, we designed a plexiglass lid with hinges in order to swing open and close. One important component of this lid are the two center pieces of plexiglass which can be seen in the above figure in pictures 1 and 2. These two pieces are used for stability for the lid and to keep the lid from hitting the wires/electrodes.

5.2.3 Custom Solar Charge Controller Enclosure Design

For this next section of the design, we designed a schematic for a custom solar charge controller enclosure in CAD. Our intent for this design is for it to be 3D printed. Unlike the battery assembly, this design is smaller and can be made using more conventional easily available 3D printers. This enclosure will contain our custom designed PCB discussed above in section 5.2.1. Below is our custom enclosure design in figure 86 pictures 1 and 2. Our design will be simple and will include an opening to receive the six contacts for the solar panel, battery, and load portion of the PCB. It will also have an opening to receive the capacitive touchscreen and each of these previously mentioned components can be seen in the below figure in picture 1. Finally, in figure 87 on the next page, the side view of the custom enclosure is shown which has an opening to receive the temperature sensor.

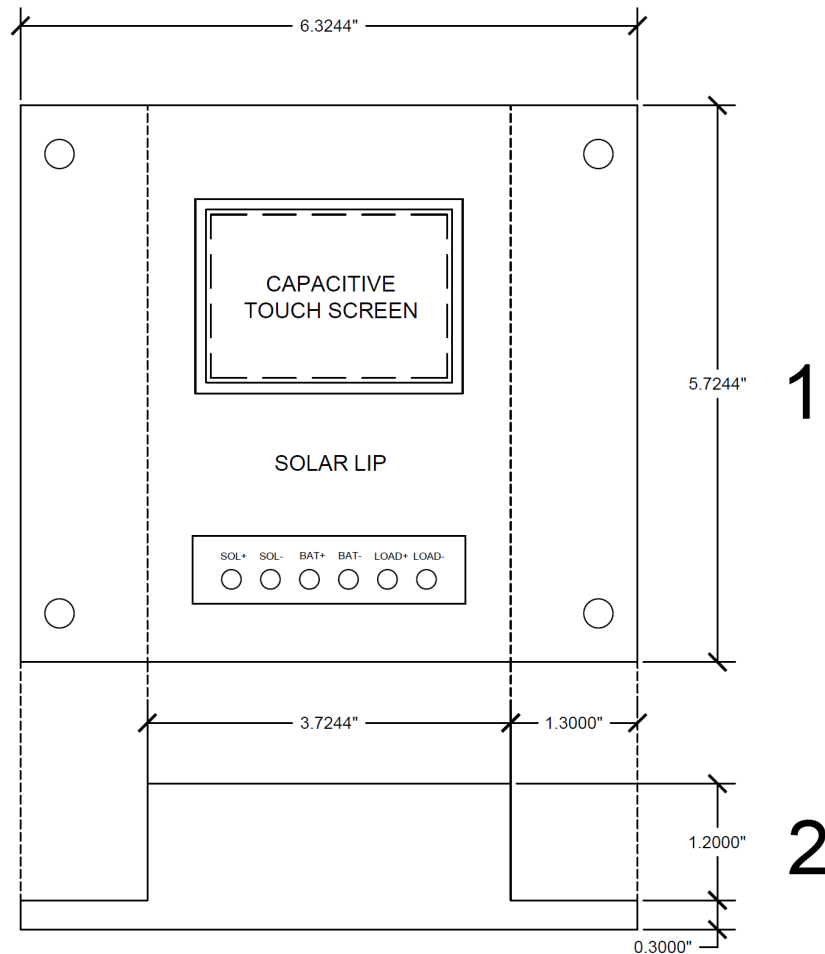


Figure 86: Custom Solar Charge Controller Enclosure Front and Bottom

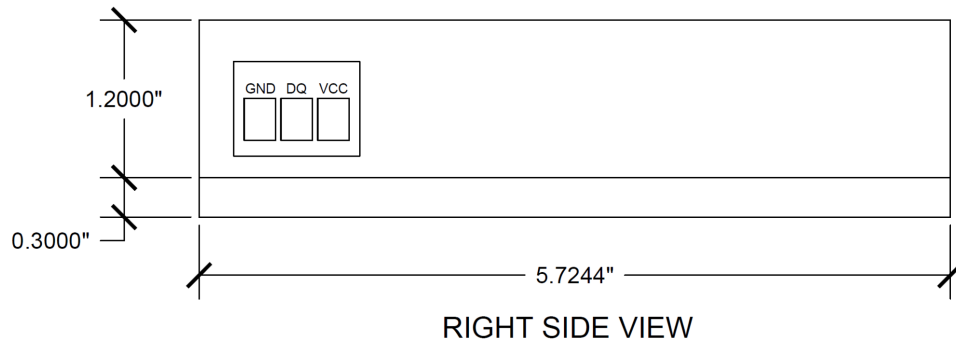


Figure 87: Custom Solar Charge Controller Enclosure Side View

5.2.4 Solar Panel Connection to Solar Charge Controller

Even though we will not be designing our own solar panel, it is important for our design to explain how we will be connecting the solar panel to the solar charge controller. Our donated solar panel already comes with 14 gauge connectors provided by the manufacturer which will be connected on the SOL+ and SOL- terminals shown in our design in figure 86 picture 1. The overall design can be seen below in figure 88.

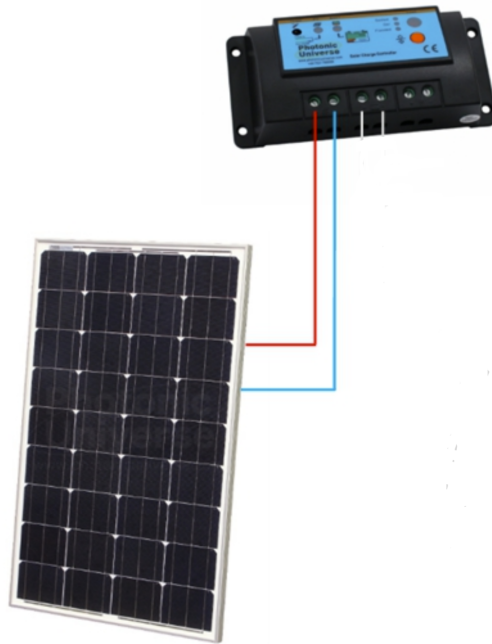


Figure 88: Connecting the Solar Panel to Our Charge Controller

5.2.5 Battery to Inverter Connection

Similar to the solar panel section, we will not be using our own inverter, but rather using a donated modified sine wave inverter. Though it is a crude representation, the figure below generally depicts how we will be connecting our donated modified sine wave inverter to our battery assembly. In the case of our design, we will have a BMS connected between the battery assembly and the inverter. As explained in section 5.2.2, we will be connecting the “P” cable to the negative terminal of the modified sine wave inverter. From here, the connected 4 gauge wire on the main positive terminal of the battery will be connected to the positive terminal of the modified sine wave inverter. Between the 4 gauge wire and the BMS this assembly can handle 60 Amps. After this assembly is complete, AC devices can be connected into the two power plugs provided by our donated modified sine wave inverter.

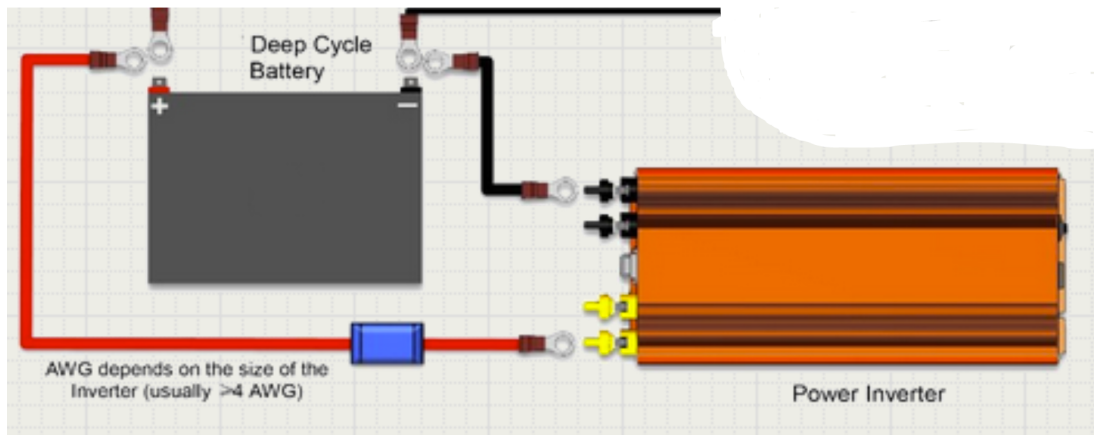


Figure 89: Connecting the Inverter to the Battery

Important Note:

Sections 6.0 - 7.0 are reserved here and will be added as we test and prototype our received equipment and design in Senior Design II.

8.0 Budget and Funding

Our budget will be self funded, excluding malfunction of equipment and breakage, the cost of materials can be found below in tabular format:

| Budget Analysis | | | |
|---|---|-----------------------|-------------------------------|
| Item | Quantity | Price Estimate | Place of origin |
| Solar Panel | 1 | Donated | Friend |
| Charge Controller (PCB Components) | 1 | \$80 | Custom Made (Varies) |
| Battery Cells | 4 | \$312.04 | AliExpress |
| Microcontroller | 1 | \$25 | Adafruit |
| Custom PCB Breakout Board | 1 | \$6.47 | JLPCB |
| BMS | 1 | \$45.92 | AliExpress |
| Capacitive LCD Display | 1 | \$39.95 | Adafruit |
| Relay | 2 | \$12 | Amazon |
| Custom Enclosure (Plexi) | 1 | \$39.44 | Home Depot |
| Hinge | 3 | \$9.98 | Home Depot |
| Wiring of different gauges | Varies | \$35 / Donated | Amazon/Friend |
| Soldering materials | 1 Soldering Iron 1 60/40 Rosin Solder 1 Rosin Paste Flux | \$65 | Amazon/ Home Depot |
| Inverter | 1 | Donated | Friend |
| Temperature Sensor | 1 | \$5.00 | Adafruit |
| Total | N/A | \$675.80 | N/A |

Table 19: Budget and Funding

8.1 Milestones

SD1 Milestones

| Description | Timeline | Completion Date |
|--|-----------------|------------------------|
| Senior Design Grouping | 1 week | 1st week (1/14/2021) |
| Project Idea Brainstorming | 1 week | 2nd week (1/21/2021) |
| Divide and Conquer 1.0 | 1 week | 3rd week (1/29/2021) |
| Divide and Conquer 1.0 Meeting | 1 week | 4th week (2/1/2021) |
| Divide and Conquer 2.0 (Project Locked in) | 1 week | 5th week (2/12/2021) |
| Initial Project Research/60 Page Draft | 7 weeks | 12th week (4/2/2021) |
| 100 Page Draft | 2 weeks | 14th week (4/16/2021) |
| Final Document | 2 weeks | 16th week (4/27/2021) |

Table 20: SD1 Milestones

SD2 Milestones

| Description | Timeline | Completion Date |
|---------------------------------|-----------------|------------------------|
| Project prototype build | 4 weeks | 4th week (6/4/2021) |
| Testing and fixes | 2 weeks | 6th week (6/18/2021) |
| Finish prototype based on fixes | 2 weeks | 8th week (6/29/2021) |
| In class presentation | TBA | TBA |
| Final document for turn-in | TBA | TBA |
| Final presentation | TBA | TBA |

Table 21: SD2 Milestones

Bibliography

- [1] “100 Watt 12 Volt Monocrystalline Solar Panel.” *HQST*, hqsolarpower.com/100-watt-12-volt-monocrystalline-solar-panel/.
- [2] “2N3904 - Bipolar (BJT) Single Transistor, NPN, 40 V, 200 mA, 625 mW, TO-92, Through Hole.” *Newark*, www.newark.com/multicomp-pro/2n3904/bipolar-transistor-npn-40v-to/dp/08N8111?CMP=AFC-SF-BNL.
- [3] (n.d.). In J. G. Proakis, *Digital Signal Processing (4th Edition)* (p. 403). Prentice Hall.
- [4] Admin. “Electrochemical Series - Definition, Chart, Applications.” *BYJUS*, 14 Oct. 2020, byjus.com/jee/electrochemical-series/.
- [5] Administrator. “How To Make 12v DC to 220v AC Converter/Inverter Circuit Design?” *Electronics Hub*, 2 Jan. 2016, www.electronicshub.org/12v-dc-220v-ac-converter-circuit/.
- [6] Administrator. “Interfacing ACS712 Current Sensor with Arduino - Measure Current with Arduino - Measuring Current with Arduino.” *Electronics Hub*, 19 July 2018, www.electronicshub.org/interfacing-ac712-current-sensor-with-arduino/.
- [7] Agarwal, Tarun, et al. “Types of Voltage Regulators : Working and Their Limitations.” *ElProCus*, 18 Jan. 2021, www.elprocus.com/types-of-voltage-regulators-and-working-principle/.
- [8] “Arduino ADC.” *Best Microcontroller Projects*, www.best-microcontroller-projects.com/arduino-adc.html.
- [9] Augusto, A., et al. “Open-Circuit Voltage.” *PVEducation*, www.pveducation.org/pvcdrom/solar-cell-operation/open-circuit-voltage.
- [10] Barai, Anup, et al. “Transportation Safety of Lithium Iron Phosphate Batteries - A Feasibility Study of Storing at Very Low States of Charge.” *Scientific Reports*, Nature Publishing Group UK, 11 July 2017, www.ncbi.nlm.nih.gov/pmc/articles/PMC5505962/.
- [11] Barr, Michael. *Embedded C Coding Standard*. Barr Group, 2018.
- [12] “Battery Characteristics.” *DoITPoMS*, www.doitpoms.ac.uk/tlplib/batteries/battery_characteristics.php.
- [13] “Battery Management System.” *Battery Management System - an Overview | ScienceDirect Topics*, www.sciencedirect.com/topics/engineering/battery-management-system.
- [14] “Battery Management System.” *Wikipedia*, Wikimedia Foundation, 8 Apr. 2021, en.wikipedia.org/wiki/Battery_management_system.

- [15] “Battery Management System Tutorial.” *Renesas*, www.renesas.com/us/en/products/power-power-management/battery-management-system-tutorial.
- [16] “Battery Temperature Compensation - SunWize: Power Independence.” *SunWize*, 14 Dec. 2017, www.sunwize.com/tech-notes/battery-temperature-compensation/#:~:text=This%20affect%20how%20much%20energy,sulfate%20when%20it%27s%20too%20cold.
- [17] Battery, Crown. “What Is a Deep Cycle Battery? .” *Crown Battery- The Power Behind Performance*, 24 Apr. 2018, 9:37AM, www.crownbattery.com/news/what-is-a-deep-cycle-battery-.
- [18] Beck, Anton. “Lithium Iron Phosphate Vs. Lithium-Ion: Differences and Advantages.” *Epec's Blog*, 20 Sept. 2019, blog.epectec.com/lithium-iron-phosphate-vs-lithium-ion-differences-and-advantages.
- [19] “Bipolar Junction Transistor (BJT) Theory Worksheet - Discrete Semiconductor Devices and Circuits.” *All About Circuits*, 29 June 2020, www.allaboutcircuits.com/worksheets/bipolar-junction-transistor-bjt-theory/.
- [20] “BU-107: Comparison Table of Secondary Batteries.” *Secondary (Rechargeable) Batteries – Battery University*, batteryuniversity.com/learn/article/secondary_batteries.
- [21] “BU-201: How Does the Lead Acid Battery Work?” *Lead-Based Batteries Information – Battery University*, batteryuniversity.com/learn/article/lead_based_batteries.
- [22] “BU-203: Nickel-Based Batteries.” *Nickel-Based Batteries Information – Battery University*, batteryuniversity.com/index.php/learn/article/nickel_based_batteries.
- [23] “BU-205: Types of Lithium-Ion.” *Types of Lithium-Ion Batteries – Battery University*, batteryuniversity.com/index.php/learn/article/types_of_lithium_ion.
- [24] “BU-302: Series and Parallel Battery Configurations.” *Serial and Parallel Battery Configurations and Information*, batteryuniversity.com/learn/article/serial_and_parallel_battery_configurations.
- [25] “BU-303: Confusion with Voltages.” *Battery Voltage Information – Battery University*, batteryuniversity.com/learn/article/confusion_with_voltages#:~:text=Lead%20Acid,cause%20the%20buildup%20of%20sulfation.
- [26] “BU-402: What Is C-Rate?” *Charles-Augustin De Coulomb's C-Rate for Batteries*, batteryuniversity.com/learn/article/what_is_the_c_rate.
- [27] “BU-501: Basics about Discharging.” *Battery Discharge Methods – Battery University*, batteryuniversity.com/learn/article/discharge_methods.

- [28] “BU-804b: Sulfation and How to Prevent It.” *Sulfation and How to Prevent It - Battery University*, batteryuniversity.com/learn/article/sulfation_and_how_to_prevent_it.
- [29] “BU-908: Battery Management System (BMS).” BU-908: Battery Management System (BMS) – Battery University, batteryuniversity.com/learn/article/how_to_monitor_a_battery.
- [30] “Charging Module for Newest Types of Rechargeable Batteries LiFePO4.” *IEEE Xplore*, ieeexplore.ieee.org/document/5423730.
- [31] Chu, Pong P. “FPGA Prototyping by Verilog Examples.” *Google Books*, Google, books.google.com/books?id=z8XhRwmWpeQC&pg=PT253&dq=uart+serial&hl=en&sa=X&ved=0ahUKEwiw25mJq_LdAhWky4MKHUI_B1A4FBDoAQgmMAA#v=onepage&q=uart%20serial&f=false.
- [32] Clark, Jim. “The Electrochemical Series.” *The Electrochemical Series*, 2002, www.chemguide.co.uk/physical/redoxeqia/ecs.html.
- [33] Clean Energy Ideas. “Monocrystalline vs Polycrystalline Solar Panels.” *Clean Energy Ideas*, 26 June 2019, www.clean-energy-ideas.com/solar/solar-panels/monocrystalline-vs-polycrystalline-solar-panels/.
- [34] Cloud, Maria. “What Is the Energy Density of a Lithium-Ion Battery?” *Home*, www.fluxpower.com/blog/what-is-the-energy-density-of-a-lithium-ion-battery#:~:text=What%20is%20Battery%20Energy%20Density,one%20watt%20for%20one%20hour.
- [35] Contributor, TechTarget. “What Is Battery Management System (BMS)? - Definition from WhatIs.com.” *WhatIs.com*, TechTarget, 16 May 2014, whatis.techtarget.com/definition/battery-management-system-BMS.
- [36] Dahl, Øyvind Nydal, et al. “How Transistors Work (NPN and MOSFET) - The Simple Explanation.” *Build Electronic Circuits*, 26 Mar. 2021, www.build-electronic-circuits.com/how-transistors-work/.
- [37] Data Sheet 2N3904
- [38] Data Sheet GV-10Li
- [39] Data Sheet IRF4905fPBF
- [40] Data Sheet IRF7240 TRPBF
- [41] Data Sheet MLX91221
- [42] Data Sheet MP2307
- [43] Data Sheet MPPT
- [44] Data Sheet PMST3904 NPN Switching Transistor

- [45] Data Sheet PS-15 Gen 3
- [46] Data Sheet PS-15M Gen 3
- [47] Data Sheet PS-30 Gen 3
- [48] Data Sheet PS-30M Gen 3
- [49] Dave. “What Is Thermal Runaway?” *Sure Power, Inc*, 15 July 2013, www.sure-power.com/2013/07/what-is-thermal-runaway/.
- [50] “Design Your Own LiFePO4 Solar Power System.” *Mobile Solar Power Made Easy!*, www.mobile-solarpower.com/design-your-own-12v-lifepo4-system.html.
- [51] D Kudryashov *et al* 2018 *J. Phys.: Conf. Ser.* 1124 041010
- [52] Dhaker, Piyu. “Introduction to SPI Interface.” *Introduction to SPI Interface | Analog Devices*, www.analog.com/en/analog-dialogue/articles/introduction-to-spi-interface.html.
- [53] Ding, Wengfeng, and Scott E. Johnson. “Polycrystalline Material.” *Polycrystalline Material - an Overview | ScienceDirect Topics*, www.sciencedirect.com/topics/engineering/polycrystalline-material.
- [54] Dube, Ryan. “Capacitive vs. Resistive Touchscreens: What Are the Differences?” *MUO*, 28 Nov. 2018, www.makeuseof.com/tag/differences-capacitive-resistive-touchscreens-si/.
- [55] Durbin, Dan, and Quinn Horn. “BU-106: Advantages of Primary Batteries.” *Primary (Non-Rechargeable) Batteries – Battery University*, 15 Feb. 2012, batteryuniversity.com/learn/article/primary_batteries.
- [56] “Electrical Relay and Solid State Relays.” *Basic Electronics Tutorials*, 11 Feb. 2018, www.electronics-tutorials.ws/io/io_5.html.
- [57] “Electrical Relay and Solid State Relays.” *Basic Electronics Tutorials*, 11 Feb. 2018, www.electronics-tutorials.ws/io/io_5.html.
- [58] “Electrochemistry (Article).” *Khan Academy*, Khan Academy, www.khanacademy.org/test-prep/mcat/physical-processes/intro-electrochemistry-mcat/a/electrochemistry.
- [59] “Electronics Fundamentals: Voltage Regulator.” *Electronics Fundamentals: The Voltage Regulator*, www.jameco.com/Jameco/workshop/learning-center/voltage-regulator.html.
- [60] EnergySage. “Types Of Thin-Film Solar Panels: What You Need To Know: EnergySage.” *Solar News*, EnergySage, 30 Oct. 2020, news.energysage.com/types-of-thin-film-solar-panels/.

[61] Engineering, Omega. “What Is a PID Controller?” [https://www.omega.com/En-US/Omega Engineering Inc](https://www.omega.com/En-US/Omega-Engineering-Inc), 17 Apr. 2019, www.omega.com/en-us/resources/pid-controllers.

[62] Engineers Edge, LLC. “Battery Definitions and Terms.” *Engineers Edge*, engineersedge.com/battery/battery_definitions.htm#:~:text=Gassing%20-%20Evolution%20of%20gas%20from,battery%20is%20on%20equalizing%20charge.

[63] “EVE Lifepo4 3.2V 280 Power Lithium Ion Battery for RV/Solar System Storage .” *EVE 3.2V 280Ah LiFePO4 Prismatic Battery Cell*, www.evlithium.com/hot-lithium-battery/946.html.

[64] Flowers, Paul, and Klaus Theopold. “17.5: Batteries and Fuel Cells.” *Chemistry LibreTexts*, Libretexts, 5 Nov. 2020, [chem.libretexts.org/Bookshelves/General_Chemistry/Book%3A_Chemistry_\(OpenSTAX\)/17%3A_Electrochemistry/17.5%3A_Batteries_and_Fuel_Cells#:~:text=a%20single%20cell,-,There%20are%20two%20basic%20types%20of%20batteries%3A%20primary%20and%20secondary,use%20E%20and%20cannot%20be%20recharged.&text=The%20second%20type%20is%20rechargeable,acid%2C%20and%20lithium%20ion%20batteries](http://chem.libretexts.org/Bookshelves/General_Chemistry/Book%3A_Chemistry_(OpenSTAX)/17%3A_Electrochemistry/17.5%3A_Batteries_and_Fuel_Cells#:~:text=a%20single%20cell,-,There%20are%20two%20basic%20types%20of%20batteries%3A%20primary%20and%20secondary,use%20E%20and%20cannot%20be%20recharged.&text=The%20second%20type%20is%20rechargeable,acid%2C%20and%20lithium%20ion%20batteries).

[65] Fulcher, Jonathan. “How Do Solar Cells Produce Electricity?” *Lexology*, 9 July 2019, www.lexology.com/library/detail.aspx?g=10aff4c1-37ba-4d43-a0ca-4154f5bd0473.

[66] “Genasun GV-10 MPPT Charge Controller for Lithium Batteries.” *AltEstore.com*, www.altestore.com/store/charge-controllers/solar-charge-controllers/mppt-solar-charge-controllers/genasun-gv-10-li-142v-mppt-charge-controller-for-lithium-batteries-p11517/.

[67] Granath, Erika, and Emmanuel Odunlade. “Different Types of Voltage Regulators and Working Principle.” *Power & Beyond*, Power & Beyond, 22 Apr. 2020, www.power-and-beyond.com/different-types-of-voltage-regulators-and-working-principle-a-919791/.

[68] Grepow. “Can We over-Charge the LiFePO4 Battery?” *Grepow Blog*, 8 July 2020, www.grepow.com/blog/can-we-over-charge-the-lifepo4-battery/#:~:text=Overcharging%20a%20battery%20means%20that%20the%20battery%20charger,When%20the%20charge%20exceeds%203.65V%2C%20it%20is%20overcharged.

[69] Hannan, M. A., et al. “Fig. 6. Lead-Acid Battery Chemistry: (a) during Discharging, (b) during...” *ResearchGate*, 12 Nov. 2020, www.researchgate.net/figure/Lead-acid-battery-chemistry-a-during-discharging-b-during-charging-and-c-LA_fig4_311305861.

[70] Heath, Janet. “PWM: Pulse Width Modulation: What Is It and How Does It Work?” *Analog IC Tips*, 6 Nov. 2018, www.analogictips.com/pulse-width-modulation-pwm/.

- [71] “How Do I Read the Solar Panel Specifications?” *Solar Power News & DIY Solar Tips*, 28 Apr. 2016,
www.altestore.com/blog/2016/04/how-do-i-read-specifications-of-my-solar-panel/#.YGaJfehKiiN.
- [72] “How Do Photovoltaics Work?” *NASA*, NASA,
science.nasa.gov/science-news/science-at-nasa/2002/solarcells.
- [73] “How Do Rechargeable (That Is, Zinc-Alkaline or Nickel-Cadmium) Batteries Work and What Makes the Reactions Reversible in Some Batteries, but Not in Others?” *Scientific American*, Scientific American, 21 Oct. 1999,
www.scientificamerican.com/article/how-do-rechargeable-that/.
- [74] “How Do Solar Panels Work? The Science of Solar Explained.” *Solect Energy*, 27 Mar. 2018, solect.com/the-science-of-solar-how-solar-panels-work/.
- [75] “How Relays Work: Relay Diagrams, Relay Definitions and Relay Types.” *How Relays Work | Relay Diagrams, Relay Definitions and Relay Types*,
www.galco.com/comp/prod/relay.htm.
- [76] “How to Read Solar-Panel Output Specifications?” *Solar 4 RVs*,
www.solar4rvs.com.au/buying/buyer-guides/how-to-read-solar-panel-specifications/.
- [77] “How The BMS Works.” *Orion Li-Ion Battery Management System*,
www.orionbms.com/general/how-it-works/.
- [78] “How To Charge Lithium Iron Phosphate (LiFePO4) Batteries.” Power Sonic, 25 Mar. 2021,
www.power-sonic.com/blog/how-to-charge-lithium-iron-phosphate-lifepo4-batteries/.
- [79] Hymel, Shawn. *What Is a Battery?*,
learn.sparkfun.com/tutorials/what-is-a-battery/all.
- [80] *I2C Info – I2C Bus, Interface and Protocol*, i2c.info/.
- [81] “IEEE 1666-2011 - IEEE Standard for Standard SystemC Language Reference Manual.” IEEE SA - The IEEE Standards Association - Home,
standards.ieee.org/standard/1666-2011.html.
- [82] “Introduction to Battery Management Systems - Technical Articles.” *All About Circuits*,
www.allaboutcircuits.com/technical-articles/introduction-to-battery-management-systems/.
- [83] “Introduction to Bipolar Junction Transistors (BJT): Bipolar Junction Transistors: Electronics Textbook.” All About Circuits,
www.allaboutcircuits.com/textbook/semiconductors/chpt-4/bipolar-junction-transistors-bjt/.

- [84] Industries, Adafruit. “1.8” SPI TFT Display, 160x128 18-Bit Color - ST7735R Driver.” *Adafruit Industries Blog RSS*, www.adafruit.com/product/618.
- [85] Industries, Adafruit. “MCP9808 High Accuracy I2C Temperature Sensor Breakout Board.” *Adafruit Industries Blog RSS*, www.adafruit.com/product/1782.
- [86] International Std. ISO/IEC 9899:TC2
- [87] “IPC Certifications.” *IPC International, Inc.*, 23 Oct. 2020, www.ipc.org/ipc-certifications.
- [88] IPC-221B Generic Standard on Printed Board Design
- [89] “IRF4905PBF - Power MOSFET, P Channel, 55 V, 74 A, 0.02 Ohm, TO-220AB, Through Hole.” *Newark*, www.newark.com/infineon/irf4905pbf/p-channel-mosfet-55v-74a-to-220ab/dp/63J7300?st=irf+4905+power+mosfet+74a+55v+to-220.
- [90] “IRF7240TRPBF.” *Newark*, www.newark.com/w/search/prl/results?st=IRF7240TRPBF&scope=partnumberlookahead&searchref=searchlookahead.
- [91] Jeremy S Cook Jeremy S. Cook has a BSME from Clemson University. “PID Controller Basics & Tutorial: PID Arduino Project.” *Arrow.com*, 1 Nov. 2019, www.arrow.com/en/research-and-events/articles/pid-controller-basics-and-tutorial-pid-implementation-in-arduino.
- [92] Kansagara, Ravi. “Understanding Total Harmonic Distortion (THD) in Power Systems - Technical Articles.” *All About Circuits*, 18 Dec. 2018, www.allaboutcircuits.com/technical-articles/understanding-thd-total-harmonic-distortion-in-power-systems/.
- [93] *Kean Diamond Wire*, keandiamondwire.com/wire%20sawing.
- [94] Kumar, Arkadeep, and Shreyes N. Melkote. “Diamond Wire Sawing of Solar Silicon Wafers: A Sustainable Manufacturing Alternative to Loose Abrasive Slurry Sawing.” *Procedia Manufacturing*, Elsevier, 7 Mar. 2018, www.sciencedirect.com/science/article/pii/S2351978918301963.
- [95] Lam, Mike. “What Is DOD for LiFePO4 Batteries?” *Medium*, Battery Lab, 3 Feb. 2020, medium.com/battery-lab/what-is-dod-for-lifepo4-batteries-335f1dbc9d3d.
- [96] Lextrait, Thomas. “Arduino: Power Consumption Compared • Thomas Lextrait.” Thomas Lextrait on Svbtile, 22 May 2016, tlextrait.svbtile.com/arduino-power-consumption-compared.
- [97] “Lithium-Based Batteries Information.” Lithium-Based Batteries Information – Battery University, batteryuniversity.com/learn/article/lithium_based_batteries.

- [98] Liu, Chaofeng, et al. "Understanding Electrochemical Potentials of Cathode Materials in Rechargeable Batteries." *Materials Today*, Elsevier, 14 Nov. 2015, www.sciencedirect.com/science/article/pii/S1369702115003181.
- [99] "Low-Cost Wafers for Solar Cells." *ScienceDaily*, 9 Oct. 2015, www.sciencedaily.com/releases/2015/10/151009083203.htm#:~:text=Silicon%20wafers%20are%20the%20heart,percent%20reduction%20in%20energy%20costs.
- [100] "Low Voltage Direct Current(LVDC) Nanogrid for Home Application." IEEE Xplore, ieeexplore.ieee.org/document/8069993.
- [101] "Manufacturing.org." *PV Manufacturing*, 18 Sept. 2020, pv-manufacturing.org/etching/.
- [102] Meyer, Paul, et al. "Morningstar ProStar PS-30 30A, Charge Controller without Display (12/24V)." *AltEstore.com*, www.altestore.com/store/charge-controllers/solar-charge-controllers/pwm-solar-charge-controllers/morningstar-prostar-ps-30-30a-pwm-charge-controller-without-display-gen-3-p789/.
- [103] "MLX91221KDC-ABR-020-SP Melexis: Mouser." *Mouser Electronics*, www.mouser.com/ProductDetail/Melexis/MLX91221KDC-ABR-020-SP?qs=81r%252BiQLm7BROD1%252ByhTK6jg%3D%3D.
- [104] "Monocrystalline Silicon Cell." *Monocrystalline Silicon Cell - an Overview | ScienceDirect Topics*, www.sciencedirect.com/topics/engineering/monocrystalline-silicon-cell.
- [105] "Morningstar ProStar MPPT 25A Solar Charge Controller with Display." *AltEstore.com*, www.altestore.com/store/charge-controllers/solar-charge-controllers/mppt-solar-charge-controllers/morningstar-prostar-mppt-25a-solar-charge-controller-with-display-p11989/.
- [106] "Morningstar ProStar PS-15 15A, Charge Controller without Display (12/24V)." *AltEstore.com*, www.altestore.com/store/charge-controllers/solar-charge-controllers/pwm-solar-charge-controllers/morningstar-prostar-ps-15-15a-charge-controller-without-display-1224v-gen3-p787/.
- [107] Mott, Vallerie. "Introduction to Chemistry." *Lumen*, courses.lumenlearning.com/introchem/chapter/other-rechargeable-batteries/#:~:text=A%20rechargeable%20battery%20is%20a,electrochemical%20reactions%20are%20electrically%20reversible.&text=Load%2Dleveling%20involves%20storing%20electric,use%20during%20peak%20load%20period.
- [108] Mott, Vallerie. "Introduction to Chemistry." *Lumen*, courses.lumenlearning.com/introchem/chapter/other-rechargeable-batteries/#:~:text=Rechargeable%20batteries%20store%20energy%20through,the%20battery%20has%20been%20drained.

[109] “MPPT Charge Controller: MPPT Solar Charge Controller: AltE.” *AltEstore.com*, www.altestore.com/store/charge-controllers/solar-charge-controllers/mppt-solar-charge-controllers-c474/.

[110] M. Y., Ayad & Becherif, Mohamed & Abdennacer, Aboubou & Henni, A.. (2011). Sliding Mode Control of Fuel Cell, Supercapacitors and Batteries Hybrid Sources for Vehicle Applications. 10.5772/15881.

[111] Nallapa, Venkatapathi R. “US7058755B2 - EEPROM Emulation in Flash Memory.” *Google Patents*, Google, patents.google.com/patent/US7058755B2/en.

[112] Nate. Analog to Digital Conversion, learn.sparkfun.com/tutorials/analog-to-digital-conversion/all#:~:text=Relating%2n.d.C%20Value%20to%20Voltage.%20The%20ADC%20reports,digital%20conversions%20are%20dependant%20on%20the%20system%20voltage.

[113] “NCP1117ST50T3G - Fixed LDO Voltage Regulator, 3.5V to 20V, 1.07V Dropout, 5Vout, 1Aout, SOT-223-3.” Newark, www.newark.com/on-semiconductor/ncp1117st50t3g/ldo-voltage-regulator-5v-1a-sot/dp/71J6563?gclid=Cj0KCQjwyZmEBhCpARIsALzmnJqZoQaHSId2XB1beR7657kdSr7BJ0XiwrJzYwJKtZEjLTyV20JZw8aAofLEALw_wcB&_kwcid=AL%218472%213%21486608219231%21p%21%21g%21%21ncp1117st50t3g&_mckv=s_dc%7Cpcrid%7C486608219231%7Cplid%7C%7Ckword%7Cncp1117st50t3g%7Cmatch%7Cp%7Cslid%7C%7Cproduct%7C%7Cpgrid%7C115553262475%7Cptaid%7Ckwd-10795717557%7C&CMP=KNC-GUSA-SKU-MDC-SEMICONDUCTORS.

[114] Notes, Electronics. “Electromechanical Relay.” *Electronics Notes*, www.electronics-notes.com/articles/electronic_components/electrical-electronic-relay/what-is-a-relay-basics.php.

[115] Notes, Electronics. “Series Voltage Regulator: Series Pass Regulator.” *Electronics Notes*, www.electronics-notes.com/articles/analogue_circuits/power-supply-electronics/linear-psu-series-regulator-circuit.php.

[116] “NPN Transistor Tutorial - The Bipolar NPN Transistor.” *Basic Electronics Tutorials*, 1 Oct. 2018, www.electronics-tutorials.ws/transistor/tran_2.html.

[117] Okonya, Johnson, et al. “Morningstar ProStar PS-30M 30A, Charge Controller with Display (12/24V).” *AltEstore.com*, www.altestore.com/store/charge-controllers/solar-charge-controllers/pwm-solar-charge-controllers/morningstar-prostar-ps-30m-30a-charge-controller-with-display-gen-3-p790/.

[118] Omar, N, and J Van Mierlo. “Nickel Cadmium Battery.” Nickel Cadmium Battery - an Overview | ScienceDirect Topics, 2014, www.sciencedirect.com/topics/chemistry/nickel-cadmium-battery.

- [119] O'Neill, Peter. "Morningstar ProStar PS-15M 15A, Charge Controller with Display (12/24V)." *AltEstore.com*,
www.altestore.com/store/charge-controllers/solar-charge-controllers/pwm-solar-charge-controllers/morningstar-prostar-ps-15m-15a-pwm-charge-controller-with-display-gen-3-p788/.
- [120] "Open Circuit and Short Circuit." *Ultimate Electronics Book*, 18 Mar. 2021,
ultimateelectronicsbook.com/open-circuit-and-short-circuit/.
- [121] Opengreenenergy, and Instructables. "ARDUINO PWM SOLAR CHARGE CONTROLLER (V 2.02)." *Instructables*, 21 July 2020,
www.instructables.com/ARDUINO-PWM-SOLAR-CHARGE-CONTROLLER-V-202/.
- [122] Patel, Darshil. "How to Design a Three-Stage Battery Charging Circuit: Custom." *Maker Pro*, Maker Pro, 14 Jan. 2020,
maker.pro/custom/tutorial/how-to-design-a-three-stage-battery-charging-circuit.
- [123] PDF, Download. "Understanding How a Voltage Regulator Works." *Understanding How a Voltage Regulator Works | Analog Devices*,
www.analog.com/en/technical-articles/how-voltage-regulator-works.html#.
- [124] Peña, Eric, and Mary Grace Legaspi. "UART: A Hardware Communication Protocol Understanding Universal Asynchronous Receiver/Transmitter." *UART: A Hardware Communication Protocol Understanding Universal Asynchronous Receiver/Transmitter | Analog Devices*,
www.analog.com/en/analog-dialogue/articles/uart-a-hardware-communication-protocol.html.
- [125] "Pololu 9V, 2.3A Step-Down Voltage Regulator D24V22F9." *Pololu Robotics & Electronics*, www.pololu.com/product/2861.
- [126] "Polycrystalline Materials & Textures." *PhysicsOpenLab*, 1 May 2018,
physicsopenlab.org/2018/05/01/texture-in-polycrystalline-materials/.
- [127] Prine-Robie, Michael. "How Does Temperature Affect Battery Performance?" *CED Greentech*, 31 Aug. 2020,
www.cedgreentech.com/article/how-does-temperature-affect-battery-performance.
- [128] "Pure Sine Wave vs. Modified Sine Wave Inverters- What's the Difference?" *Solar Power News & DIY Solar Tips*, 27 Oct. 2015,
www.altestore.com/blog/2015/10/pure-sine-wave-vs-modified-sine-wave-whats-the-difference/#.YIdgK5BKiiN.
- [129] "PWM Solar Charge Controller: PWM Charge Controller: AltE." *AltEstore.com*,
www.altestore.com/store/charge-controllers/solar-charge-controllers/pwm-solar-charge-controllers-c477/?page=1.
- [130] Ramdas. *AMBA Bus Protocols - AXI, AHB, APB - Understanding Architecture and References*, 16 Aug. 2018, verificationexcellence.in/amba-bus-architecture/.

- [131] “Resistive or Capacitive Touch Screen: Which Is Better.” *Orient Display*, www.orientdisplay.com/knowledge-base/touch-panel-basics/resistive-or-capacitive-touch-screen-which-is-better/#:~:text=Capacitive%20vs.%20Resistive%20Touch%20Screens%20%20%20,%20Relatively%20low%20%2014%20more%20rows.
- [132] Robinson, Allan. “Voltage Regulator: Theory of Operation.” *Sciencing*, 24 Apr. 2017, sciencing.com/voltage-regulator-theory-operation-2451.html.
- [133] Roderick, Ryan. “A Look Inside Battery-Management Systems.” *Electronic Design*, 26 Mar. 2015, www.electronicdesign.com/power-management/article/21800666/a-look-inside-batterym-anagement-systems.
- [134] Rozenblat, Lazar. “YOUR GUIDE TO DC to AC POWER INVERTERS.” *Power Inverter Circuits: DC-AC Converter*, www.smeps.us/power-inverter.html.
- [135] “Schottky Diode or Schottky Barrier Semiconductor Diode.” *Basic Electronics Tutorials*, 11 July 2019, www.electronics-tutorials.ws/diode/schottky-diode.html.
- [136] Scott, Kevin. “Paralleling Linear Regulators Made Easy.” *Paralleling Linear Regulators Made Easy | Analog Devices*, www.analog.com/en/technical-articles/paralleling-linear-regulators-made-easy.html#:~:text=Connecting%20multiple%20linear%20regulators%20in,currents%20a%20solution%20can%20deliver.&text=Two%20voltage%20reference%2Dbased%20linear,will%20not%20share%20current%20equally.
- [137] Shapley, Patricia. *Galvanic and Electrolytic Cells*, University of Illinois, 2012, butane.chem.uiuc.edu/pshapley/genchem2/c6/1.html.
- [138] “Solar Panel Voltage Regulator-OLYS.” 深圳市奥林斯科技有限公司, www.olyssolar.com/product_Info-4-46.html?gclid=Cj0KCQjwgtWDBhDZARIsADEKwgPZhYnJ4hWmfWCW_hY03awKJDI5HgmKSyLN6ggybzhMfqeDzrBVHogaAtd7EALw_wcB.
- [139] “Solid State Relay or Solid State Switch.” *Basic Electronics Tutorials*, 24 Aug. 2019, www.electronics-tutorials.ws/power/solid-state-relay.html.
- [140] Sopori, Bhushan, et al. “Characterizing Damage on Si Wafer Surfaces Cut by Slurry and Diamond Wire Sawing.” *IEEE Xplore*, ieeexplore.ieee.org/document/6744298.
- [141] “SPI Versus I2C: How to Choose the Best Protocol for Your Memory Chips.” *Altium*, resources.altium.com/p/spi-versus-i2c-how-choose-best-protocol-your-memory-chips.
- [142] “SPI vs I2C Protocols - Pros and Cons.” *Arrow.com*, 5 Sept. 2020, www.arrow.com/en/research-and-events/articles/spi-vs-i2c-protocols-pros-and-cons#:~:text=SPI%20vs%20I2C%20SPI%20and%20I2C%20were%20both,generally%20operate%20in%20the%203.3%20or%205V%20range.

- [143] St. Michael, Stephen. "The Advanced Microcontroller Bus Architecture: An Introduction - Technical Articles." *All About Circuits*, www.allaboutcircuits.com/technical-articles/introduction-to-the-advanced-microcontroller-bus-architecture.
- [144] Stein, Andrea. "How It Works: Voltage Relay." *Sciencing*, 21 July 2017, sciencing.com/how-it-works-voltage-relay-13401385.html.
- [145] Svarc, Jason. "Most Efficient Solar Panels 2021." *CLEAN ENERGY REVIEWS*, *CLEAN ENERGY REVIEWS*, 24 Mar. 2021, www.cleanenergyreviews.info/blog/most-efficient-solar-panels.
- [146] "Temperature Effects on Batteries." *Intercel Services B.V.*, 9 July 2020, www.intercel.eu/frequently-asked-questions/temperature-effects-on-batteries/#:~:text=Even%20though%20battery%20capacity%20at,life%20is%20cut%20in%20half.
- [147] Thoubboron, Kerry. "DOD Battery: What Does Depth of Discharge Mean?: EnergySage." *Solar News*, EnergySage, 3 June 2019, news.energysage.com/depth-discharge-dod-mean-battery-important/.
- [148] "Transient-Voltage-Suppression Diode." *Wikipedia*, Wikimedia Foundation, 1 Jan. 2021, en.wikipedia.org/wiki/Transient-voltage-suppression_diode.
- [149] Turashoff, Michael. "The Difference Between Galvanic Cells and Electrolytic Cells." *News about Energy Storage, Batteries, Climate Change and the Environment*, 10 July 2014, www.upsbatterycenter.com/blog/difference-galvanic-cells-electrolytic-cells/.
- [150] "Types of Batteries: The Rechargeable Battery Association." *PRBA*, 1 June 2012, www.prba.org/battery-safety-market-info/types-of-batteries/.
- [151] "Types of Solar Panels: Which One Is the Best Choice?" *Solar Reviews*, 10 Jan. 2021, www.solarreviews.com/blog/pros-and-cons-of-monocrystalline-vs-polycrystalline-solar-panels#mono.
- [152] "Understanding the Differences Between UART and I2C." *Total Phase Blog*, 16 Dec. 2020, www.totalphase.com/blog/2020/12/differences-between-uart-i2c/.
- [153] User Manual GV-10-Li
- [154] User Manual MPPT
- [155] User Manual PS-MPPT-25
- [156] User Manual PS-MPPT-25M
- [157] User Manual PS-MPPT-40
- [158] User Manual PS-MPPT-40M

- [159] “Voltage Regulation: Transformers: Electronics Textbook.” *All About Circuits*, www.allaboutcircuits.com/textbook/alternating-current/chpt-9/voltage-regulation/.
- [160] “Voltage Regulator Types and Working Principle: Article: MPS.” *Voltage Regulator Types and Working Principle | Article | MPS*, www.monolithicpower.com/en/voltage-regulator-types.
- [161] “Voltage Regulators,Circuits,Types,Working Principle, Design, Applications.” *Electronic Circuits and Diagrams-Electronic Projects and Design*, 9 Aug. 2018, www.circuitstoday.com/voltage-regulators.
- [162] “VRLA Battery.” *Wikipedia*, Wikimedia Foundation, 7 Apr. 2021, en.wikipedia.org/wiki/VRLA_battery#:~:text=A%20valve%20regulated%20lead%E2%80%93acid,positive%20plates%20so%20that%20oxygen.
- [163] “What Are Electromechanical Relays?” *Types of Relays*, relays.weebly.com/electromechanical-relays.html#:~:text=Electromechanical%20relays%20are%20switches%20that,controlled%20by%20one%20single%20signal.
- [164] “What Is a Relay? Definition, Working Principle and Construction.” *Circuit Globe*, 11 Feb. 2017, circuitglobe.com/relay.html.
- [165] “What Is a Solar Charge Controller?” *AltEstore.com*, www.altestore.com/store/info/solar-charge-controller/.
- [166] “What is the difference between a normal lead-acid car battery and a deep cycle battery?” 1 April 2000. HowStuffWorks.com. <https://auto.howstuffworks.com/question219.htm> <26 April 2021
- [167] Williams, David. “Understanding Total Harmonic Distortion (THD) in Power Systems - Technical Articles.” *All About Circuits*, 15 Mar. 2017, www.allaboutcircuits.com/technical-articles/understanding-thd-total-harmonic-distortion-in-power-systems/.
- [168] Williams, K., et al. “Reactive Ion Beam Etching of Ferroelectric Materials Using an RF Inductively Coupled Ion Beam Source.” *IEEE Xplore*, ieeexplore.ieee.org/document/598141.
- [169] Woodford, Chris. “How Do Batteries Work? A Simple Introduction.” *Explain That Stuff*, 2006, www.explainthatstuff.com/batteries.html.
- [170] Woodford, Chris. “How Do Relays Work?” *Explain That Stuff*, 19 Aug. 2020, www.explainthatstuff.com/howrelayswork.html.
- [171] Woodford, Chris. “How Do Transistors Work?” *Explain That Stuff*, 21 Sept. 2020, www.explainthatstuff.com/howtransistorswork.html.
- [172] “Working of Relays-How Relay Works,Basics,Design,Construction,Application.” *Electronic Circuits and Diagrams-Electronic Projects and Design*, 14 Aug. 2018, www.circuitstoday.com/working-of-relays.

[173] Yuanjian Jiang, et al. "Optimization of a Silicon Wafer Texturing Process by Modifying the Texturing Temperature for Heterojunction Solar Cell Applications." *RSC Advances*, Royal Society of Chemistry, 5 Aug. 2015, pubs.rsc.org/en/content/articlehtml/2015/ra/c5ra09739h#:~:text=Silicon%20surface%20texturing%20is%20a,%E3%80%89%2Doriented%20monocrystalline%20silicon%20wafers.

[174] ZHCSolar. "MPPT vs PWM : Which Charge Controller Should You Choose?" *ZHCSolar*, 8 Mar. 2021, zhcsolar.com/mppt-vs-pwm/.

[175] PS-MPPT-25 data sheet

[176] PS-MPPT-25M data sheet

[177] PS-MPPT-40 data sheet

[178] PS-MPPT-40M data sheet

[179]"Inverter Types & Working Principle: Sine Wave, Square Wave, Modified Sine Wave Inverter Working." *Electrical Academia*, 12 Sept. 2019, electricalacademia.com/renewable-energy/inverter-types-working-principle-sine-wave-square-wave-modified-sine-wave-inverter-working/.

[180]"NMOS vs PMOS | Difference Between NMOS and PMOS Types." *NMOS vs PMOS | Difference between NMOS and PMOS Types*, www.rfwireless-world.com/Terminology/NMOS-vs-PMOS.html.

[181]"Difference Between NMOS PMOS and CMOS Transistors." *Electrotopic.com*, 10 Nov. 2019, electrotopic.com/difference-between-nmos-pmos-and-cmos-transistors/.

[182] Orunmila "The Problems of I2C - common problems and errors with using I2C" *microforum.cc*, 28, June.2019, www.microforum.cc/blogs/entry/42-the-problems-of-i2c-common-problems-and-errors-with-using-i2c

[183] "Viewing Angle of an LCD" *liquidcrystaltechnologies.com*, http://www.liquidcrystaltechnologies.com/tech_support/viewangle.htm